The TIAM-UCL Model (Version 4.1.1) Documentation

June 2020

Steve Pye
Isabela Butnar
Jen Cronin
Dan Welsby
James Price
Olivier Dessens
Baltazar Solano Rodríguez
Matthew Winning
Gabrial Anandarajah
Daniel Scamman
Ilkka Keppo

Contents

Acronyms

BECCS	Bioenergy with CCS
BEVs	Battery Electric Vehicles
CAT	Centre for Alternative Technology
CCAs	Climate Change Agreements
CCC	Committee on Climate Change
CCS	Carbon Capture and Storage
CfDs	Contracts for Difference
CNG	Compressed Natural Gas
COP21	21st session of the Conference of the Parties to the UNFCCC
DDPP	Deep Decarbonisation Pathways Project
DECC	Department of Energy & Climate Change
DTI	Department of Trade and Industry
ECO	Energy Company Obligation
EMR	Electricity Market Reform
ETI	Energy Technologies Institute
ETSAP	Energy Technology Systems Analysis Programme
EU ETS	European Union Emissions Trading Scheme
GHG	Greenhouse Gas
H_2FC	Hydrogen Fuel Cell
HGVs	Heavy Goods Vehicles
IA&S	International aviation and shipping
IEA	International Energy Agency
IPCC	Intergovernmental Panel on Climate Change
LDVs	Light Duty Vehicles (cars, vans)
LEVs	Low Emission Vehicles
OLEV	Office of Low Emission Vehicles
PHEVs	Plug-in Hybrid Electric Vehicles
RCEP	Royal Commission on Environmental Pollution
RCP	Representative Concentration Pathways
RHI	Renewable Heat Incentive
SMR	Steam Methane Reformer
TIMES	The Integrated MARKAL-EFOM System
UKERC	UK Energy Research Centre
UKTM	UK TIMES Model
UNEP	United Nations Environmental Programme
UNSDSN	UN Sustainable Development Solutions Network

1. Model overview

This document describes the global energy system model TIAM-UCL, which stands for TIMES Integrated Assessment Model at University College London. This document replaces the previous TIAM-UCL documentation, by Anandarajah et al. [1].

TIAM-UCL is an energy-economy model of the global energy system. It is built in the TIMES framework, a modelling framework that uses an optimisation approach to explore cost-optimal systems. The representation of the global energy system includes primary energy sources (oil, gas, coal, nuclear, biomass, and renewables) from production through to their conversion (e.g. electricity production), their transport and distribution, and their eventual use to meet energy demands across a range of economic sectors. Using a scenario-based approach, the evolution of the system to meet future energy service demands (including mobility, lighting, residential and industrial heat and cooling), can be simulated, driven by the least-cost objective.

The model splits the globe up into 16 regions, including the UK, which allows for a detailed characterisation of regional energy sectors, and the trade flows between them. Future demands for energy services, which increase due to population and economic growth, drive the evolution of the energy system that must meet these demand requirements. These demands are dynamic, in that they can rise or fall in response to changes in the cost of providing energy services via the use of long run price elasticities. Therefore, reductions of energy service demands also provide flexibility for reducing emissions. The model can also be hard-linked to a simple CGE model to assess impacts of the energy system on the broader economy, and the subsequent feedback on energy demand.

Decisions around what energy sector investments to make across regions to meet these demands are determined on the basis of the most cost-effective investments, taking into account the existing system in 2015, energy resource potential, technology availability, and crucially policy constraints such as emissions reduction targets. Using linear programming, the model solves to minimise the discounted total system cost over the full time horizon of the model, based on a discount factor of 3.5%. The model time horizon runs to 2100, in line with the timescale typically used in these simulations.

The model does have the ability to remove emissions from the atmosphere via negative emissions, based on a set of BECCS technologies (in power generation, industry, and in H_2 and biofuel production) and Direct Air Capture and Storage (DACS).

A climate module is also integrated into the model framework, calibrated to the climate model MAGICC [2], allowing for a simplified representation of the climate system. It ensures that any future energy system is consistent with a given temperature objective, such as limiting warming to 1.5°C or 2°C by 2100 and beyond. To this end, the climate module is run out well beyond 2100 to ensure emission levels in 2100, and the underlying energy system, are consistent with maintaining a stable temperature from that point onwards. As described later, this approach is coupled with carbon budgets in order to be more representative of the most up-to-date climate science assessed by the IPCC that used multiple lines of evidence to estimate carbon budgets and not just simple climate models.

For CH_4 and N_2O emission levels, non-energy sector related emissions (outside of the energy system) are fixed based on RCP trajectories. However, emissions of non-CO_2 GHGs from the energy system are endogenously modelled, with mitigation options available, for example, to reduce CH_4 leakage from oil and gas extraction and supply activities. This allows the model to replicate the crucial role of increasing the stringency of environmental regulation for oil and gas systems. The sum of the exogenous and endogenous emissions are required (via a constraint) to be below a declining emission trajectory out to 2100. For CH_4 and N_2O these constraints are derived separately and are based on the mean of pathways used in the IPCC Special Report on 1.5°C (here after SR1.5).

The model also has a backstop mechanism, meaning that if it does not have sufficient mitigation options to remain within a given carbon budgets or temperature limit, it can deploy this mechanism. However, it only does so as a last resort, as the option is costed well above the highest cost technological option in the model, at £5000/tCO_2. The purpose of this backstop mechanism is not to represent a 'unicorn' technology, but rather to allow the model to solve so that other insights can be gained e.g. which sectors have highest residual emissions? To what extent is the carbon budget exceeded? Its use in this context can be found in a number of analyses [3,4].

A schematic of the model structure is provided in Table 1. Energy service demands drive the demand for energy (left-hand side), which are met by the energy supply system (right hand side). Costs are accounted for (top-right), with the objective of the model to minimise these as far as possible. Energy services can be responsive to changes in their price, either modelled via price elasticities or via linkages with the macroeconomic module. A climate module (bottom right) calculates impacts of emissions on global temperatures; however, there are no feedbacks from changes in climate on the energy system.

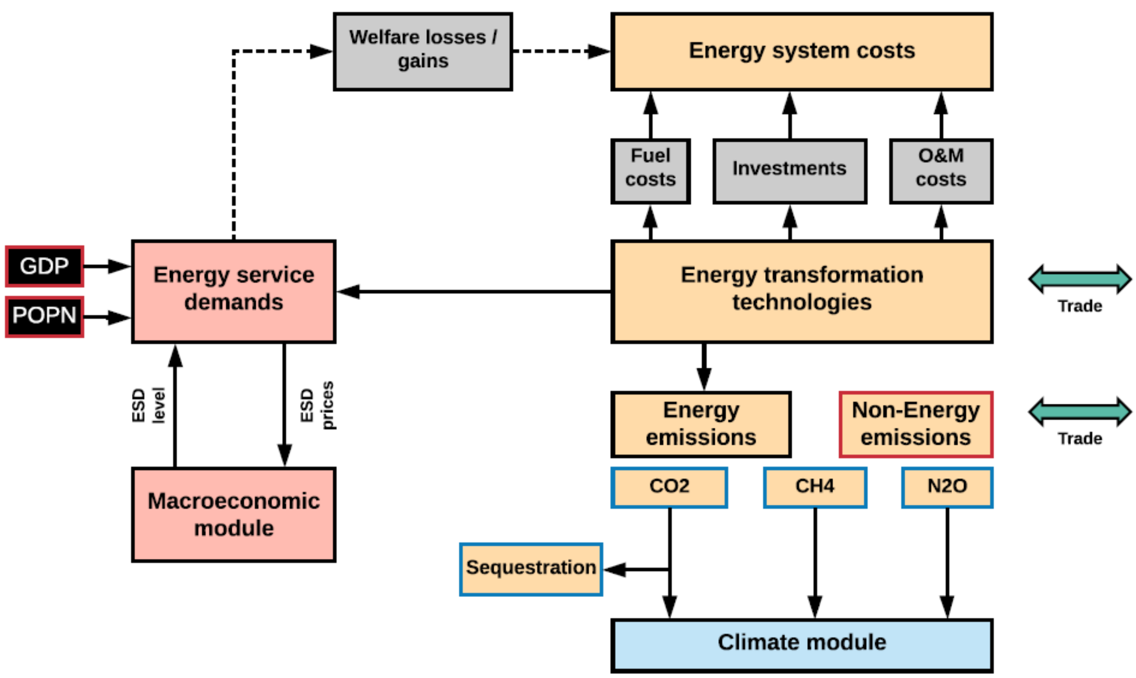

Figure 1. General structure of TIAM-UCL

Fossil fuel resource assessments have been a key focus of research using TIAM-UCL. However, a range of papers have been published, focusing on a diverse set of topics:

- fossil fuel resource assessment [5–9]

- fossil fuel trade [10]
- bioenergy use [11]
- industrial energy demand [12]
- energy demand response [13]
- technology learning [14]
- transport decarbonisation [15,16]
- role of CCS [17]
- model scenario comparison [18]
- macroeconomic impacts [19]
- climate ambition [3,4,20–22]

1.1. Model approach (paradigm)

The model is a multi-region, multi-sector energy system model, linked to both the wider economy via a simple macro-economic module and to the wider climate system, via a climate module (detailed in section 8).

The energy system model is built using the TIMES model framework [23], which uses a linear programming approach to explore cost-optimal configurations of the future energy system. The model objective is to minimize total discounted system costs[1]. Features of this formulation include perfect competition (no market power held by specific firms) and perfect foresight (market players have all information, now in the future, to inform investment decisions). The macroeconomic model, described further in section 2.3, uses a simple one sector CGE model to estimate the impact of the energy system on the wider economy.

The regional structure of the model is shown in section 1.2, the temporal structure in 1.3 and the sectoral structure in section 1.4.

1.2. Regional disaggregation

The model is split into 16 regions, including 1) Africa (AFR), 2) Australia (AUS), 3) Canada (CAN), 4) Central and South America (CSA), 5) China (CHI), 6) Eastern Europe (EEU), 7) Former Soviet Union (FSU), 8) India (IND), 9) Japan (JAP), 10) Mexico (MEX), 11) Middle-east (MEA), 12) Other Developing Asia (ODA), 13) South Korea (SKO), 14) United Kingdom (UK), 15) USA (USA) and 16) Western Europe (WEU).

The countries that are included in each region are listed in Appendix 1.

[1] Or when accounting for demand response to price (in the elastic demand formulation), maximising consumer surplus.

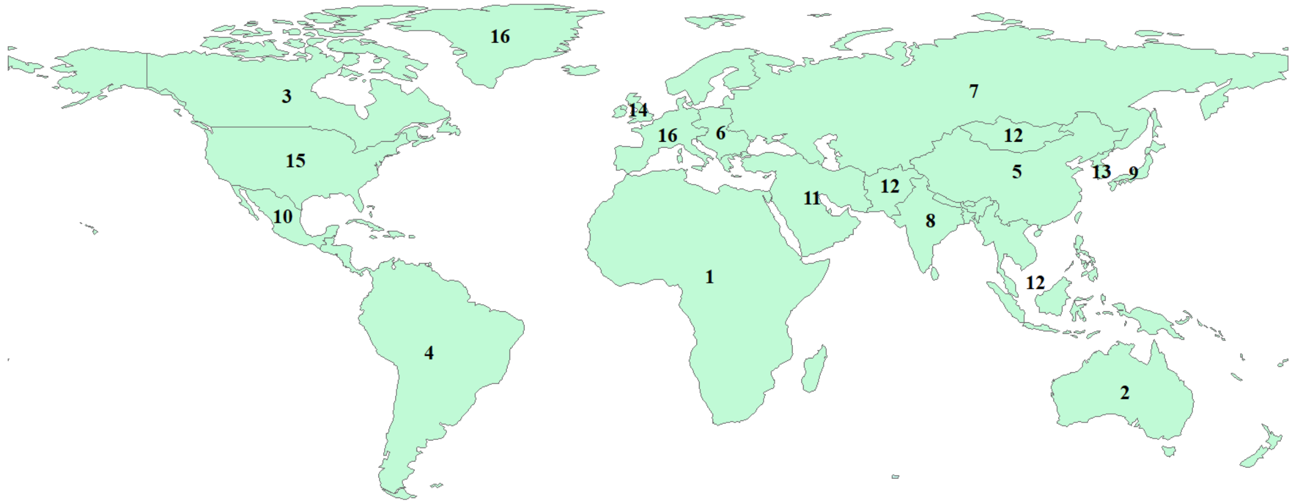

Figure 2. TIAM-UCL regions (from Welsby [24] **)**

A key feature of the regional disaggregation is that energy commodities can be traded, important for simulating global markets (and prices). In addition, GHG commodities can also be traded, allowing for the formation of carbon markets. The simulation of such markets only makes sense where GHG targets are regionally differentiated, providing incentives for regions to explore offsetting opportunities via such markets.

A more detailed description of fossil fuel trade is provided in section 3.1.4. Biomass trade is described in Section 3.2 and Appendix 7.

1.3. Temporal structure

TIAM-UCL is an inter-temporal optimization model, solving for the perfect-foresight equilibrium of the global energy system between the years 2005-2100. While the model can be run in different time step configurations, the model typically uses five-year time steps until 2060, and ten-year time steps thereafter.

Within a given year, the structure consists of six periods (or *time slices*), based on three seasons (summer, winter and intermediate), and two diurnal periods (Day, 16 hours and night, 8 hours). This is important to represent changes in electricity and heat load based on sector demand profiles.

1.4. Structure of energy sector

Within each region, the structure of the energy system is represented as shown in Figure 3. However, this is not a closed system, with trade in energy commodities and CO_2 / GHG certificates (offsets) possible (if enabled). The structure is fairly typical of this type of model, with a resource sector representing the fossil and renewable resources available across different regions. An upstream sector extract, processes and distributes those resources, and supplies them to the power and end use sectors directly, or enables secondary transformation (hydrogen, biofuels). Five end use sectors use the energy supplied to meet energy service demands for a range of services (mobility, industrial products, thermal comfort in buildings). CO_2 can also be captured and stored at different points across the system and transported and stored. At all parts of the energy system, GHG emissions are accounted for.

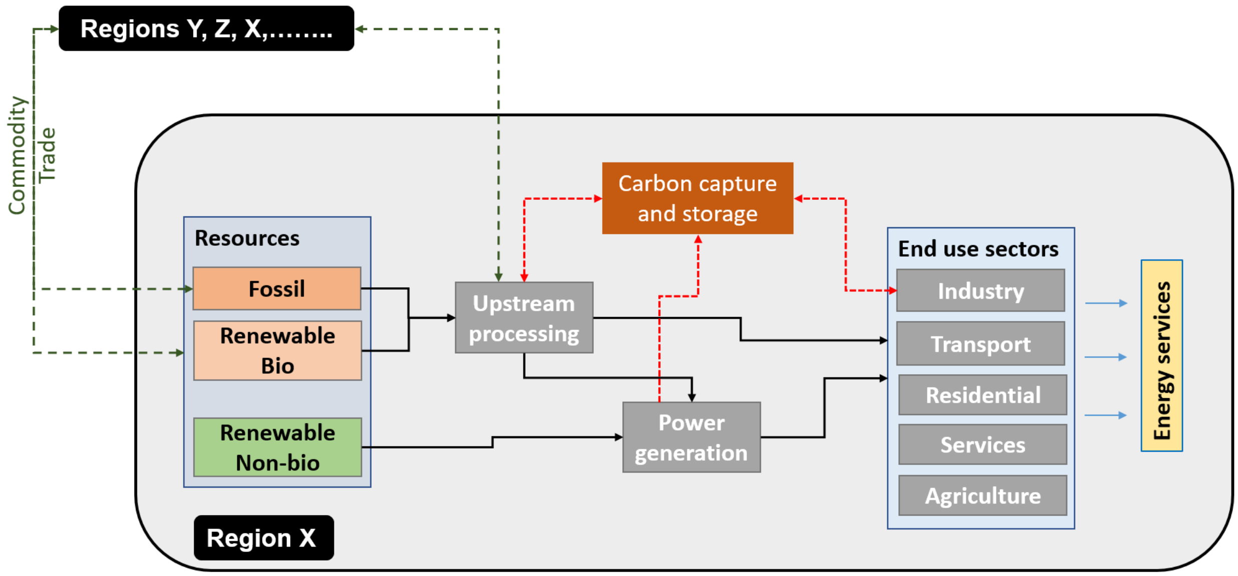

Figure 3. TIAM-UCL energy system

1.5. Policies

Individual country or regional level policies are usually not modelled in detail, except for nationally determining contributions (NDCs) which are increasingly used as a reference case against which to compare more ambitious climate policies [19]. In the main, as with other IAMs, TIAM-UCL is primarily used to explore alternative futures under different levels of climate ambition, assuming global action is taken to effect this change. TIAM-UCL has also been used to investigate scenarios of differentiated regional action, in which developed countries take a lead in cutting emissions with some nations and regions ahead of others in developing climate policy that will enable deeper emission reductions than suggested by the scenarios of unified global action [25].

The model has a range of features, listed in Table 1.

Table 1. Key features of TIAM-UCL

Key feature	Description	Section (for more detail)
Model paradigm	Energy system optimisation (LP) model; similar paradigm to the MESSAGE model [26].	
Macroeconomic formulation	Hard linkage to simple single sector CGE model.	2.3

Regional representation	16 regions	1.2; Appendix 1
Investment decisions	Assessment of all costs (capex, O&M, fuel) over the model time horizon, subject to 3.5% (SRTP[2]) discount rate. Capex annualised based on cost of capital rate over economic lifetime, varied by technology group / region.	
Energy commodity trade linkages	Commodity flows between regions are enabled for all fossil fuels, and bioenergy.	3.1.4 and 3.3
Energy supply sector representation	Power generation, biofuel production, hydrogen production	4.0
End use sector representation	Transport, residential, commercial, agriculture, industry	6.0
Climate policy targets	Global temperature targets via climate module and carbon budget. Regional targets using carbon pricing or emission caps, with the option to trade / offset.	7.0, 8.0
Technological change / learning	Exogenously determined technological learning, informed by other literature. An endogenous technology learning (ETL) extension to TIMES exists [27] and has been implemented previously in TIAM-UCL [14].	
Land use	TIAM-UCL does not have a linkage to a bespoke land use model.	3.2

[2] SRTP refers to the Social Rate of Time Preference

2. Projected demands

2.1. Energy service demands

TIAM-UCL represents the demand for final energy across the four sub-sectors in the model (commercial, residential, transport, industry) in the form of a set of exogenously prescribed end-use energy service demands (ESD). These are defined at the regional level and include services such as residential space heating, domestic aviation and iron and steel production (see Table 2 for a full list).

Table 2. List of energy service demands

Code	Service demand	Unit	Driver
ICH	Chemicals	PJ	PICH
IIS	Iron and Steel	Mt	PIIS
INF	Non-ferrous metals	Mt	PINF
INM	Non Metals	Mt; PJ	PINM
ILP	Pulp and Paper	Mt	PILP
IOI	Other Industries	PJ	POI
NEO	Industrial and Other Non Energy Uses	PJ	GDP
ONO	Other non-specified consumption	PJ	GDP
AGR	Agricultural demand	PJ	PAGR
CC1	Commercial Cooling - Region 1	PJ	PSER
CCK	Commercial Cooking	PJ	PSER
CH1	Commercial Space Heat - Region 1	PJ	PSER
CHW	Commercial Hot Water	PJ	PSER
CLA	Commercial Lighting	PJ	PSER
COE	Commercial Office Equipment	PJ	PSER
CRF	Commercial Refrigeration	PJ	PSER
RC1	Residential Cooling - Region 1	PJ	HOU/GDPPHOU*
RCD	Residential Clothes Drying	PJ	HOU/GDPPHOU*
RCW	Residential Clothes Washing	PJ	HOU/GDPPHOU*
RDW	Residential Dishwashing	PJ	HOU/GDPPHOU*
REA	Residential Other Electric	PJ	HOU/GDPPHOU*
RH1	Residential Space Heat - Region 1	PJ	HOU
RHW	Residential Hot Water	PJ	POP
RK1	Residential Cooking - Region 1	PJ	POP
RL1	Residential Lighting - Region 1	PJ	GDPP
RRF	Residential Refrigeration	PJ	HOU/GDPPHOU*
NEU	Non Energy Uses	PJ	GDP
TAD	Domestic Aviation	PJ	GDP
TAI	International Aviation	PJ	GDP
TRB	Road Bus Demand	Bv-km	POP
TRC	Road Commercial Trucks Demand	Bv-km	GDP
TRE	Road Three Wheels Demand	Bv-km	POP
TRH	Road Heavy Trucks Demand	Bv-km	GDP
TRL	Road Light Vehicle Demand	Bv-km	GDP
TRM	Road Medium Trucks Demand	Bv-km	GDP
TRT	Road Auto Demand	Bv-km	GDPP
TRW	Road Two Wheels Demand	Bv-km	POP
TTF	Rail-Freight	PJ	GDP
TTP	Rail-Passengers	PJ	POP
TWD	Domestic Internal Navigation	PJ	GDP
TWI	International Navigation	PJ	GDP

*Driver is GDPPHOU for AFR, CHI, CSA, EEU, FSU, IND, MEA, MEX, ODA and SKO

Each service demand is projected from 2005-2100 by relating it to a given demand driver and using the expression:

$$ESD_t = ESD_{t-1}\left(\frac{Driver_t}{Driver_{t-1}}\right)^{\propto_t}$$

Here α is a decoupling factor which is used to adjust the strength of the relationship between demand driver and ESD, thereby reflecting shifts in the wider socio-economic system. Drivers are listed in Table 2 and their code explained in Table 3. The ESDs ICH, IIS, INF, INM, ILP and AGR do not use a decoupling factor and are directly linked to their respective drivers.

Table 3. List of drivers for projecting energy service demands

Driver	Description
PICH	Production of chemicals
PIIS	Production of iron and steel
PINF	Production of non-ferrous metals
PINM	Production of cement
PILP	Production of pulp and paper
PIOI	Production of other industries
PAGR	Production of agriculture (linked to calories consumed)
PSER	Services (directly linked to GDP growth)
HOU	Number of households
POP	Population
GDP	GDP
GDPP	GDP per capita
GDPPHOU	GDP per capita per household

2.2. Shared Socio-economic Pathways

The Shared Socio-economic Pathways (SSPs) have been developed by the Integrated Assessment Modelling community as a means of mapping out a set of future narratives for the evolution of the global socio-economic system across a multi-dimensional matrix [28]. A simplified version is shown in Figure 4 which plots the SSPs on axes of challenges to mitigation/adaption. Broadly speaking, SSP1 can be viewed as a world in which society re-orientates itself toward more sustainable lifestyles, population growth is reduced and global GDP per capita is high and so challenges are low. SSP3, by contrast, is a world much less focused on sustainability with high population growth and low GDP per capita thus resulting in high challenges to both mitigation and adaption. SSP2 is then the middle of the road scenario between these two extremes with SSP4/5 fleshing the off diagonal elements.

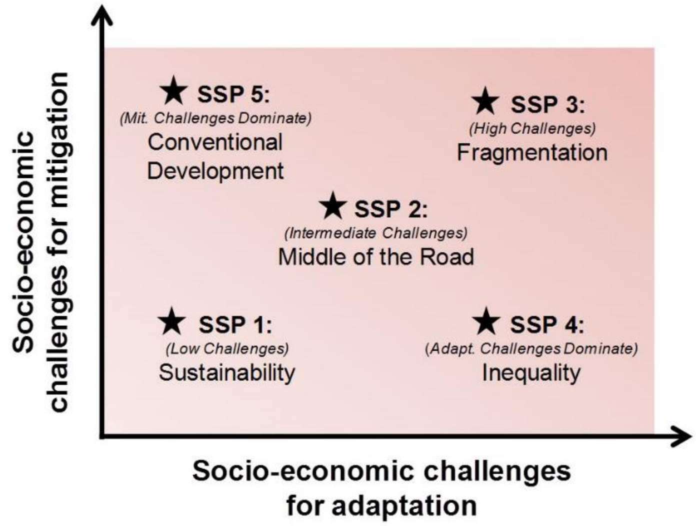

Figure 4. Shared Socio-economic Pathways (SSPs) narratives, reproduced from [28]

TIAM-UCL has a simplified representation of the SSPs which include appropriately aligned regional GDP and population projections between 2005-2100 and scaled biomass availability. We have also made efforts to adjust and calibrate the model's default ESD trajectories to match the SSP marker model for each SSP. This has been achieved by approximately aligning global final energy consumption between TIAM-UCL and each SSP marker model. Furthermore, in order to bring our SSP ESDs projections towards historical data (i.e. calibrated demands), individual service demands in each region have been inflated or deflated based on shifts in the energy system and energy demand in recent years. To-date, there are on-going efforts to translate more of the qualitative elements of the SSPs into the model's ESD pathways, coupled macro-economic model and price elasticities.

Macro Stand-Alone (MSA) is a single-agent, single-sector, multi-regional, general equilibrium Ramsey optimal-growth model which maximises discounted utility of a single consumer-producer agent [29]. This enables the estimation of changes in consumption, production and investment as well as GDP losses (or gains) for each region compared to the baseline scenario. Energy cost outputs from the initial TIMES model run are used as inputs to the non-linear MSA model which then solves and returns changed energy service demands back to TIMES which then begins the solution process again for the updated demands. This iterative process continues until convergence is achieved between the two models. TIAM-UCL can be solved with or without the linkage to MSA depending upon the research question.[3]

The data required for MSA calibration is initial GDP level of each region, the GDP growth rate projections for each region (which should be synchronous with the TIMES demand drivers), and the calibration parameters e.g. elasticity of substitution between energy and the capital/labour composite, which are listed along with equations in Kypreos and Lehtila [29].

Each region will have its own initial energy system mix, as well as differing resource endowments, all of which will determine the extent to which it is impacted by emissions targets – the ambition of which will also affect regional economic impacts. Most analyses assume all regions have the same elasticity of substitution parameter between the labour/capital composite and energy in the production function of 0.2.[4]

[3] Running the model with the TIMES_MSA hard link adds significantly to the solution time.

[4] The elasticity of 0.2 represents a combination of both short-run and long-run elasticities and is taken from the Kypreos and Lehtila [29].

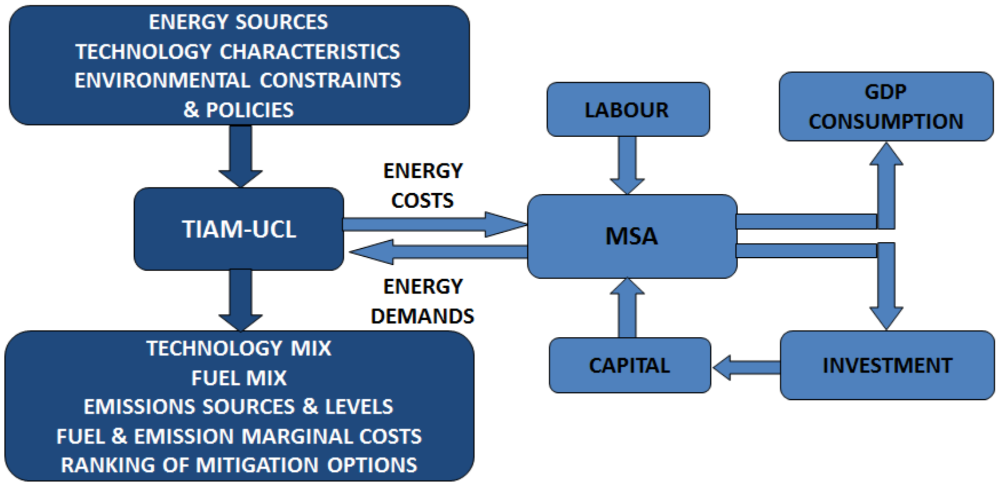

Figure 5. Schematic of the TIAM-UCL – MSA framework

The modelling analysis considers only the costs of changes to the energy system and omits the negative impact and damages of climate change on the economy. These are typically omitted due to the timing of the damages which mostly occur beyond the time frame of the study i.e. 2050 onwards at an exponential rate [30]. The latest implementation of the macro MSA module in TIAM-UCL can be found in Winning et al. [19].

3. Primary Energy resources

3.1. Fossil fuels

The fossil fuel upstream sector in TIAM-UCL incorporates the availability and costs of primary energy resources, all extraction processes, and any upgrading / processing required which yields energy commodity carriers that can be used as inputs into end-use sectors. For fossil fuel resources, this translates as all processes across the system, from extraction of resource out of the ground to a form where it can be input into another sector and/or traded to another region. Table 4 lists the different parts of the upstream fossil fuel sector, and where additional detail can be found on each in Appendix 2.

Table 4. Structure of Appendix 2

Upstream focus	Section	Commodity	Section
Primary energy resources and the extraction of exhaustible primary commodities	A2.1	Coal	A2.1.1
		Natural gas	A2.1.2
		Oil	A2.1.3
Primary transformation (upgrading and/or processing)	A2.2	Coal	A2.2.1
		Natural gas	A2.2.2
		Oil	A2.2.3
Secondary transformation (refining)	A2.3		
Trade	A2.4	Coal	A2.4.1
		Natural gas	A2.4.2
		Oil	A2.4.3
Key upstream constraints	A2.5	Coal	A2.5.1
		Natural gas and oil	A2.5.2

3.1.1. Coal

Coal consists of two categories of resource - brown coal (lignite) and hard coal (sub-bituminous, bituminous and anthracite). The resource base is split into three cost tranches, to allow for more accessible and higher quality resources to be depleted first, before moving to more expensive extraction of (potentially) harder to exploit resources. The distribution of resources / reserves assigned to each cost category varies by region and is influenced by the proportion of the total resource base which can be considered reserves[5], with the remainder of resources split between the middle and highest cost categories.

[5] Reserves are defined as geologically proven with current technologies, and commercially viable to extract at current market prices/cost conditions.

3.1.2. Gas

The underlying availability and cost of natural gas in TIAM-UCL is disaggregated into the following geological categories:

- Non-associated conventional gas proved reserves
- Non-associated conventional gas reserve additions
- Non-associated conventional gas new discoveries
- Associated natural gas
- Arctic conventional natural gas resources
- Shale gas
- Coal bed methane
- Tight natural gas

The disaggregation is based on McGlade [31]. However, the characterisation of these resources has been further developed by Welsby [24], based on a detailed field-level assessments of resource availabilities and costs. Resource assessments were generally conducted at disaggregated field-/play-level, and then aggregated into the regions of TIAM-UCL using probability distributions, and taking into account any correlation between discrete estimates etc. These were then applied to depletion curves which were formed from a database of field-/play-level costs where possible. The database was then extended to fields for which costs were either not known (i.e. no publicly available indication of field supply costs) or have not yet been developed. This means the representation of natural gas supply costs is driven by statistically significant coefficients of field-/play-level supply costs, aggregated into a representative cost depletion curves. The supply costs curves based on regional breakdown and resource category are shown in Figure 6.

a)

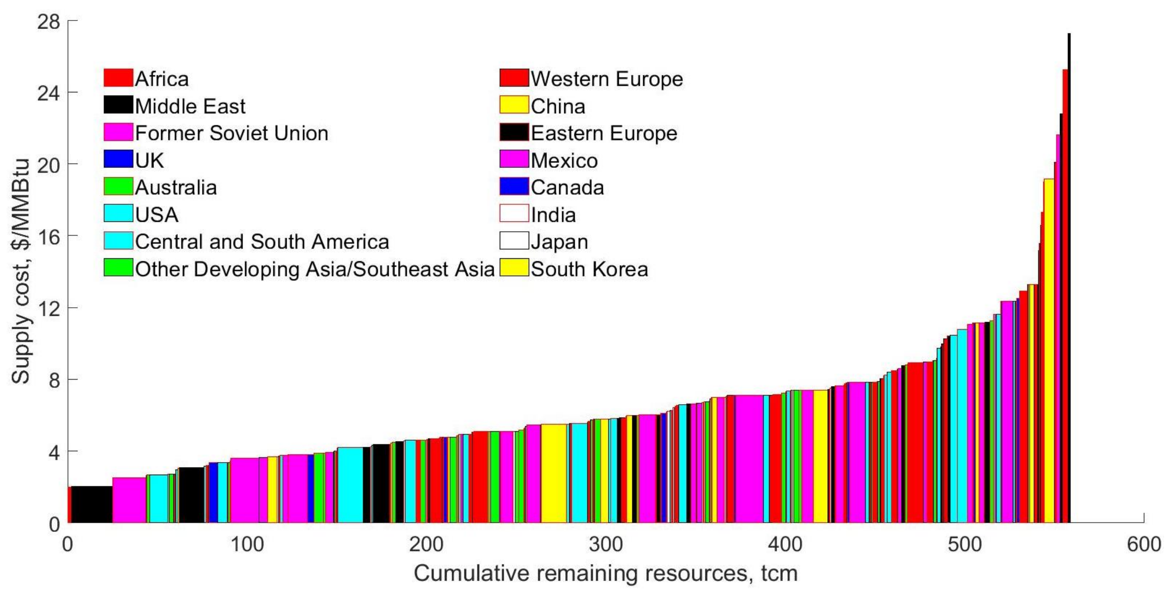

b)

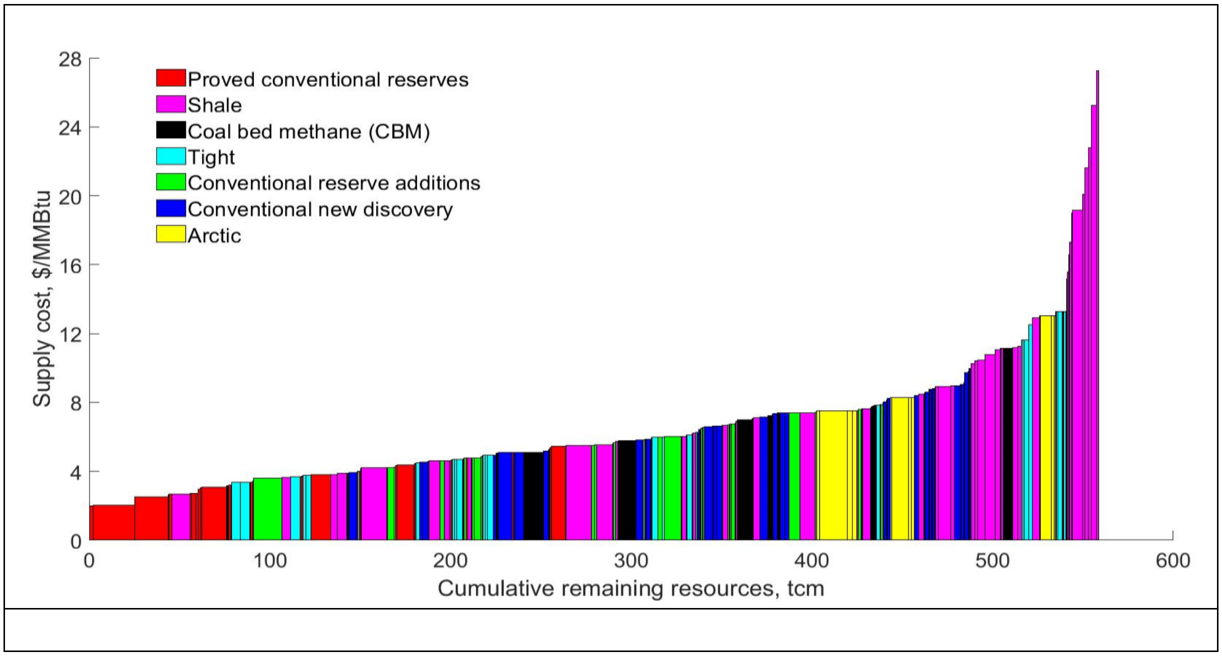

Figure 6. Natural gas global supply cost curve from 2015 by a) TIAM-UCL region and b) resource category.

Once extracted, the model represents processing of natural gas to remove impurities and ensure it is of pipeline / liquefaction quality. Regionalised operation and maintenance costs are associated with this processing step, as well as historical capacities. Additionally, a distinction is made between the processing of non-associated conventional natural gas, and unconventional natural gas. Once processed (taking into account emissions intensities, efficiencies, and any required energy inputs), the resulting energy commodity can either be traded internationally, via pipeline or LNG, or can be used as 'useful' input downstream, such as secondary transformation in the power generation sector, or directly used in the end use sectors.

3.1.3. Oil

The representation of oil in TIAM-UCL is predominantly based on the work by McGlade [31], which focused on quantifying uncertainties in the outlook for oil and natural gas, and in particular in the availability and costs of these energy carriers. As with natural gas, oil is split into different geological categories, each with specific availabilities and supply cost dynamics:

- Conventional oil proved reserves
- Conventional oil reserve additions
- Conventional oil new discoveries
- Arctic oil
- Mined shale oil
- In-situ shale oil
- Light tight oil
- Mined oil sands
- In-situ oil sands (ultra-heavy oil)

The representation of uncertainty in TIAM-UCL for oil availability and costs differs between conventional and unconventional oil. For conventional oil, direct estimates of reserve and/or resource availability were taken from the literature and input into probability distributions, with corresponding assumptions on correlation between the estimates. For unconventional oil (e.g. mined bitumen), two parameters were assigned probability distributions: a range of estimates for original oil in-place (OOIP) and a range of estimates of a recovery factor (i.e. between 0 and 1, which determines the proportion of the in-place resource base which is technically recoverable). These two distributions were then combined using random repeated sampling (Monte Carlo simulations) to form regional estimates [31]. The combination is the product of the OOIP and the recovery factor, repeated a large number of times to generate an aggregated distribution. These estimates of the resource base for each category of oil were then combined with cost depletion curves, mostly formed from IEA data on cost ranges, and used to generate supply cost curves.

As for gas, the supply cost curve is split into three parts for input into TIAM-UCL: the first 50% of the resource base considered the lowest cost, then the next 30%, and finally the most expensive oil representing the last 20% of the resource base. Figure 7 show the global supply cost curve for oil in TIAM-UCL split by region (a) and resource category (b).

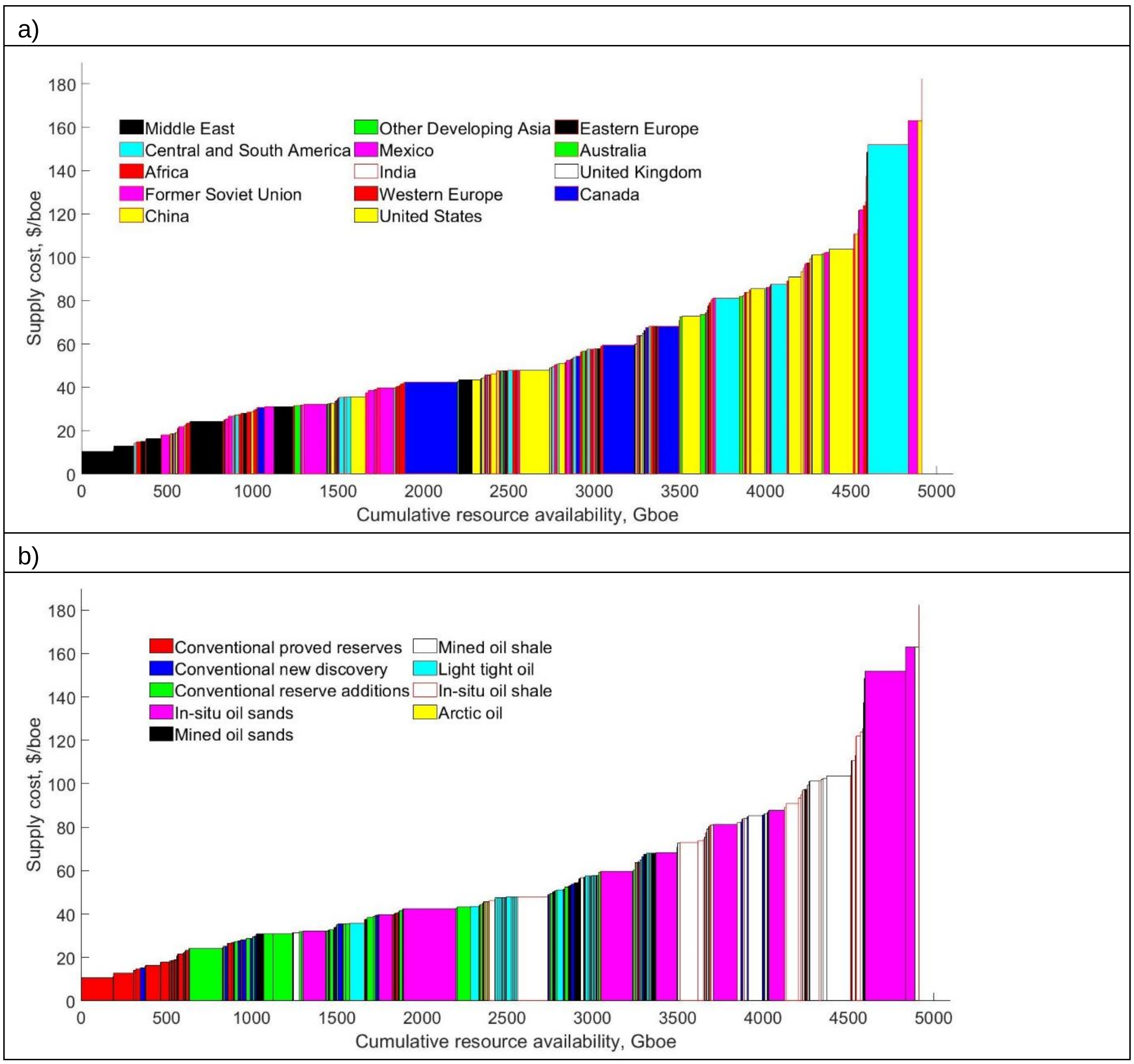

Figure 7. Oil supply cost curve from 2015 by a) TIAM-UCL region and b) resource category.

Oil generally requires the most refining / upgrading / processing in the upstream sector before it can be sent further downstream (e.g. crude oil as a traded commodity, or derived naphtha as a feedstock into petrochemical production of plastics etc.). In particular for some forms of unconventional oil, a huge operation is required to upgrade the oil to 'useful' forms of energy (e.g. crude oil), which requires large scale investment in upgrading infrastructure and intensive energy inputs into the processes. For example, extra-heavy oil and bitumen oil require significant upgrading to reduce the viscosity of the oil from a tar-like liquid (hence the name tar-sands) to a less viscous compound which can be transported by pipeline. A significant part of the improvements made to the upstream sector of TIAM-UCL by McGlade [31] was to provide insights into the costs and availability of unconventional oil production. These costs and material[6] flows through the reference energy system could then be assessed until, for example, mined bitumen is upgraded to synthetic crude oil which can then be transported and/or used as a useful energy carrier. These upstream processes which upgrade and/or process the initial outputs of the mining process require energy inputs, which have a range of efficiencies and costs. Therefore the output commodity 'price' of these processes (useful energy carriers), will have a premium above the cost of the mining process. This was of particular importance for bitumen and extra-heavy oil, where the upgrading process can account for upwards of 50%[7] of the production cost (i.e. generating synthetic crude).

TIAM-UCL has a range of secondary transformation processes which produce refined petroleum products. As with the primary transformation processes, refinery activity in TIAM-UCL requires energy inputs, which have costs associated, as well as the efficiency of the technology.

3.1.4. Fossil trade

All traded commodities in TIAM-UCL must first be processed/transformed into 'transportable' energy carriers, as described in earlier sections. An underlying matrix is then defined by the user, which determines inter-regional trade flows. For flexible forms of transportation (i.e. by maritime transport), the number of trade links will thus be higher than more constrictive forms of trading energy commodities (e.g. by pipeline, which are not just restricted by cost but also by geopolitical and geographical constraints).

It is assumed in TIAM-UCL that only higher grade coal is traded; i.e. sub-bituminous, bituminous and anthracite. All trade flows for coal have been recalibrated in the model to ensure that 2015-2020 flows of coal around the world are consistent with historical data [32–38]. As with natural gas (and oil) discussed subsequently, the trade of coal incurs costs, namely for its transportation via international shipping or across land-borders (i.e. by rail). The transportation costs, as with natural gas and oil, are determined based on average shipping/train capacities and rental rates, and the distance between the regions. However, unlike natural gas which requires processing, transformation and transportation

[6] Including externalities associated with production of oil and gas, such as fugitive emissions, flaring, emissions from the upgrading process, etc.

[7] For example, McGlade (2013, p. 124) identifies the difference in costs (driven by energy requirements to upgrade, and the initial complexity/efficiency of the original mining process) between in-situ and mined bitumen, with mined the upgrading costs of mined bitumen reaching over 50% ($22/bbl) of the total production cost ($40/bbl). It should be noted these figures do not include fiscal regime costs.

infrastructure (e.g. liquefaction plants and pipelines), coal can be more easily transported and therefore no investment costs are required.

Natural gas trade in TIAM-UCL is split between pipeline gas and liquefied natural gas (LNG). Both are constrained firstly by the underlying trade matrix shown above. Additionally, trade volumes and infrastructure have been calibrated to 2015/2020-2025, with **under construction** infrastructure (both pipeline and LNG) fixed to come online in the model by 2020/2025, depending on an estimated start-date [39–47].

Liquefied natural gas trade in TIAM-UCL includes infrastructural parameters (liquefaction and regasification capacities, and build constraints) and cost parameters (CAPEX on new infrastructure, OPEX on the liquefaction/regasification process, and a shipping cost). For pipeline investment costs and capacity additions in the near-term, individual project costs and capacity have been added where appropriate (e.g. pipeline cost and maximum volume from Russia to China between 2015 and 2020 are based on the under-construction Power of Siberia pipeline, which is due to come online in 2020).

The trade of oil commodities is split into various different products, which are outputs of processing/transformation processes in the upstream: crude oil, heavy fuel oil, naphtha, natural gas liquids[8], diesel. As with natural gas trade via LNG tankers, the variable cost of transporting oil via tankers is assumed to be a function of the distance between ports, the speed of the tanker, and the average capacity of a ship travelling from the exporter to the importer.

3.2. Biomass

TIAM-UCL distinguishes between six types of bioenergy feedstock:

- Municipal waste (BIOBMU), represents wastes produced by households, industry, hospitals and the tertiary sector that are collected by local authorities;
- Industrial waste (BIOBIN), comprises solid and liquid products such as tyres, sulphite lyes (black liquor) and animal waste products;
- Landfill gas (BIOLFG), is methane produced and recovered from controlled landfill sites;
- Solid biomass (BIOSLD), comprises woody residues from forestry and agriculture (stems and branches, un-merchantable trees from pruning and thinning operations, residues from sawmill and plywood production, timber and paper scrap, aboveground stalks, husks, shells and cobs);
- Dedicated energy crops (BIOCRP), are grassy and woody crops grown specifically for energy purposes;
- First generation liquid biofuels (BIOLIQ) produced from food crops such as bioethanol from sugarcane and corn are represented as the liquid fuels directly rather than the primary crop resource.

For each of these fractions cost supply curves are specified for each of the 16 regions, i.e. the amount of biomass available at different costs in each region. For specific details on biomass availability and costs, please see Annex 7.

The only bioenergy feedstocks available for international trade are solid biomass and energy crops, while the waste feedstocks are assumed to be used within each region. Only solid biomass and energy crops can

[8] Longer chain hydrocarbons which are separated from the gas stream in processing plants, most of which form liquids at surface temperature and pressure, and includes ethane, propane, butane (Schlumberger, 2019)

be used for BECCS in the model; the waste fractions are used directly in the residential and industrial sectors. The costs of biomass collection and transport within each region are included in the regional costs of biomass production (see Appendix 7). The cost and emissions of international transport of the two traded bioenergy commodities are modelled endogenously in TIAM-UCL as a function of the distance between regions. The cost and associated GHG emissions of the traded commodities are endogenously computed by the model to account for shipping costs and emissions. There is no subsidy nor tax applied to bioenergy feedstocks.

CO_2 emissions associated with land-use change for energy crop cultivation are included in the model, while the other biomass fractions are assumed to produce no land-use change. Emissions coefficients are applied for CO_2, CH_4 and N_2O depending on how the biomass is used. It is estimated that approximately 5% of the biomass carbon content is lost during storage, drying and transport. Net CO_2 emissions associated with other land-use and land-use change are represented by an emissions pathway, which is an input to the TIAM model (Pye et al. 2019). In addition, the energy crops produced in our scenarios cause emissions which vary from15–25 $kgCO_2/GJ$ between regions. These represent the impact of bringing degraded land into cultivation in terms of land-use (LU) and land-use change (LUC). The first is linked to planting, growing and harvesting the biomass; the second, to switching land from its current use to the production of energy crops [48]. The resulting emission factors are attached to the technologies which produce the energy crops: each unit of crops produced is linked to a corresponding level of CO_2 emission. We do not consider indirect LUC potentially caused by energy crops expansion and LUC emissions for other biomass fractions (Butnar et al., 2020).

3.3. Other renewables

TIAM-UCL models the following renewable energy sources:

- Centralised and decentralized onshore wind.
- Offshore wind.
- Centralised and decentralized solar photovoltaics (PV)
- Concentrated solar power (CSP)
- Hydropower – both run-of-river and reservoir
- Tidal power
- Geothermal at various depths

Resource potentials for each technology are expressed as technical capacity deployment potentials for each region in the model. For onshore and offshore wind these are taken from [49]. For countries covered by that study we use the fraction of total land area available for deployment and convert that to a capacity potential assuming 3 MW/km2 for onshore and 5MW/km2 for offshore (see [50] for more details). For countries not covered we take the global average fraction of total land area available across the countries and apply that to each region using land area data from the World Bank.

In the case of solar PV, we use land area data for each region and assume a maximum of 6% can be used for deployment based on [51]. We convert this to a technical capacity potential assuming 40 MW/km2 [50]. The potentials of other renewables are taken from the ETSAP version of TIAM.

4. Energy supply sectors

A key part of the energy system is the conversion of primary energy into secondary energy carriers via specific energy conversion technologies. In this section, we cover electricity, hydrogen and biofuel production. The technologies used to represent these conversion processes include a range of parameters including -

- Capital expenditure, specified on an 'overnight' basis. Except for the ETL version of the model, all cost improvements are exogenously defined.
- Costs of capital are also included, based on the economic lifetime of the investment
- Fixed yearly operating and maintenance costs, typically expressed as a percentage of investment.
- Variable operating costs (excluding fuel costs).
- Conversion efficiencies
- Technical lifetime of the technology asset
- Capacity factor concerning the annual utilisation of the capacity in place

Importantly, TIAM-UCL tracks the stock of technologies over time, meaning that investments are made on the basis that the technology will be in use for its lifetime. However, early retirement of technologies is possible.

4.1. Power generation

The electricity and heat generation sector represents the main technology groups across the range of fossil-based and renewables sources. The existing system is represented in generic terms whilst the options for future investments are characterised in more detail. Electricity and heat supply is temporally disaggregated across six periods (or *time slices*), based on three season and two diurnal periods (Day / night) to represent changes in load based on sector demand profiles.

This sector is divided in the following technology types -

- Electricity generation plant, providing electricity to the grid
- Public CHP plant, providing electricity to the grid and heat to local networks
- Public heat generation plant (heat only plants), providing heat to local networks

Electricity generation plant are additionally categorised as providing electricity to the centralised or decentralised grid. Decentralised producers tend to be small scale, connected to the distribution network or serving local grids, while centralised producers are connected to the transmission network.

Key technologies represented in this sector are shown in

Table 5 below. Cost and efficiency assumptions for these technologies can be found in Appendix 4.

Table 5. List of power generation technologies

Resource group	Technology
Bioenergy	MSW combustion Bioenergy combustion Bioenergy combustion (decentralised) Bioenergy gasification Bioenergy gasification (decentralised)
Fossil fuels (unabated)	Coal IGCC Coal super critical Coal ultra super critical Gas CCGT Oil generation (dcn) Oil generation
Fossil fuels (CCS)	Coal IGCC w/CCS Coal USC w/CCS Gas CCGT w/CCS
Non-bioenergy renewables	Geothermal shallow Geothermal deep Geothermal very deep Hydro dam Solar CSP Solar PV Tidal Offshore wind Onshore wind
Nuclear	Nuclear Advanced LWR
Storage	Storage

Figure 8 illustrates how some of the key low carbon technologies deploy under different climate targets, relative to the range of IAM scenarios for 1.5°C.

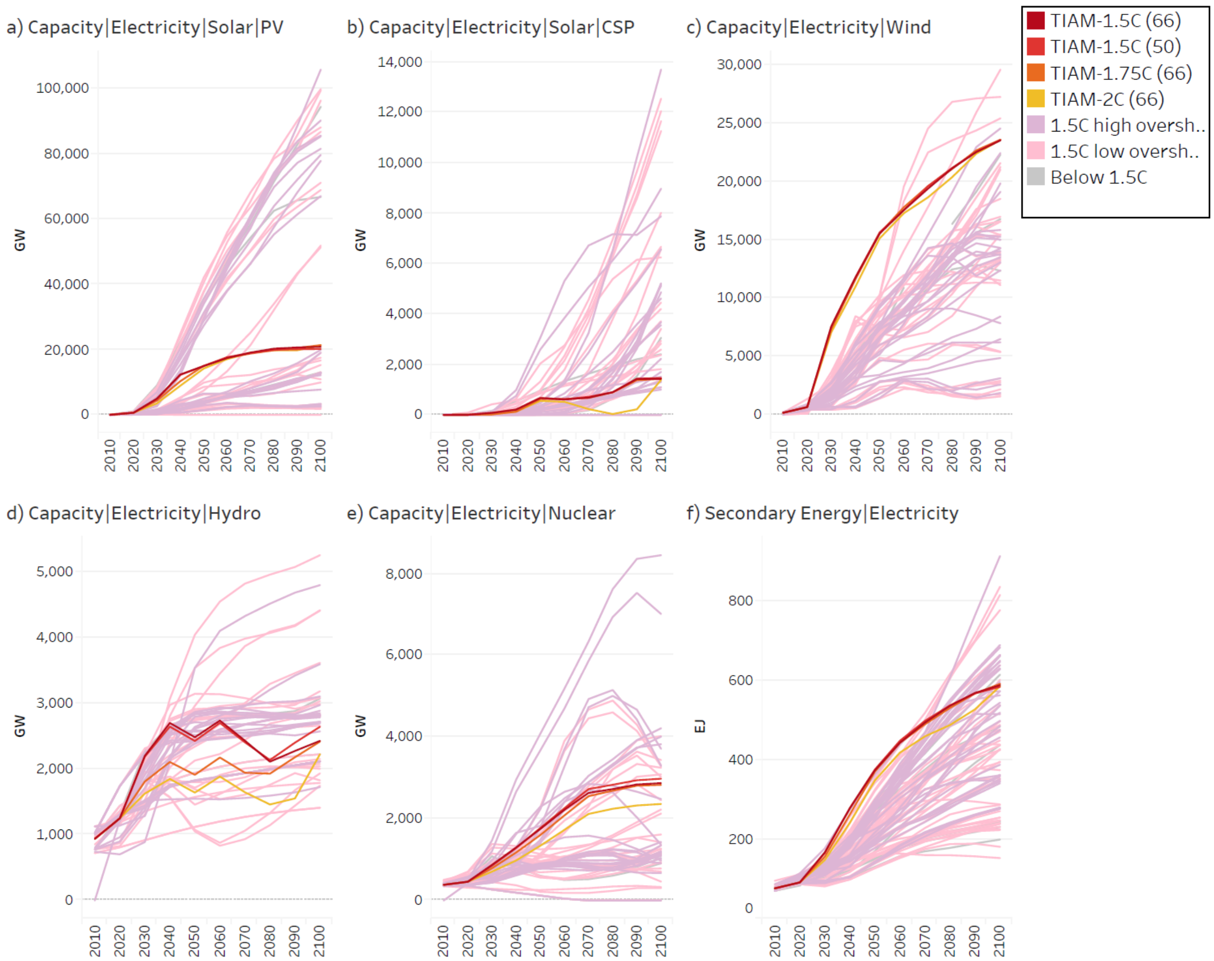

Figure 8. Power generation for selected technologies for a selection of TIAM-UCL runs [4]**, compared to scenarios in the IAMC 1.5°C database** [52]

4.2. Other conversion sectors

4.2.1. Hydrogen

Hydrogen infrastructure is well represented in TIAM-UCL from production to transportation to distribution to end-use devices. On the supply side, hydrogen production technologies are divided into three different scales: centralised large-scale production (Figure 9), centralised medium scale production (Figure 10) and decentralised small-scale production (Figure 11). Large-scale plants are based on biomass, coal and gas with continuous production of hydrogen. These plants are available with and without CCS technology. Hydrogen produced from centralised plants are transported with two different transportation options: long-distance pipe line transportation (gaseous hydrogen) and liquefaction plus trucks (liquid hydrogen). Liquefaction plants can be built at the production site or away from the site (close to demand) as shown in Figure 10. Hydrogen liquid is distributed to transport sector from both liquefaction plants with different transportation costs (for truck1 and truck 2). Hydrogen produced from these large centralised plants is also available for upstream sector for liquid fuel production such coal/gas to liquid (synthetic fuel) and biomass to liquid.

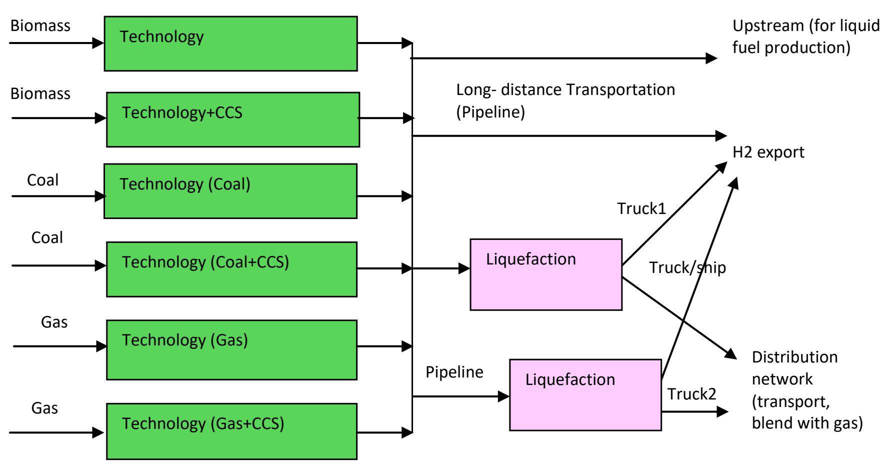

Figure 9. Centralised (large) H_2 production

Centralised plants in medium scale, based on biomass and gas, are available with or without CCS. Technologies that produces hydrogen from electricity are also included in the medium size plants. These are centralised plants (medium size) and assumed to be built closer to demands leading to short distance transportation requirements. Separate sector fuel technologies are modelled to generate input fuels such as HELC (electricity for hydrogen), HNGA (natural gas for hydrogen) and HBIO (biomass for hydrogen) in order to include distribution cost for the input fuels. Hydrogen produced can be transported through pipelines (gaseous hydrogen) or by truck as liquid hydrogen assuming liquefaction plants are built at the production site. Hydrogen is blended with gas and supplied to end-use sectors such as residential, commercial and industry sectors. Hydrogen (gas and liquid) is available to transport and industry sectors. Different technologies will be modelled for hydrogen production, storage and electricity production (from hydrogen).

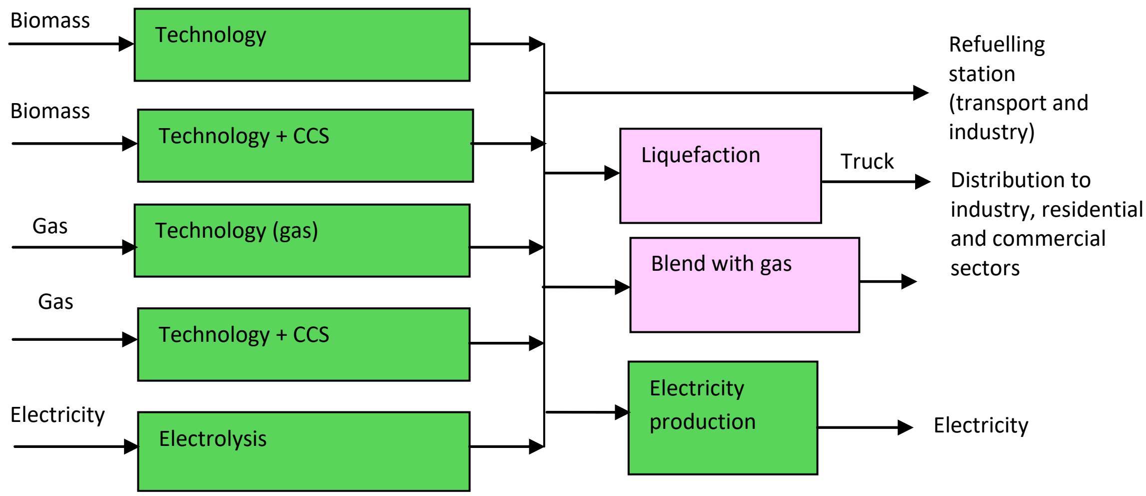

Figure 10. Centralised (mid-size) H_2 production

Decentralised small-scale plants are based on electricity, gas and biomass. There are different options for electricity supply for electrolysis. Hydrogen from electrolysis can be produced using centralised electricity from main grid (HELC) and decentralised electricity (ELCD) generated by decentralised wind and solar plants (Figure 12). Investment cost of decentralised technologies includes station (refuelling) cost. Hydrogen produced can be supplied to transport sector and other end-use sectors by directly and blending it with natural gas. It is also assumed that these small-scale plants can be built at the refuelling stations. Figure 12 presents the overall representation of hydrogen infrastructure in TIAM-UCL after improvement under UKSHEC project.[9]

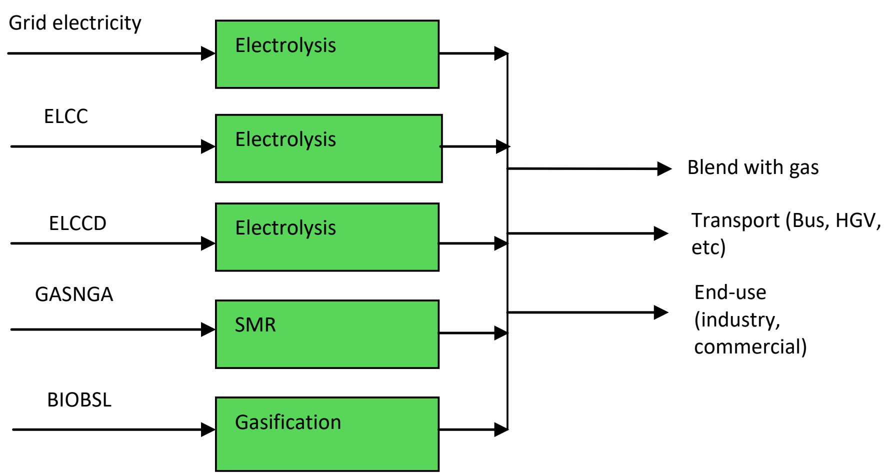

Figure 11. Decentralised (small) H_2 production

Hydrogen technology data are under three different categories: production, transportation, liquefaction, distribution, refuelling stations and end-use sector (only vehicle technologies). This section provides only supply-side data including transportation and distribution network. Hydrogen production data is resented in Table 1 in Appendix 5. These data are based on the review by Dodds and McDowall (A review

[9] https://www.ucl.ac.uk/bartlett/energy/research-projects/2019/feb/hydrogen-energy-research-programme

of hydrogen delivery technologies for energy system models) (2012). Detailed descriptions of data sources and assumptions are available in the report. Hydrogen transportation, liquefaction, distribution and refuelling station data are presented in Table 2 in Appendix 5. Average distance for the long-distance pipe line (and tanker for liquid hydrogen) is 800 km and for distribution network is 100 km for tanker as well as distribution pipelines.

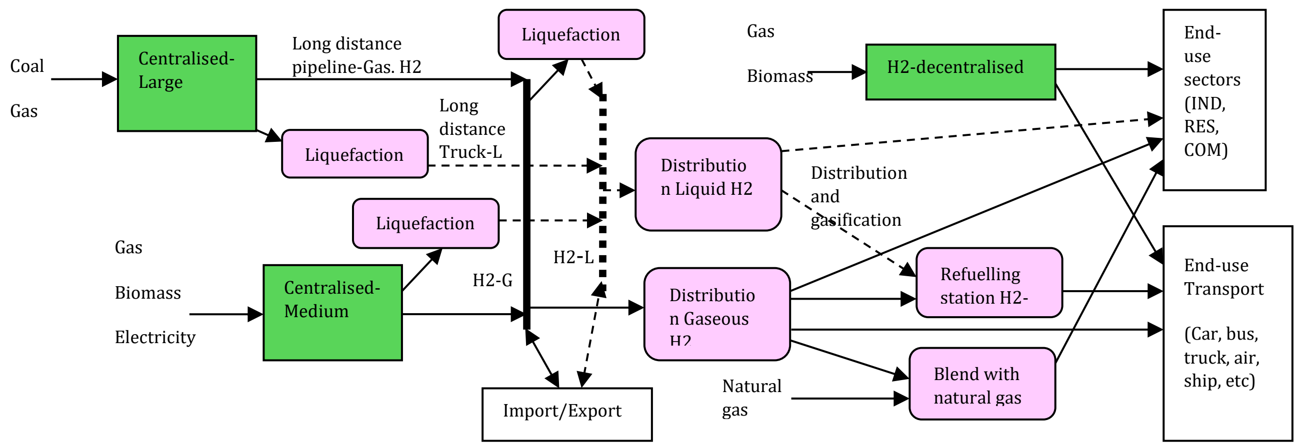

Figure 12. Hydrogen infrastructure in TIAM-UCL

4.2.2. Biotechnologies

A range of commodities can be produced from biomass in TIAM-UCL: (i) electricity generated by combustion or gasification of biomass with and without (w and w/o) CCS; (ii) heat from biomass in combined heat and power w/o CCS and in large-scale plants w CCS; (iii) hydrogen from small-, medium- and large-scale biomass plants; and (iv) transport fuels produced through Fischer Tropsch (FT) processes available w and w/o CCS. Bioenergy technologies w/o CCS can use any biomass fraction, but BECCS relies only on energy crops and solid biomass. A schematic representation of bioenergy pathways in TIAM-UCL is given in Figure 13 (Butnar et al., 2020). The techno-economic assumptions used to describe these technologies are listed in 4.2.2.

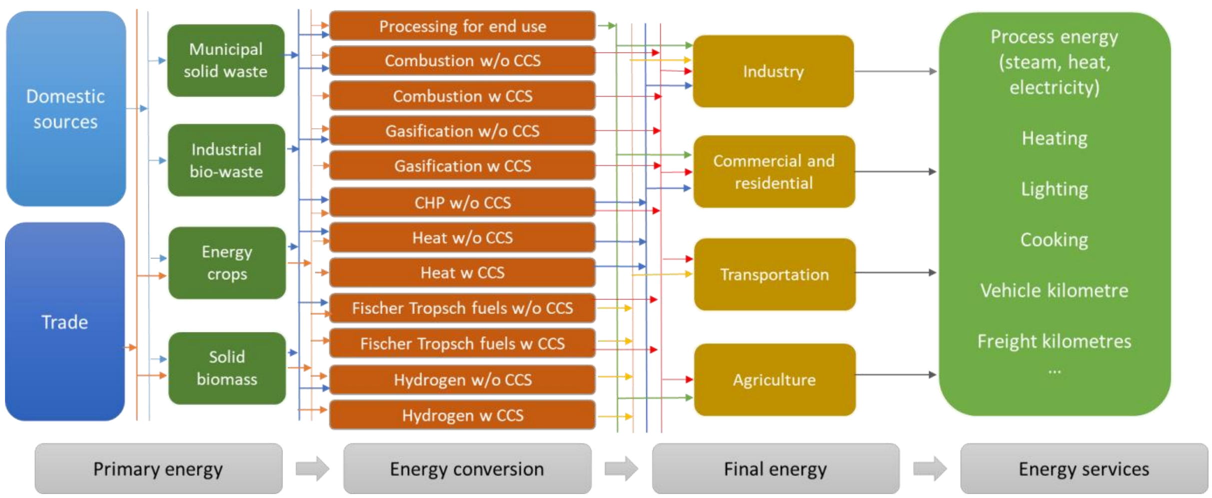

Figure 13. Bioenergy supply chains in TIAM-UCL starting with the supply of biomass resources (left of the figure), either by domestic production (blue arrows) or international trade (orange arrows, only available for solid biomass and energy crops). While tradable biomass can be used as input into all bio-technologies w and w/o CCS (orange arrows), the waste fractions can be used only for producing bioenergy w/o CCS (dark blue arrows). The resulting bioenergy flows are coloured by type of energy: green arrows for biomass pellets which can be used in several end use sectors, red arrows for bio-electricity, blue arrows for heat for industry and buildings, and yellow arrows for transport bio-fuels and bio-hydrogen used in the transport and industry sectors. The green box on the right of the diagram shows final energy services, defined exogenously.

5. CCS and other NETs

The current set-up of the model for CCS reflects revisions undertaken as part of a recent UCL research work in collaboration with the Global CCS Institute [53]. CCS applications are available in the following sectors: electricity and heat, hydrogen, synthetic fuel (via Fischer Tropsch processes), and in the industry. The latter includes CCS for combustion emissions from process heat production in iron and steel, non-metallic minerals and other industry sub-sectors. There is also a CCS technology that captures CO_2 process emissions from the use of petrochemical feedstocks.

Cost and performance information can be found in [53]. CCS can grow at between 2-5% for annum (industry, power at the upper end), starting from 2030 and reaching 15-24 GtCO2 by 2100. CO_2 captures rates of 90% are assumed for all fossil CCS technologies.

BECCS

CCS is available for various bioenergy process in TIAM, see Figure 14, including power generation by combustion or gasification of energy crops or of solid biomass (agricultural and forestall residues), heat by combustion of solid biomass, and hydrogen production from a mix of solid biomass and energy crops. CCS is also available on the production of advanced transport fuels produced through Fischer Tropsch (FT) processes either from energy crops or biomass. The techno-economic assumptions of these technologies are given in Table A. 20 in Appendix 6.

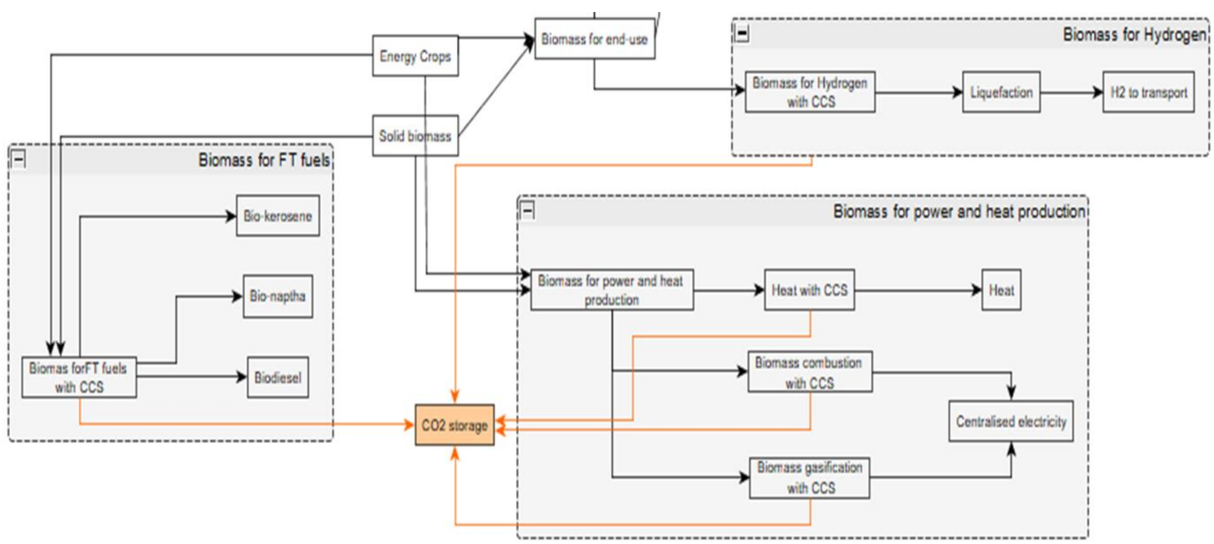

Figure 14. Schematic view of BECCS in TIAM-UCL v 4.1.1

DACS

The current DACS representation in TIAM-UCL is based on the two-loop hydroxide-carbonate system, parametrised based on Socolow et al. [54], Chen and Tavoni [55], and other literature references, see Table A. 23 in Appendix 8.

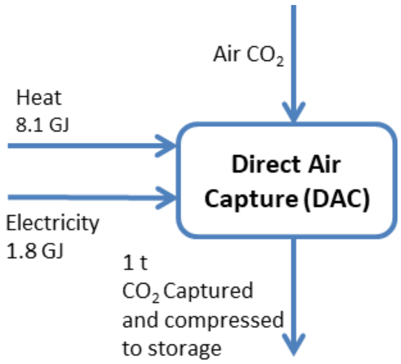
Air CO_2
Heat
8.1 GJ
Direct Air
Capture (DAC)
Electricity
1.8 GJ
1 t
CO_2 Captured
and compressed
to storage

6. End use sectors

6.1. Industry

The industrial sector is currently modelled in TIAM-UCL in a stylized manner. It includes eight sub-sectors, represented in Table 6 together with the technologies they include. These technologies represent all the energy inputs to different sub-sectors and processes, but they are not producing specific industrial goods to be used elsewhere in the energy system. In the same way, material recycling within each industrial sub-sector is not modelled in the current version.

Each set of technologies has an existing and a new technology version. The existing technologies are modelled only as consumption of energy to provide specific sub-sector energy demand. No investment can be made into the existing technologies, which are replaced at the end of their lives by new technologies, which are modelled including investment and operational costs, life time, capacity factor, efficiency (which improves over time), and process emissions. In the current version, TIAM-UCL v 4.1.1., these process emissions are not attributable to an industrial product, nor to an industrial sub-sector, but are reported as generic industry emissions.

Table 6. Main industry model characteristics

Industrial subsector breakdown	Technologies included	Industrial goods	Efficiency improvements	Process emissions
Pulp and paper	Heat auto-production (various fuels) Steam auto-production (various fuels) Machine drive (various fuels) Electro-chemical processes	No	Exogenous	Yes[a]
Chemicals[b]	Technologies to convert various fuels to non-energy petrochemical feedstock[c] Technologies to convert various fuels to other chemicals Heat auto-production (various fuels) Steam auto-production (various fuels) Machine drive (various fuels) Electro-chemical processes	No	Exogenous	Yes[a]
Iron and steel	Technologies consuming coke and petroleum coke for iron and steel production Heat auto-production (various fuels)[c] Steam auto-production (various fuels) Machine drive (various fuels) Electro-chemical processes	No	Exogenous	Yes[a]
Non-metallic minerals	Technologies consuming various fuels for non-metals production Heat auto-production (various fuels)[c]	No	Exogenous	Yes[a]

	Steam auto-production (various fuels) Machine drive (various fuels) Electro-chemical processes			
Non-ferrous minerals	Technologies consuming various fuels for non-metals production Heat auto-production (various fuels) Steam auto-production (various fuels) Machine drive (various fuels) Electro-chemical processes	No	Exogenous	Yes[a]
Other industries	Technologies consuming various fuels for other industrial production Heat auto-production (various fuels)[c] Steam auto-production (various fuels) Machine drive (various fuels) Electro-chemical processes	No	Exogenous	Yes[a]
Industry and other non-energy consumption	Technologies consuming various fuels for industrial and non-energy production	No	Exogenous	Yes[a]
Other non-specified consumption	Technologies consuming various fuels for other non-specified production	No	Exogenous	Yes[a]

[a] All process emissions are recorded as generic industry emissions, i.e. not specific to each sub-sector.

[b] Note that transport fuels (including biofuels and synthetic fuels) are modelled in the upstream sector, while lubricants used for transport are modelled within the transport sector.

[c] Technologies also available fitted with Carbon Capture and Storage (CCS), but only fueled by coal or gas, i.e. BECCS is not available in the industry sector.

The energy demand of each industrial sub-sector is met through a competition between all the available technologies for that sector, except for the “Industry and other non-energy consumption” and “Other non-specified consumption” for which fixed shared of fuels in the fuel mix are exogenously specified for different periods to 2100, i.e. 2010, 2020, 2030, 2050 and 2100.

The industrial energy and material demands are projected to 2100 using general **economic and demographic drivers**, such as population, GDP, GDP per capita, and sectoral output. Please see Section 2.1 for related assumptions on these drivers. The assumed global demand growth of each industrial subsector relative to 2005 is represented in Figure 15.

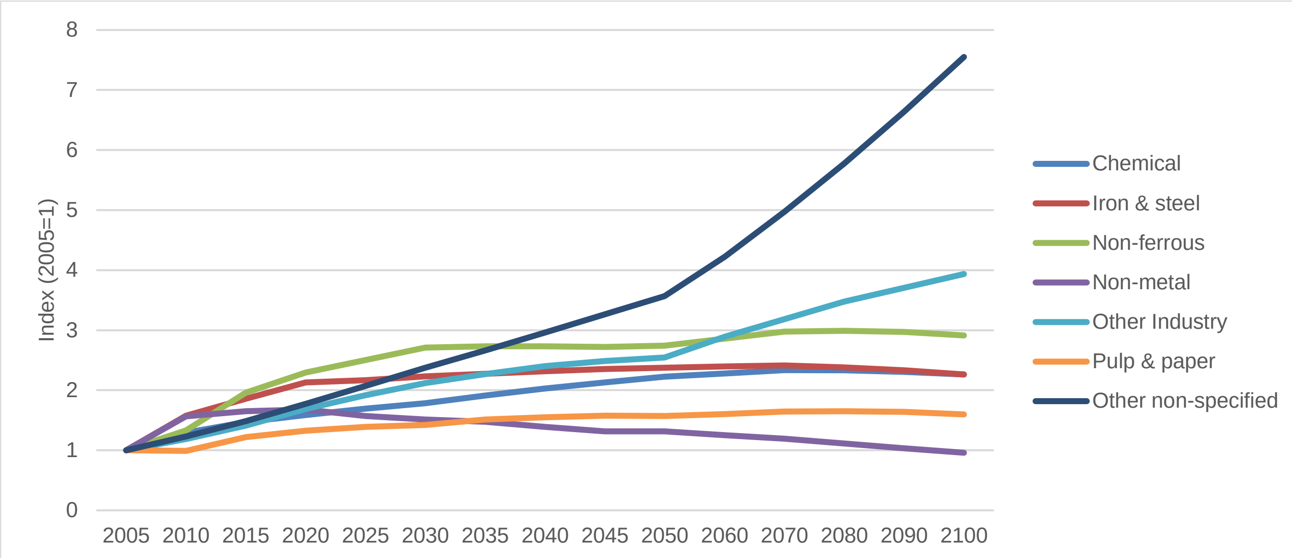

Figure 15. Projected industrial energy demand by sector in the Baseline

The **policy measures** which can be applied to the industrial sector include carbon tax/cap, permit trading, technology subsidy, efficiency requirements. The policy impact is reflected through price mechanisms and model constraints.

The **industrial fuel mix** in the Baseline is mainly composed of fossil fuels, see Figure 16. Coal and gas supply more than half of the final energy demand in the industry, while biomass and electricity cover less than a quarter. The composition of the mix changes considerably under a 2DS mitigation scenario run, showing a strong move away from fossil fuel, especially from coal and oil, and an increased electrification of the industry. The share of biomass in the final energy demand for the industry stays the same. The share of renewables remains insignificant event under a mitigation scenario, showing the reduced mitigation options available for the industry in the current model version, 4.1.1.

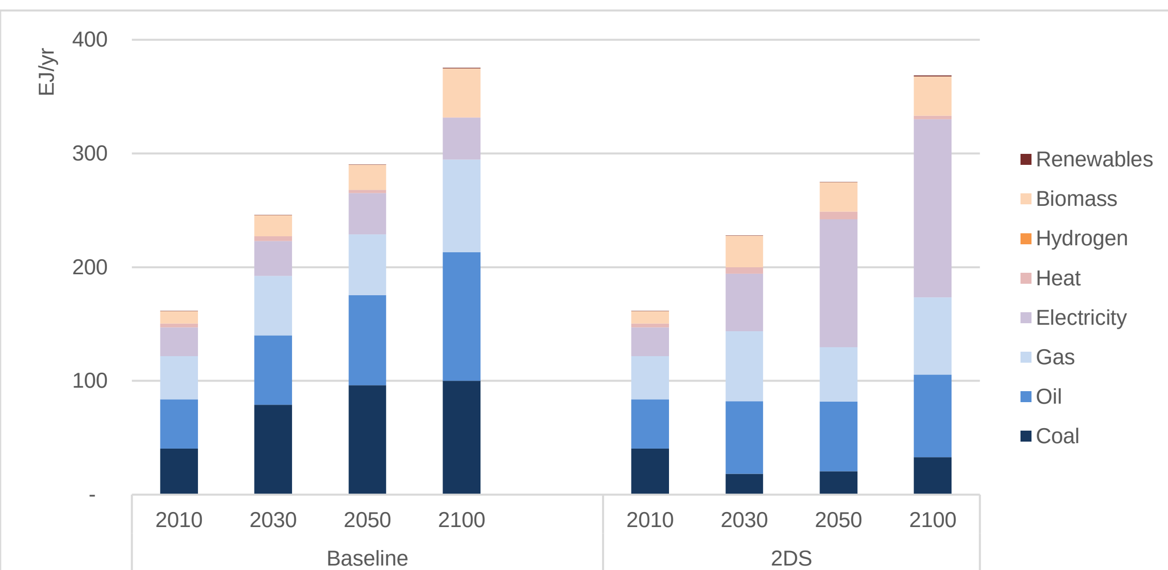

Figure 16. Final Energy demand of the industry per fuel type in different periods in the Baseline vs a 2DS mitigation scenario.

Industrial CCS is available only fitted to heat auto-generation plants which use coal or gas as a feedstock. This option is available only in the chemical industry, when producing heat for non-energy petrochemical feedstock, in the iron and steel industry, non-metallic industry, and other industry. Note that although biomass can be used in the industry, in the current model version, 4.1.1, they cannot be fitted with CCS. The reason behind this is partially the fact that the industry can use a variety of biomass feedstocks, including waste streams, which in TIAM-UCL cannot be used for BECCS.

6.2. Buildings

The buildings end-use sector in TIAM-UCL is driven by both residential and commercial energy service demands. Table 7 shows each residential energy service demand, the activity unit, and the corresponding socioeconomic driver (as discussed in Section 2, each service demand is assigned a driver of growth, as well as decoupling and/or sensitivity factors which inflate/deflate the growth of the demand above/below the driver alone).

Table 7. Residential energy service demands

Energy service demand (Code[10])	Activity unit	Socioeconomic driver
Cooking (RK*)	PJ	Population
Space heating (RH*)	PJ	Households (number)^{OECD}, GDP/household$^{Non\text{-}OECD}$
Space cooling (RC*)	PJ	Households (number)^{OECD}, GDP/household$^{Non\text{-}OECD}$
Lighting (RL*)	PJ	GDP/capita^{OECD}, GDP/household$^{Non\text{-}OECD}$
Refrigeration (RRF)	PJ	Households (number)^{OECD}, GDP/household$^{Non\text{-}OECD}$
Hot water (RHW)	PJ	Population
Clothes drying (RCD)	PJ	Households (number)^{OECD}, GDP/household$^{Non\text{-}OECD}$
Clothes washing (RCW)	PJ	Households (number)^{OECD}, GDP/household$^{Non\text{-}OECD}$
Dishwashing (RDW)	PJ	Households (number)^{OECD}, GDP/household$^{Non\text{-}OECD}$
Other electric (REA)	PJ	GDP/capita^{OECD}, GDP/household$^{Non\text{-}OECD}$
Other (ROT)	PJ	GDP/capita^{OECD}, GDP/household$^{Non\text{-}OECD}$

* = energy service demand is disaggregated into rural and urban

[10] As represented in Table 2

For reference, the commercial sector has similar energy service demands (lighting, heating, cooling), however the socioeconomic driver for each energy service in the commercial sector is a composite of GDP growth between *t-1* and *t*, multiplied by GDP in *t-1*, and raised to an exponent depending on whether GDP/capita is above or below a certain threshold (i.e. a proxy for whether the economy has transitioned to a 'service' economy)[11]. Therefore, as the modelling horizon expands out to 2100, there is an assumption that each economy will transition to more service-intensive economic activity. However, and as mentioned in the discussion on the shared socioeconomic pathways, the period in which an economy becomes more service-intensive differs between each pathway (for example in SSP1, Africa changes to a growth exponent (1.25) in 2055, whereas in an SSP2 pathway, this transition does not take place until 2065).

The residential and commercial sectors have a range of technologies, with different energy commodity inputs, varying cost, efficiencies, and in some cases technology vintages (i.e. modelling efficiency/cost gains as experience is accumulated etc. through new releases of the same technology). The energy commodities used in the buildings sector either come from the energy supply sector (e.g. electricity, hydrogen from steam reformation/electrolysis, natural gas which has been processed and transported to local distribution networks) or directly from primary energy resources (e.g. biomass). The buildings sector is different to others in terms of its geographic disaggregation in TIAM-UCL as the energy services required are split into rural and urban demand, allowing for user constraints based on a range of specific rural-urban characteristics. For example, the spatial aggregation of TIAM-UCL does not allow for a particularly robust representation of the investment costs of implementing a widespread distribution network for natural gas to satisfy urban and rural residential and commercial service demand. Therefore, for regions with a large, and relatively cheap, natural gas resource base, large volumes of gas could find its way into the residential sector whereas in reality the costs required to construct such a distribution network is prohibitive; the main example in the model is Africa. Therefore user constraints have been added constraining the penetration of natural gas as an energy vector for some energy services (e.g. rural and urban cooking etc.) in Africa, Other Developing Asia, India, and China. The functional form of these constraints is shown below, taken from Welsby [24].

$$ESD_{r,t} = \sum_{i=1}^{n} X_i = \alpha \sum_{i=1}^{1} X_i + \beta \sum_{i=2}^{n} X_i \tag{8.2}$$

Where,

$ESD_{r,t}$ = rural residential energy service demand in region *r*, in time period *t*

X_i = all energy commodity input vectors which can meet ESD_r, *for i=1:n*

for α + β = 1,

α = maximum share coefficient for energy commodity input X_1 (i.e. natural gas)

β = minimum share coefficient for vector of energy commodity inputs X_2:X_n

[11] The exponent is assumed to be 1.25 for a service economy, and 0.9 for a developing economy.

These constraints were used widely for residential service demands in Africa and India, to ensure that energy commodity vectors into the demand technologies were consistent with IEA data in the near-term. For reference, residential gas consumption in Africa is ~ 415 PJ in 2017[12], with the recalibrated TIAM-UCL consumption figure around 10% higher at 460 PJ.

As with the other end-use sectors, a fleet of additional technologies are available for the model to invest in (beyond the base year) to satisfy the energy service demands for buildings in each country, including lower carbon alternatives for sectoral decarbonisation (e.g. heat pumps for residential and commercial heating, which require electricity as an input). These new technologies correspond to a specific commodity input (e.g. a residential cooking technology using liquefied petroleum gas), and have varying efficiencies, costs, and hurdle rates applied. An additional assumption is that the existing technologies from the base year are replaced, with traditional biomass as an input energy vector phased out of the energy system, and replaced with a range of other technologies (including other more efficient and cleaner-burning biomass technologies).

6.3. Transport

The transport sector in TIAM-UCL is fully based on a cost-optimisation paradigm; it does not capture the preferences of consumers, vehicle purchase decisions are made based on capital, maintenance and fuel costs alone. Although non-financial attributes are not considered (such as range anxiety or refueling availability for electric vehicles), the model can provide useful insights into the evolution of the transport sector and its implications on the whole energy system.

The transport sector is characterized by 14 energy-services plus one non-energy use demand segment. The road transport sector considers two and three wheels vehicles, cars, light duty vehicles, commercial, medium and heavy trucks and buses. Additionally, the model considers rail transport of passengers and freight, domestic and international navigation as well as domestic and international aviation. The projected demand for each one of these energy services is assumed to evolve as a function of GDP, population, or GDPP as indicated in Table 8. The shift between transport modes (e.g. from cars to buses or trains) is not possible in the standard TIAM-UCL version; each service demand is an exogenous model input.

Table 8. Residential energy service demands

Domestic aviation	PJ	GDP
International aviation	PJ	GDP
Road buses	Bvkm	POP
Road commercial trucks	Bvkm	GDP
Road three wheels	Bvkm	POP
Road heavy trucks	Bvkm	GDP
Road light vehicles	Bvkm	GDP

[12] IEA Energy Balances, 2019

Road medium trucks	Bvkm	GDP
Road cars	Bvkm	GDPP
Road two wheels	Bvkm	POP
Rail-freight	PJ	GDP
Rail-passengers	PJ	POP
Domestic internal navigation	PJ	GDP
International navigation	PJ	GDP

There is a range of fuels represented in TIAM-UCL to supply existing and new transport technologies, for all transport service demands: coal, natural gas, LPG, gasoline, diesel, kerosene, heavy fuel oil, electricity, bio-ethanol, hydrogen and methanol. These fuels have a supply chain and system architecture associated, from the upstream sector through to end-use services, as shown in Figure X.

Figure 17. Simplified structure of the transport sector in TIAM-UCL

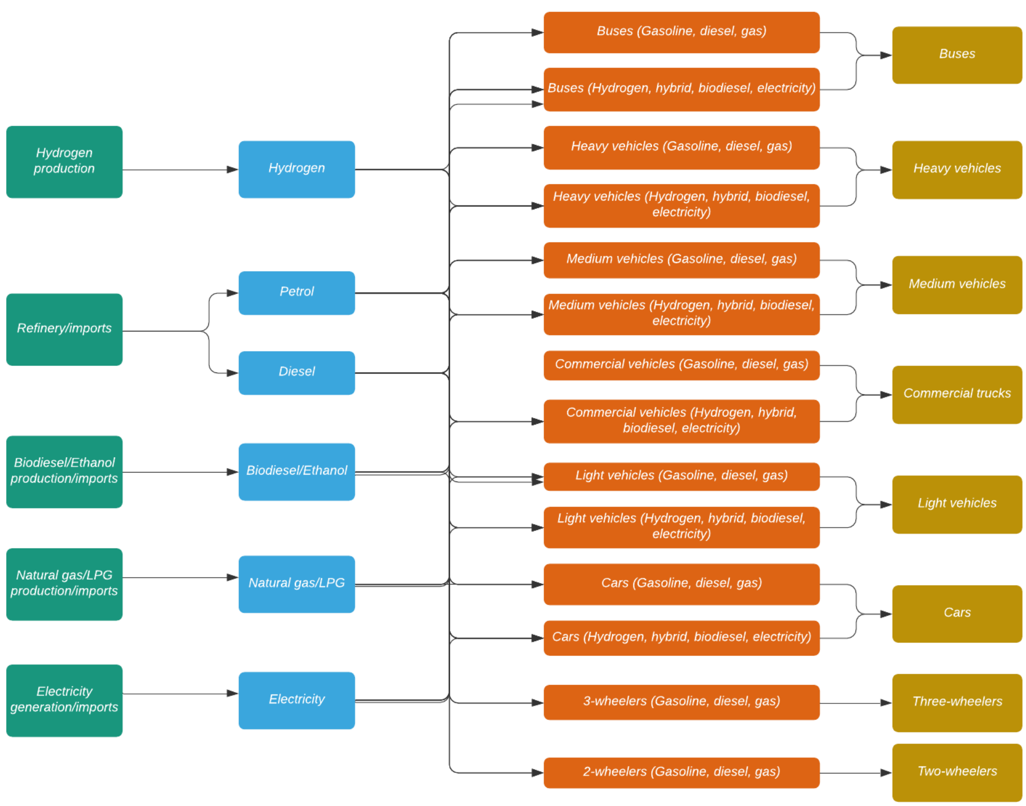

6.4. Agriculture

Agriculture sector is modelled with single energy-service and the energy-service demand can be met by different fuels, mix of which is fixed. There is no technology choice and fuel choice allowed in agriculture sector and no new technology sheets available. Agriculture sector is simplistically modelled in TIAM-UCL, in part because it accounts for a very small fraction of total final energy. Note that the agricultural sector only covers energy use in the agricultural sector.

7. Climate module

A climate module is also integrated into the model framework, calibrated to the MAGICC simple climate model used by the IPCC [2], allowing for a simplified representation of the climate system. It ensures that any future energy system is consistent with a given temperature objective, such as limiting warming to 1.5°C or 2°C by 2100 and beyond. To this end, the climate module takes into consideration the different stages needed to calculate global surface temperature change from greenhouse gas emissions, as described in Figure 18:

1) from emissions to atmospheric concentrations

2) from concentrations to radiative forcing

3) from radiative forcing to realised temperature

Note that the climate module calculates only a single "global" value for temperature change with no regional differentiation. The underlying mathematical structure of the module is based on a linear recursive approach from Nordhaus and Boyer [40]. This is a well-documented, albeit simple approach, which gives a good approximation of more complex climate models [38]. The mathematical equations with their parameters are presented in an annex of this report.

The climate module interacts with the main TIAM model only in "constraining" the emissions of GHGs (and the technology chosen within the energy system). In its present form, the module doesn't interact with demand (heating or cooling for example), supply (hydro, wind for example) or most globally the energy system infrastructure (extreme events).

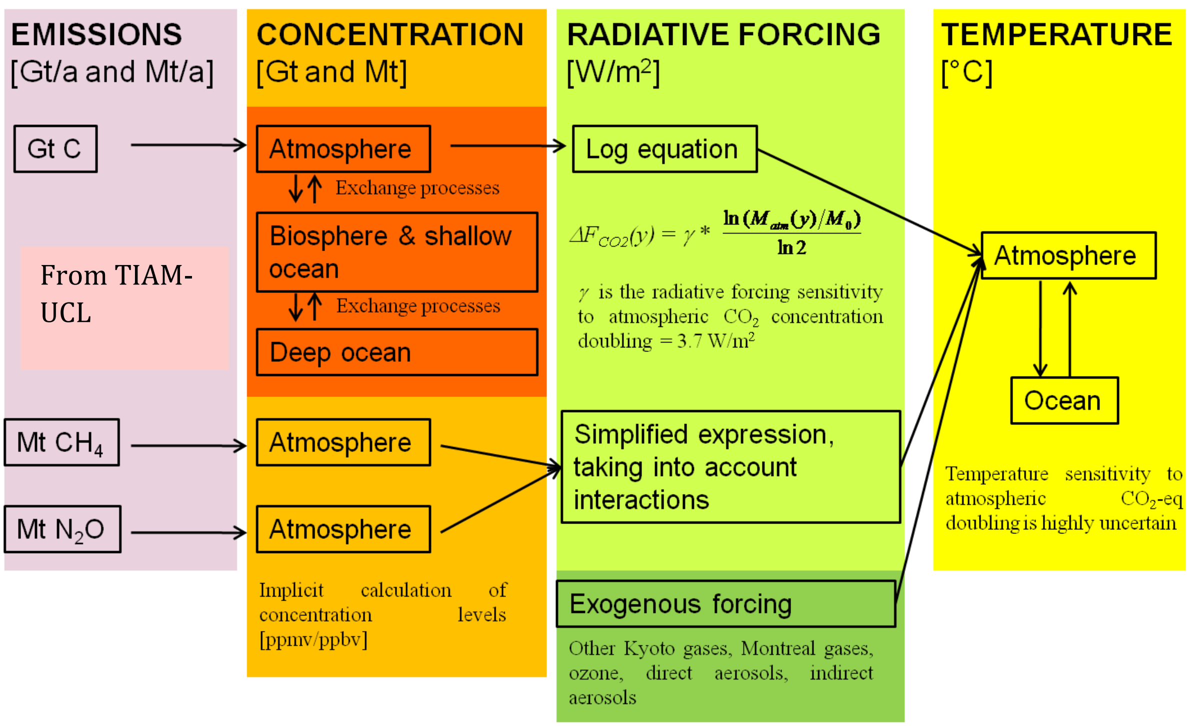

Figure 18. Overview of the TIAM climate module representation.

The climate module uses GHG emissions both from the energy system (endogenous) and other GHG emissions from sectors, such as agriculture or land use change, not explicitly represented (exogenous). Successively, it calculates changes in the concentration of CO_2, CH_4 and N_2O, the change in radiative forcing over pre-industrial times from all three gases adding an exogenously defined additional forcing (for the other GHGs and radiatively active parameters such as aerosols and clouds not represented) and finally the global temperature change over pre-industrial times for the atmosphere.

Note that the radiative forcing from CO_2 in the "climate system" is non linearly responding to the atmospheric concentration of CO_2. In consequence, there is an approximation to "linearise" the radiative response of CO_2 in the TIAM climate module; the modeller has to use the right calibrated parameters for the temperature achieved. The different calibration can be found in scenario files.

The model handles emissions of 3 specific gases: CO_2, CH_4 and N_2O until the calculation of the radiative forcing. For CO_2, CH_4 and N_2O emission levels, non-energy sector related emissions (outside of the energy system) are fixed based on exogenous trajectories (usually RCPs). The sum of the exogenous and endogenous emissions are required to consider the full effects of anthropogenic emissions on the climate system. These exogenous emissions need to be in-line with the climate policy applied to the TIAM model; as consequences different "scenarios" have been created representing different levels of emissions. The modeller should choose the "non-CO_2" exogenous emissions (and file scenario) matching the climate policy modelled (3^{o}C, 2 ^{o}C or 1.5 ^{o}C).

In some cases, policies (such as NDC) relies on "CO2-equivalent" information. For this purpose, the model converts the non-CO2 greenhouse gases into CO2-equivalents GHGs. The calculation uses a simplified correlation between these gases extracted from their global warming potential (GWP); a technique presented in the IPCC; the use of the latest values is recommended (WG1, Chapter 8, AR5). The commodity GHGs is not used in the climate module calculation but can be used in reporting results and constraining the scenarios.

Different constraints can be applied to the climate module to represent "climate policy goals": a temperature target (at a point in time or a strict limit not to overshoot), a certain level of CO_2 concentration in the atmosphere (450ppm), but it could also be specific emission pathway (following for example the RCP – Representative Concentration Pathway). These approaches can be coupled with carbon budgets in order to be more representative of the most up-to-date climate science assessed by the IPCC that used multiple lines of evidence to estimate carbon budgets and not just simple climate models.

8. References

[1] G. Anandarajah, S. Pye, W. Usher, F. Kesicki, C. Mcglade, TIAM-UCL Global model documentation, UCL, 2011.

[2] M. Meinshausen, S.C.B. Raper, T.M.L. Wigley, Emulating coupled atmosphere-ocean and carbon cycle models with a simpler model, MAGICC6 - Part 1: Model description and calibration, Atmos. Chem. Phys. 11 (2011) 1417–1456. https://doi.org/10.5194/acp-11-1417-2011.

[3] M. Winning, S. Pye, J. Glynn, D. Scamman, D. Welsby, How Low Can We Go? The Implications of Delayed Ratcheting and Negative Emissions Technologies on Achieving Well Below 2 °C, 2018. https://doi.org/10.1007/978-3-319-74424-7_4.

[4] S. Pye, J. Price, J. Cronin, I. Butnar, D. Welsby, Modelling 'leadership - driven' scenarios of the global mitigation effort, 2019.

[5] C. McGlade, P. Ekins, Un-burnable oil: An examination of oil resource utilisation in a decarbonised energy system, Energy Policy. 64 (2014) 102–112. https://doi.org/10.1016/j.enpol.2013.09.042.

[6] C. McGlade, P. Ekins, The geographical distribution of fossil fuels unused when limiting global warming to 2 °C, Nature. 517 (2015) 187–190. https://doi.org/10.1038/nature14016.

[7] C.E. McGlade, M. Bradshaw, G. Anandarajah, J. Watson, P. Ekins, A bridge to a low carbon future? Modelling the long-term global potential of natural gas, UKERC Research Report, London, UK, 2014.

[8] S. Bradley, G. Lahn, S. Pye, Carbon Risk and Resilience: How Energy Transition is Changing the Prospects for Developing Countries with Fossil Fuels, London, UK, 2018.

[9] N. Bauer, C. McGlade, J. Hilaire, P. Ekins, Divestment prevails over the green paradox when anticipating strong future climate policies, Nat. Clim. Chang. (2018). https://doi.org/10.1038/s41558-017-0053-1.

[10] S. Pye, C. McGlade, C. Bataille, G. Anandarajah, A. Denis-Ryan, V. Potashnikov, Exploring national decarbonization pathways and global energy trade flows: a multi-scale analysis, Clim. Policy. 16 (2016) S92–S109. https://doi.org/10.1080/14693062.2016.1179619.

[11] I. Butnar, O. Broad, B. Solano Rodriguez, P.E. Dodds, The role of bioenergy for global deep decarbonization: CO2 removal or low-carbon energy?, GCB Bioenergy. (2020). https://doi.org/10.1111/gcbb.12666.

[12] O.Y. Edelenbosch, K. Kermeli, W. Crijns-Graus, E. Worrell, R. Bibas, B. Fais, S. Fujimori, P. Kyle, F. Sano, D.P. van Vuuren, Comparing projections of industrial energy demand and greenhouse gas emissions in long-term energy models, Energy. 122 (2017) 701–710. https://doi.org/10.1016/j.energy.2017.01.017.

[13] F. Kesicki, G. Anandarajah, The role of energy-service demand reduction in global climate change mitigation: Combining energy modelling and decomposition analysis, Energy Policy. 39 (2011) 7224–7233.

[14] G. Anandarajah, W. McDowall, P. Ekins, Decarbonising road transport with hydrogen and electricity: Long term global technology learning scenarios, Int. J. Hydrogen Energy. 38 (2013) 3419–3432. https://doi.org/10.1016/j.ijhydene.2012.12.110.

[15] O.Y. Edelenbosch, D.L. McCollum, D.P. van Vuuren, C. Bertram, S. Carrara, H. Daly, S. Fujimori, A. Kitous, P. Kyle, E. Ó Broin, P. Karkatsoulis, F. Sano, Decomposing passenger transport futures: Comparing results of global integrated assessment models, Transp. Res. Part D Transp. Environ. 55 (2017) 281–293. https://doi.org/10.1016/j.trd.2016.07.003.

[16] D.L. McCollum, C. Wilson, M. Bevione, S. Carrara, O.Y. Edelenbosch, J. Emmerling, C. Guivarch, P. Karkatsoulis, I. Keppo, V. Krey, Z. Lin, E. Broin, L. Paroussos, H. Pettifor, K. Ramea, K. Riahi, F. Sano, B.S. Rodriguez, D.P. van Vuuren, Interaction of consumer preferences and climate policies in the global transition to low-carbon vehicles, Nat. Energy. 3 (2018) 1–10. https://doi.org/10.1038/s41560-018-0195-z.

[17] P. Ekins, N. Hughes, S. Pye, M. Winning, R. Macrory, B. Milligan, S. Haszeldine, J. Watson, The role of CCS in meeting climate policy targets, Unviersity College London, UK, 2017.

[18] G. Marangoni, M. Tavoni, V. Bosetti, E. Borgonovo, P. Capros, O. Fricko, D.E.H.J. Gernaat, C. Guivarch, P. Havlik, D. Huppmann, N. Johnson, P. Karkatsoulis, I. Keppo, V. Krey, E.Ó. Broin, J. Price, D.P. VanVuuren, Sensitivity of projected long-term CO2 emissions across the Shared Socioeconomic Pathways, Nat. Clim. Chang. 7 (2017) 113–117. https://doi.org/10.1038/nclimate3199.

[19] M. Winning, J. Price, P. Ekins, S. Pye, J. Glynn, J. Watson, C. McGlade, Nationally Determined Contributions under the Paris Agreement and the costs of delayed action, Clim. Policy. (2019) 1–12.

[20] O. Dessens, G. Anandarajah, A. Gambhir, Limiting global warming to 2 °C: What do the latest

mitigation studies tell us about costs, technologies and other impacts?, Energy Strateg. Rev. 13–14 (2016) 67–76. https://doi.org/10.1016/j.esr.2016.08.004.
[21] G. Anandarajah, A. Gambhir, India's CO2 emission pathways to 2050: What role can renewables play?, Appl. Energy. (2014). https://doi.org/10.1016/j.apenergy.2014.06.026.
[22] A.J. Cronin, S. Pye, J. Price, I. Butnar, Biomass , afforestation and energy demand reduction : trade-offs in the route to decarbonisation, (2020).
[23] R. Loulou, U. Remme, A. Kanudia, A. Lehtila, G. Goldstein, Documentation for the TIMES model, Part II, 2005.
[24] Daniel Welsby, Modelling uncertainty in global gas resources and markets (forthcoming), University College London, 2020.
[25] S. Pye, J. Price, J. Cronin, I. Butnar, D. Welsby, Modelling ' leadership - driven ' scenarios of the global mitigation effort. the Committee on Climate Change's (CCC) 2019 report Net Zero: The UK's contribution to stopping global warming., London, UK, 2019. https://www.theccc.org.uk/wp-content/uploads/2019/05/Modelling-'leadership-driven'-scenarios-of-the-global-mitigation-effort.pdf.
[26] H. Müller-Merbach, The energy supply model MESSAGE, Eur. J. Oper. Res. 12 (1983) 408. https://doi.org/10.1016/0377-2217(83)90165-0.
[27] R. Loulou, G. Goldstein, A. Kanudia, A. Lehtila, U. Remme, Documentation for the TIMES Model: Part I, 2016.
[28] B.C. O'Neill, E. Kriegler, K.L. Ebi, E. Kemp-Benedict, K. Riahi, D.S. Rothman, B.J. van Ruijven, D.P. van Vuuren, J. Birkmann, K. Kok, M. Levy, W. Solecki, The roads ahead: Narratives for shared socioeconomic pathways describing world futures in the 21st century, Glob. Environ. Chang. 42 (2017) 169–180. https://doi.org/10.1016/j.gloenvcha.2015.01.004.
[29] S. Kypreos, A. Lehtila, TIMES-MACRO: decomposition into hard-linked LP and NLP problems, https://iea-etsap.org/docs/TIMES-Macro-MSA.pdf, 2014.
[30] A. Hof, P. Boot, D. van Vuuren, J. van Minnen, Costs and benefits of climate change adaptation and mitigation: An assessment on different regional scales, Hague, PBL Netherlands Environ. Assess. Agency. (2014) 1–34.
[31] C. McGlade, Uncertainties in the outlook for oil and gas, UCL (University College London), 2014. http://discovery.ucl.ac.uk/1418473/.
[32] IRENA, Renewables 2O18. Analysis and Forecasts to 2O23. Executive summary., 2018. https://doi.org/10.1787/coal_mar-2017-en.
[33] IEA, Coal Information 2018, OECD, 2018. https://doi.org/10.1787/coal-2018-en.
[34] IEA, Coal Information 2019, OECD, 2019. https://doi.org/10.1787/4a69d8c8-en.
[35] BP, Statistical review of world energy, 2017, London, UK, 2017.
[36] BP, Statistical Review of World Energy 2016, London, UK, 2016.
[37] BP, Statistical review of world energy 2018, London, UK, 2018.
[38] BP, Statistical Review of World Energy 2019. 68th Edition, London, UK, 2019. https://doi.org/10.1001/jama.1973.03220300055017.
[39] IGU, World LNG Report - 2015 Edition, 2015. https://www.igu.org/sites/default/files/node-page-field_file/IGU-World LNG Report-2015 Edition.pdf.
[40] IGU, 2016 World LNG Report, 2016. https://www.igu.org/download/file/fid/2123.
[41] IGU, 2017 World LNG Report, Int. Gas Union (IGU. 53 (2017) 1–30. https://www.igu.org/sites/default/files/103419-World_IGU_Report_no crops.pdf.
[42] IGU, 2018 World LNG Report, 2018. https://www.igu.org/sites/default/files/node-document-field_file/IGU_LNG_2018_0.pdf.
[43] IGU, 2019 World LNG Report, 2019. https://www.igu.org/sites/default/files/node-news_item-field_file/IGU Annual Report 2019_23 loresfinal.pdf.
[44] International Energy Agency (IEA), Natural Gas Information 2015, 2015. http://www.oecd-ilibrary.org/energy/natural-gas-information-2015_nat_gas-2015-en.
[45] OECD, IEA, Natural Gas Information 2016, 2016. https://doi.org/10.1787/nat_gas-2015-en.
[46] IEA, Natural gas information 2017, (2019).
[47] IEA, Natural gas Information 2018, 2018. https://www.oecd-ilibrary.org/docserver/nat_gas-2018-en.pdf?expires=1555420714&id=id&accname=ocid177247&checksum=F6E6FB230BC555867B7203FAB591C478%0Ahttp://www.oecd-ilibrary.org/natural-gas-information-2009_5ksm9lzw666d.pdf;jsessionid=ntmkxq1eg89e.x-oecd-l.
[48] V. Daioglou, J.C. Doelman, E. Stehfest, C. Müller, B. Wicke, A. Faaij, D.P. van Vuuren, Greenhouse gas emission curves for advanced biofuel supply chains, Nat. Clim. Chang. (2017). https://doi.org/10.1038/s41558-017-0006-8.

[49] K. Eurek, P. Sullivan, M. Gleason, D. Hettinger, D. Heimiller, A. Lopez, An improved global wind resource estimate for integrated assessment models, Energy Econ. 64 (2017) 552–567. https://doi.org/10.1016/j.eneco.2016.11.015.

[50] J. Price, M. Zeyringer, D. Konadu, Z. Sobral Mourão, A. Moore, E. Sharp, Low carbon electricity systems for Great Britain in 2050: An energy-land-water perspective, Appl. Energy. 228 (2018) 928–941. https://doi.org/10.1016/j.apenergy.2018.06.127.

[51] J. Price, K. Mainzer, S. Petrovic, M. Zeyringer, R. McKenna, The implications of landscape visual impact on future highly renewable power systems: a case study for Great Britain, IEEE Trans. Power Syst. 8950 (2020) 1–1. https://doi.org/10.1109/tpwrs.2020.2992061.

[52] D. Huppmann, J. Rogelj, E. Kriegler, V. Krey, K. Riahi, A new scenario resource for integrated 1.5 °C research, Nat. Clim. Chang. (2018). https://doi.org/10.1038/s41558-018-0317-4.

[53] P. Ekins, N. Hughes, S. Pye, M. Winning, R. Macrory, B. Milligan, S. Haszeldine, J. Watson, The role of CCS in meeting climate policy targets. A report commissioned by the Global CCS Institute, 2017.

[54] R. Socolow, M. Desmond, R. Aines, J. Blackstock, O. Bolland, T. Kaarsberg, N. Lewis, M. Mazzotti, A. Pfeffer, K. Sawyer, J. Siirola, B. Smit, J. Wilcox, Direct Air Capture of CO 2 with Chemicals Panel on Public Affairs, Am. Phys. Soc. - Panel Public Aff. (2011) 100.

[55] C. Chen, M. Tavoni, Direct air capture of CO2and climate stabilization: A model based assessment, Clim. Change. 118 (2013) 59–72. https://doi.org/10.1007/s10584-013-0714-7.

[56] EIA, Trends in U.S. Oil and Natural Gas Upstream Costs, US Energy Information Administration, 2016.

[57] AER, Natural Gas Supply Costs, Alberta Energy Regulator, 2018.

[58] Carbon Limits, Associated Petroleum Gas Flaring Study for Russia, Kazakhstan, Turkmenistan and Azerbaijan, EBRD, 2013.

[59] I. Advisory, Middle East Natural Gas, 2015. http://ipaadvisory.co.uk/media/1144/middle-east-gas-pricing-15_08_11.pdf.

[60] D. Santley, R. Schlotterer, A. Eberhard, Harnessing African Natural Gas: A New Opportunity for Africa's Energy Agenda?, World Bank, Washington, DC, The World Bank, Washington DC, USA, 2014.

[61] A. Aissaoui, Algerian Gas: Troubling Trends, Troubled Policies, Oxford Institute for Energy Studies, Oxford Institute for Energy Studies, Oxford, UK, 2016.

[62] IMCO, A changing world : Mexico facing the 21 st century energy revolution, 2014.

[63] IEA, Coal Information 2016, OECD, 2016. https://doi.org/10.1787/coal-2016-en.

[64] IEA, Coal Information 2017, OECD, 2017. https://doi.org/10.1787/coal-2017-en.

[65] IEA, Coal Information 2015, OECD, 2015. https://doi.org/10.1787/coal-2015-en.

[66] B. Songhurst, LNG plant cost escalation, Oxford Institute for Energy Studies, Oxford Institute for Energy Studies, Oxford, UK, 2014.

[67] B. Songhurst, LNG Plant Cost Reduction 2014–18, Oxford Institute for Energy Studies, Oxford Institute for Energy Studies, Oxford, UK, 2018.

[68] C. McGlade, M. Bradshaw, G. Anandarajah, J. Watson, P. Ekins, A Bridge to a Low-Carbon Future? Modelling the Long-Term Global Potential of Natural Gas, UKERC Research Report, UKERC Research Report, London, UK, 2014.

[69] R. Loulou, M. Labriet, A. Lehtila, TIMES Climate Module, http://iea-etsap.org/docs/TIMES-Climate-Module.pdf, 2010.

[70] D.P. van Vuuren, J. Edmonds, M. Kainuma, K. Riahi, A. Thomson, K. Hibbard, G.C. Hurtt, T. Kram, V. Krey, J.F. Lamarque, T. Masui, M. Meinshausen, N. Nakicenovic, S.J. Smith, S.K. Rose, The representative concentration pathways: An overview, Clim. Change. 109 (2011) 5–31. https://doi.org/10.1007/s10584-011-0148-z.

[71] W.D. Nordhaus, J. Boyer, Roll the DICE again: the economics of global warming, Draft Version. 28 (1999) 1999.

[72] P. Forster, V. Ramaswamy, P. Artaxo, T. Berntsen, R. Betts, D.W. Fahey, J. Haywood, J. Lean, D.C. Lowe, G. Myhre, Changes in atmospheric constituents and in radiative forcing. Chapter 2, in: Clim. Chang. 2007. Phys. Sci. Basis, 2007.

[73] V. Ramaswamy, O. Boucher, J. Haigh, D. Hauglustaine, J. Haywood, G. Myhre, T. Nakajima, G. Shi, S. Solomon, Radiative forcing of climate change. In: Houghton JT et al (eds) Climate change 2001: the scientific basis., Cambridge University Press, Cambridge, United Kingdom and New York, NY, USA., 2001.

[74] E.S. Rubin, J.E. Davison, H.J. Herzog, The cost of CO2 capture and storage, Int. J. Greenh. Gas Control. (2015). https://doi.org/10.1016/j.ijggc.2015.05.018.

[75] IRENA International Renewable Energy Agency, Renewable Power Generation Costs in 2017, 2018. https://doi.org/10.1007/SpringerReference_7300.

[76] IEA PVPS, Trends 2018 in Photovoltaic applications, 2018.
[77] I. Butnar, O. Broad, B. Solano Rodriguez, P.E. Dodds, The role of bioenergy for global deep decarbonisation: CO 2 removal or low-carbon energy?, GCB Bioenergy. (2019) gcbb.12666. https://doi.org/10.1111/gcbb.12666.
[78] J. Fargione, J. Hill, D. Tilman, S. Polasky, P. Hawthorne, Land clearing and the biofuel carbon debt., Science. 319 (2008) 1235–8. https://doi.org/10.1126/science.1152747.
[79] H. Valin, D. Peters, M. van den Berg, S. Frank, P. Havlik, N. Forsell, C. Hamelinck, J. Pirker, A. Mosnier, J. Balkovic, The land use change impact of biofuels consumed in the EU, Quantif. Area Greenh. Gas Impacts. (2015).
[80] V. Daioglou, E. Stehfest, B. Wicke, A. Faaij, D.P. van Vuuren, Projections of the availability and cost of residues from agriculture and forestry, GCB Bioenergy. 8 (2016) 456–470. https://doi.org/10.1111/gcbb.12285.
[81] Ricardo-AEA, Biomass Feedstock Availability. Final report for BEIS., London, UK, 2017. https://www.gov.uk/government/publications/uk-and-global-bioenergy-resource-model.
[82] D.P. van Vuuren, J. van Vliet, E. Stehfest, Future bio-energy potential under various natural constraints, Energy Policy. 37 (2009) 4220–4230. https://doi.org/10.1016/j.enpol.2009.05.029.
[83] M. Hoogwijk, A. Faaij, B. de Vries, W. Turkenburg, Exploration of regional and global cost-supply curves of biomass energy from short-rotation crops at abandoned cropland and rest land under four IPCC SRES land-use scenarios, Biomass and Bioenergy. 33 (2009) 26–43. https://doi.org/10.1016/j.biombioe.2008.04.005.
[84] F. Creutzig, N.H. Ravindranath, G. Berndes, S. Bolwig, R. Bright, F. Cherubini, H. Chum, E. Corbera, M. Delucchi, A. Faaij, J. Fargione, H. Haberl, G. Heath, O. Lucon, R. Plevin, A. Popp, C. Robledo-Abad, S. Rose, P. Smith, A. Stromman, S. Suh, O. Masera, Bioenergy and climate change mitigation: An assessment, GCB Bioenergy. 7 (2015) 916–944. https://doi.org/10.1111/gcbb.12205.
[85] A. Marcucci, S. Kypreos, E. Panos, The road to achieving the long-term Paris targets: energy transition and the role of direct air capture, Clim. Change. 144 (2017) 181–193. https://doi.org/10.1007/s10584-017-2051-8.
[86] S. Fuss, W.F. Lamb, M.W. Callaghan, J. Hilaire, F. Creutzig, T. Amann, T. Beringer, W. de Oliveira Garcia, J. Hartmann, T. Khanna, G. Luderer, G.F. Nemet, J. Rogelj, P. Smith, J.L.V. Vicente, J. Wilcox, M. del Mar Zamora Dominguez, J.C. Minx, Negative emissions—Part 2: Costs, potentials and side effects, Environ. Res. Lett. 13 (2018) 063002. https://doi.org/10.1088/1748-9326/aabf9f.
[87] B. Metz, L. Meyer, O. Davidson, H. de Coninck, M. Loos, IPCC Special Report on Carbon Dioxide Capture and Storage, Cambridge University Press, 2005.
[88] G. Anandarajah, S. Pye, W. Usher, F. Kesicki, C. McGlade, TIAM-UCL Global Model Documentation Working Paper, London, UK, 2011. https://www.ucl.ac.uk/drupal/site_energy-models/sites/energy-models/files/tiam-ucl-manual.pdf.

Appendices

Appendix 0. TIAM-UCL version control

This documentation corresponds to core model version 4.1.1.

Appendix 1. Countries included in model regions

Table A. 1. List of regions and countries in the 16 region TIAM-UCL model

Africa (AFR)	Algeria, Angola, Benin, Botswana, Burkina Faso, Burundi, Cameroon, Cape Verde, Central African Republic, Chad, Comoros, Congo, Côte d'Ivoire, Democratic Republic of the Congo, Djibouti, Egypt, Equatorial Guinea, Eritrea, Ethiopia, Gabon, Gambia, Ghana, Guinea, Guinea-Bissau, Kenya, Lesotho, Liberia, Libya, Madagascar, Malawi, Mali, Mauritania, Morocco, Mozambique, Namibia, Niger, Nigeria, Rwanda, Sao Tome and Principe, Senegal, Seychelles, Sierra Leone, Somalia, South Africa, South Sudan, Sudan, Swaziland, Togo, Tunisia, Uganda, United Republic of Tanzania, Zambia, Zimbabwe
Australia (AUS)	Australia, New Zealand
Canada (CAN)	Canada
Central and South America (CSA)	Anguilla, Antigua and Barbuda, Argentina, Aruba, Bahamas, Barbados, Belize, Bermuda, Bolivia, Brazil, Cayman Islands, Chile, Colombia, Costa Rica, Cuba, Dominica, Dominican Republic, Ecuador, El Salvador, Falkland Islands, Grenada, Guatemala, Guyana, Haiti, Honduras, Jamaica, Martinique, Netherlands Antilles, Nicaragua, Panama, Paraguay, Peru, Saint Kitts and Nevis, Saint Lucia, Saint Vincent and the Grenadines, Suriname, Trinidad and Tobago, Uruguay, Venezuela (Bolivarian Republic of)
China (CHI)	China, Taiwan, Tibet
Eastern Europe (EEU)	Bosnia and Herzegovina, Bulgaria, Croatia, Czech Republic, Hungary, Montenegro, Poland, Romania, Serbia, Slovakia, Slovenia, The former Yugoslav Republic of Macedonia
Former Soviet Union (FSU)	Armenia, Azerbaijan, Belarus, Estonia, Georgia, Kazakhstan, Kyrgyzstan, Latvia, Lithuania, Republic of Moldova, Russian Federation, Tajikistan, Turkmenistan, Ukraine, Uzbekistan
India (IND)	India
Japan (JAP)	Japan
Mexico (MEX)	Bahrain, Brunei Darussalam, Cyprus, Iran (Islamic Republic of), Israel, Jordan, Kuwait, Lebanon, Occupied Palestinian Territory, Oman, Qatar, Saudi Arabia, Syrian Arab Republic, Turkey, United Arab Emirates, Yemen
Middle-east (MEA)	Mexico
Other Developing Asia (ODA)	Afghanistan, American Samoa, Bangladesh, Bhutan, Cambodia, Democratic People's Republic of Korea, Fiji, French Polynesia, Indonesia, Kiribati, Lao People's Democratic Republic, Malaysia, Maldives, Mauritius, Mongolia, Myanmar, Nepal, New Caledonia, Pakistan, Papua New Guinea, Philippines, Samoa, Singapore, Solomon Islands, Sri Lanka, Thailand, Timor-Leste, Tonga, Vanuatu, Vietnam
South Korea (SKO)	Republic of Korea
United Kingdom (UK)	United Kingdom
USA (USA)	United States of America
Western Europe (WEU)	Albania, Andorra, Austria, Belgium, Denmark, Faroe Islands, Finland, France, Germany, Gibraltar, Greece, Greenland, Iceland, Ireland, Italy, Luxembourg, Malta, Monaco, Netherlands, Norway, Portugal, San Marino, Spain, Sweden, Switzerland, Vatican

Appendix 2. Fossil fuels

The fossil fuel upstream sector in TIAM-UCL incorporates the availability and costs of primary energy resources, all extraction processes, and any upgrading/processing required which yields energy commodity carriers that can be used as inputs into end-use sectors. For fossil fuel resources, this translates as all processes across the reference energy system from getting the resource out of the ground to a form where it can be input into another sector and/or traded as a to another region. Table A. 2 shows the breakdown of this overview of the upstream sector in TIAM-UCL.

Table A. 2. Overview of upstream sector documentation

Upstream focus	Section	Commodity	Section
Primary energy resources and the extraction of exhaustible primary commodities	A2.1	Coal	A2.1.1
		Natural gas	A2.1.2
		Oil	A2.1.3
Primary transformation (upgrading and/or processing)	A2.2	Coal	A2.2.1
		Natural gas	A2.2.2
		Oil	A2.2.3
Secondary transformation (refining)	A2.3		
Trade	A2.4	Coal	1.4.1
		Natural gas	1.4.2
		Oil	1.4.3
Key upstream constraints	1.5	Coal	1.5.1
		Natural gas and oil	1.5.2

A2.1 Primary energy resources and the extraction of exhaustible primary commodities

Primary energy resources, both for renewable and non-renewable commodity feedstocks are represented in the upstream sector of TIAM-UCL. Given the huge range of uncertainty around primary energy resources, where possible TIAM-UCL employs methods which utilise stochastic or probabilistic estimates in order to take account of possible ranges of estimates, as well as allowing sensitivity analysis to be conducted from the outputs of probability distributions where used. All primary resources in TIAM-UCL are subsequently used further downstream in some other process, and may require additional processing/upgrading (e.g. oil and natural gas), or as a direct input into transformation processes (e.g. solar radiation into solar PV electricity generation).

Primary extraction in TIAM-UCL is represented by a range of 'mining' processes, with the costs reflecting a range of factors including:

- Technology maturity (e.g. if a technology has been developed over time in a certain region, and experience has been accrued (learning-by-doing), then the technology can be relatively mature and potential cost reductions/efficiency gains can be experienced. For example, shale gas drilling experience was accrued over decades in the United States, both through learning-by-doing (e.g. multiple wells per drilling pad) and fiscal incentives (tax breaks) which reduced costs, and therefore US shale gas costs are lower than other regions.

- Technical difficulty (generally driven by the geology of the formation in question, i.e. the source rock). Higher mining costs are incurred for fossil resources which require additional stimulation to lead to economic flow rates, such as hydraulic fracturing for tight reservoirs of oil/gas
- Production flow rates, linked to the above technical difficulty. Additionally, various source rocks yield different production flow dynamics, e.g. across the lifetime of a well, production characteristics for conventional and unconventional gas vary -
    - Conventional non-associated natural gas would generally exhibit slower growth rates up to peak production, a longer production plateau period, and slower rates of production decline
    - Unconventional shale gas wells would generally exhibit rapid production growth up to a maximum, a shorter plateau vis-à-vis conventional gas, and faster decline rates

A2.1.1 Coal

Primary coal resources in TIAM-UCL are split into two categories, utilizing the original TIAM-ETSAP data collected by Remme et. al. [ref], and recalibrated for the individual regions of TIAM-UCL using data from the BGR [ref] -

- Brown coal (lignite): lower energy content, with average heating value ranging from 5.57-17 MJ/kg
- Hard coal (sub-bituminous, bituminous and anthracite): higher energy content, with average heating value ranging from 17.58-27.55 MJ/kg

As with oil and natural gas, the extraction technologies for coal split the resource base into cost tranches, in order to reflect (albeit relatively simplistically), cost depletion dynamics. In short, as the more accessible and higher quality resources are depleted, the model must move to more expensive extraction of (potentially) harder to exploit resources. Coal is split into hard coal and brown coal, with the representative mining technologies for both categories split into three cost categories. The distribution of resources/reserves assigned to each cost category varies by region, and is influenced by the proportion of the total resource base which can be considered reserves[13], with the remainder of resources split between the middle and highest cost categories.

Figure A. 1 shows a cost depletion curve for global coal resources, and the corresponding global supply cost curve constructed from the cost depletion curve. Additionally, Figure A. 2 shows a global supply cost curve broken down into the regions of TIAM-UCL.

a)

[13] Reserves are defined as geologically proven with current technologies, and commercially viable to extract at current market prices/cost conditions.

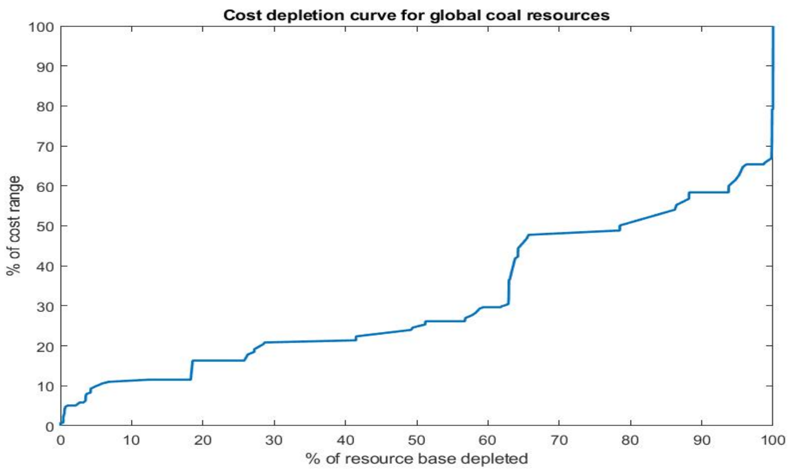

b)

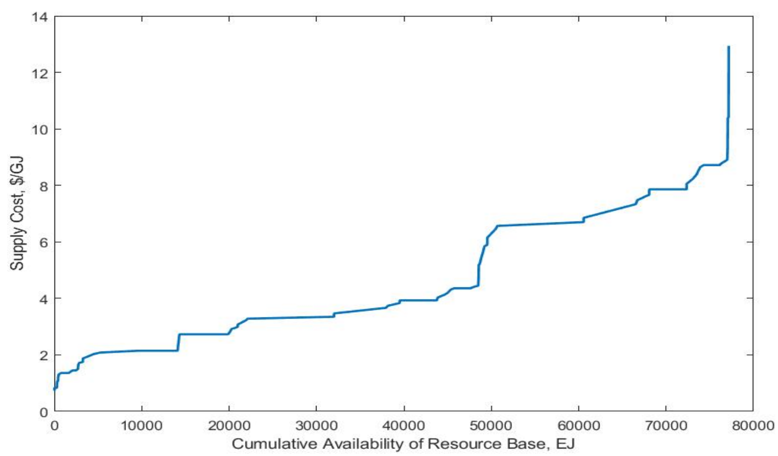

Figure A. 1. a) Cost depletion curve derived from TIAM-UCL resources and costs for global coal; b) supply cost curve derived from the cost depletion curve in 1.1 (a) for global coal resources

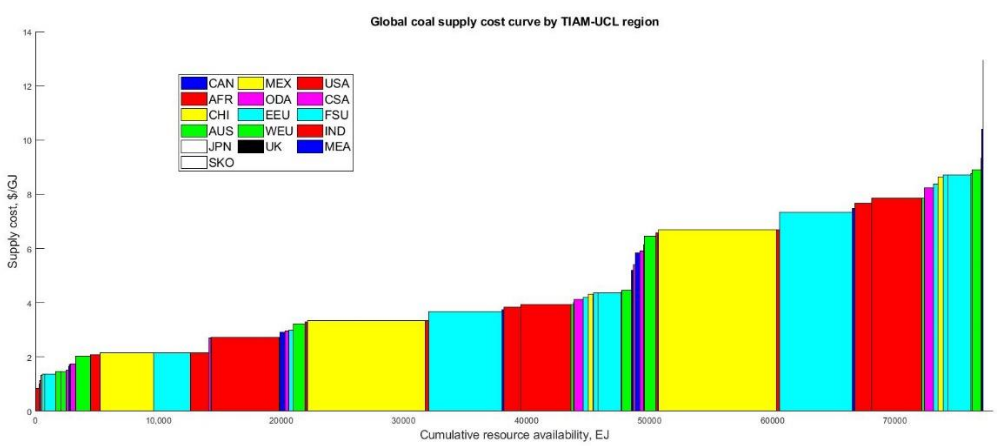

Figure A. 2. **Global supply cost curve for coal from Figure 1.1 (b) broken down into TIAM-UCL regions**

A2.1.2 Natural gas

The underlying availability and cost of natural gas in TIAM-UCL is disaggregated into the following geological categories:

- Non-associated conventional gas proved reserves
- Non-associated conventional gas reserve additions
- Non-associated conventional gas new discoveries
- Associated natural gas
- Arctic conventional natural gas resources
- Shale gas
- Coal bed methane
- Tight natural gas

As with oil, the disaggregation of natural gas in TIAM-UCL is based on McGlade [31]. This analysis was then extended in a forthcoming thesis by Welsby [24], with field-level assessments of resource availabilities and costs. Resource assessments were generally conducted at disaggregated field-/play-level, and then aggregated into the regions of TIAM-UCL using probability distributions, and taking into account any correlation between discrete estimates etc. These were then applied to depletion curves which were formed from a database of field-/play-level costs where possible. The database was then extended to fields for which costs were either not known (i.e. no publically available indication of field supply costs) or have not yet been developed. This means the representation of natural gas supply costs in TIAM-UCL is driven by statistically significant coefficients of field-/play-level supply costs, aggregated into a representative cost depletion curves.

Figure A. 3 (a,b) shows the central supply cost curves for conventional non-associated natural gas resources (a significant focus of the work by Welsby [24] and an aggregated global supply cost curve for all natural gas resource categories. The aggregated global curves below were mainly formed from field-/play-level data and have been aggregated from the TIAM-UCL regions. This means that some of the supply cost outputs will be higher/lower than the more disaggregated curves which formed the basis for these global supply cost curves.

a)

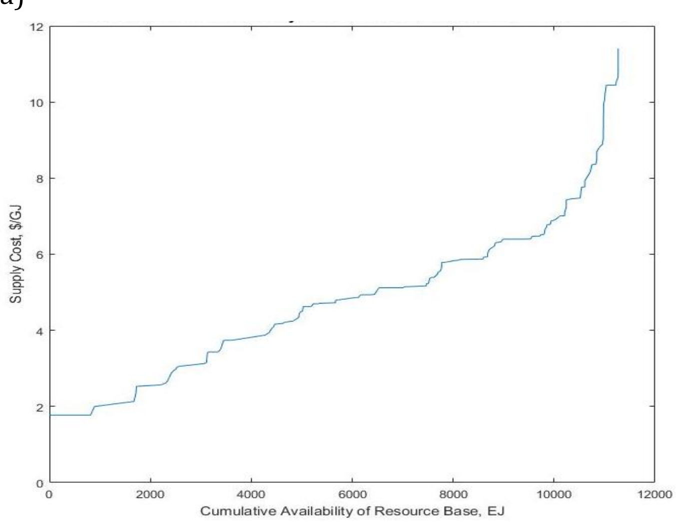

b)

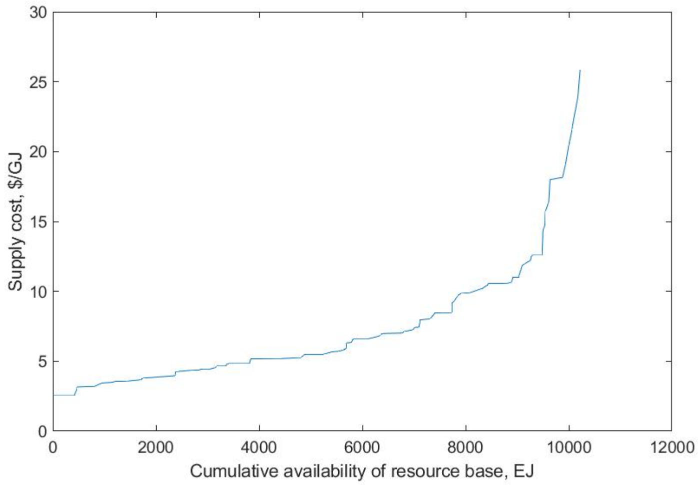

Figure A. 3. Global central (P50) supply cost curve for a) non-associated conventional natural gas and b) unconventional natural gas resources

Additionally, Figure A. 4 shows a) the regional breakdown of the resource distribution, and b) the supply cost with each resource category identified. For reference, none of the figures in this section include associated natural gas resources in the supply cost curves, as these are calculated separately, with resource availabilities calculated by McGlade [31] and Welsby [24], and an endogenous decision within the model of whether to produce the gas or flare/vent it.

a)

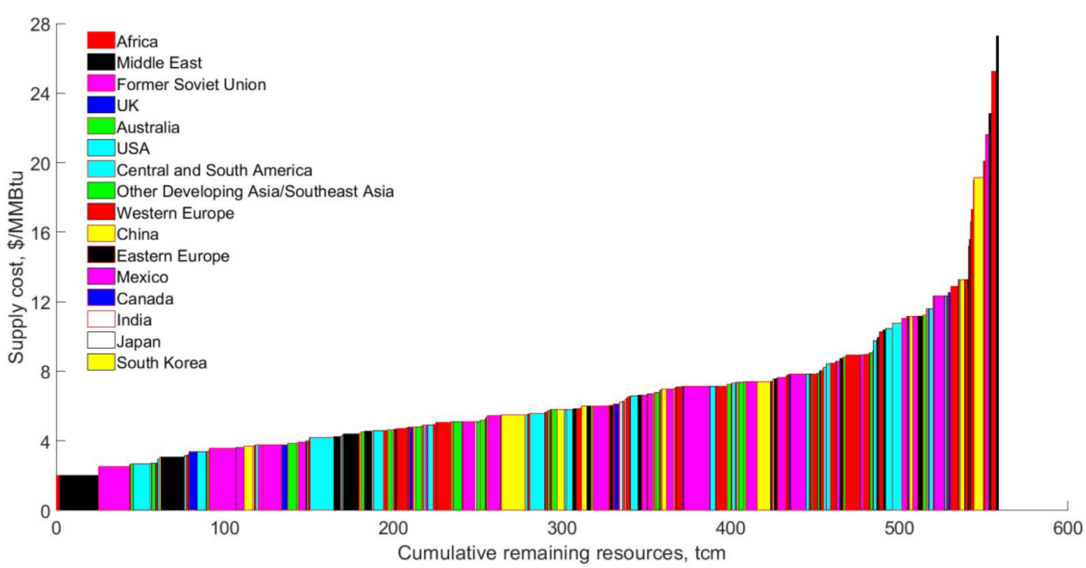

b)

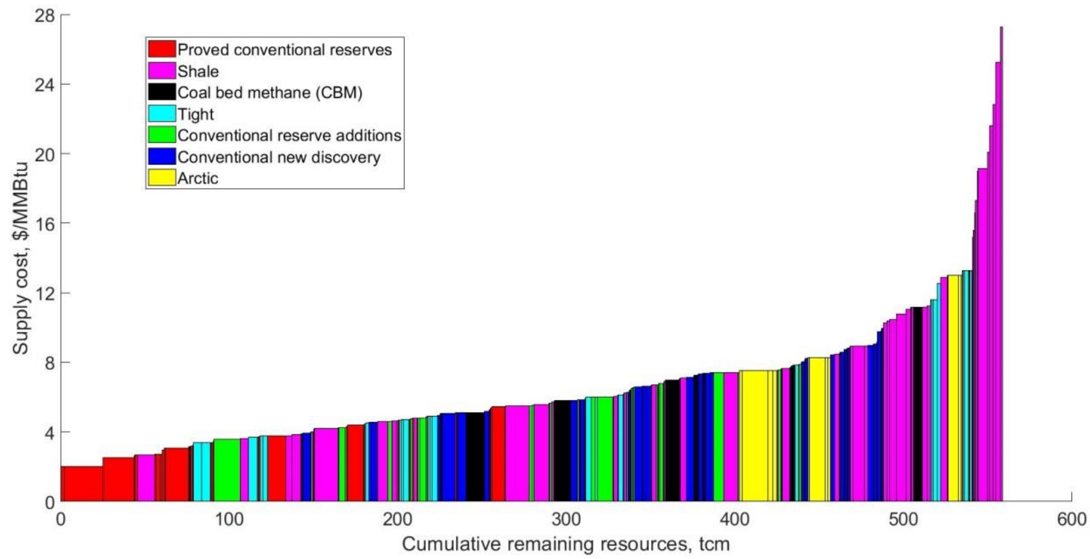

Figure A. 4. Global gas supply cost curve by a) region b) resource category

On a regional level, Figure A. 5 a shows the aggregated output distribution for combining play-level estimates of shale gas for the Central and South America region in TIAM-UCL, and Figure A. 5b shows the depletion analysis using US shale play cost analogues and linear regression using the geological characteristics of individual plays in South America (e.g. shale reservoir depth, thickness, etc.). These are then combined to form a (central) supply cost curve, shown in Figure A. 5c. These figures are taken from the forthcoming PhD thesis from Welsby [24].

a)

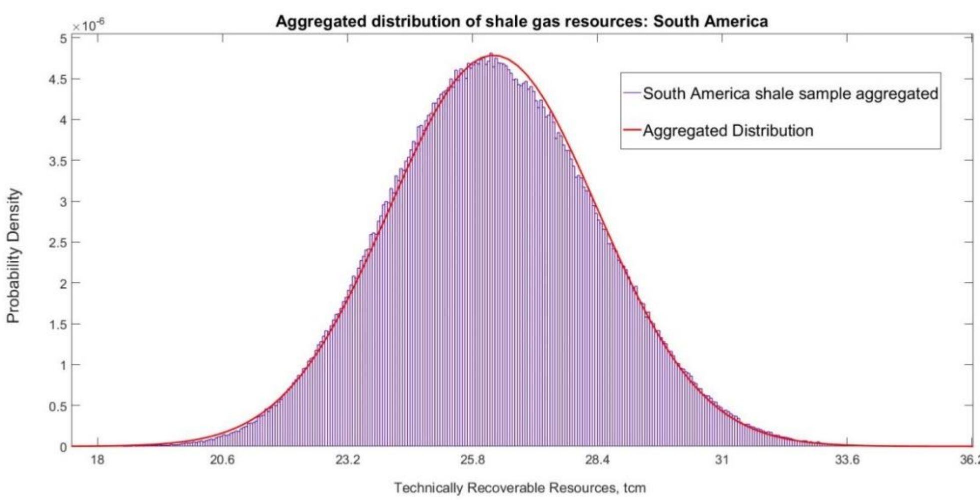

b)

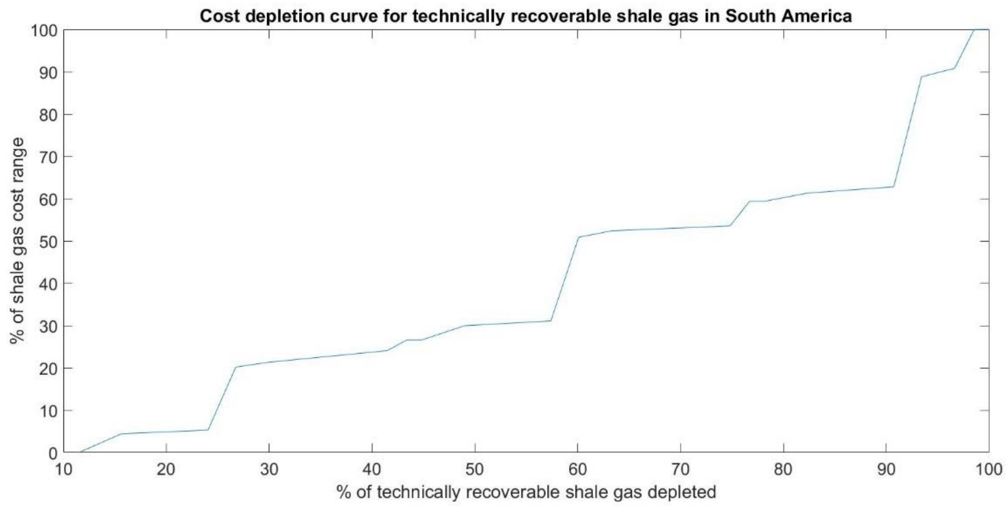

c)

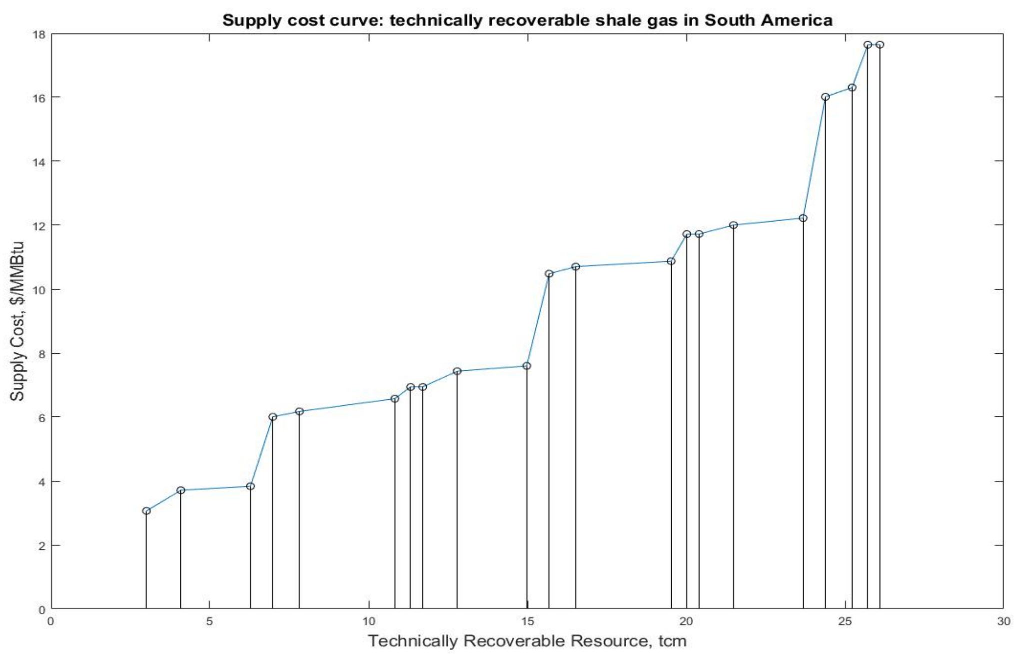

Figure A. 5. a) Aggregated distribution for estimates of technically recoverable resources of shale gas in individual plays in Central and South America (CSA) region in TIAM-UCL; b) Cost depletion curve for shale gas in Central and South America, and c) central supply cost curve for technically recoverable resources of shale gas for Central and South America (CSA)

Primary extraction of natural gas is split by region and into the different geological categories mentioned previously. For each category, the supply cost curves shown above are then disaggregated into a three-step supply cost curve, with the first 50% of the resource base in the lowest cost bracket, then the next 30% in the middle cost category, and finally the last 20% in the highest cost category. An example of this split is shown in Figure A2.6 taken from the work conducted on field-level analysis of the drivers of natural gas supply costs undertaken by Welsby [24]. Figure A. 6 shows the constructed supply cost curve for the Middle East OPEC region in TIAM-UCL, with the low, middle and high cost ranges, and the corresponding quantity of proved non-associated gas reserves which can be extracted at each cost. For reference, the higher end of the cost range for the Middle East OPEC region would be sour gas deposits in the UAE and Saudi Arabia, some of which lie at significant reservoir depths[14].

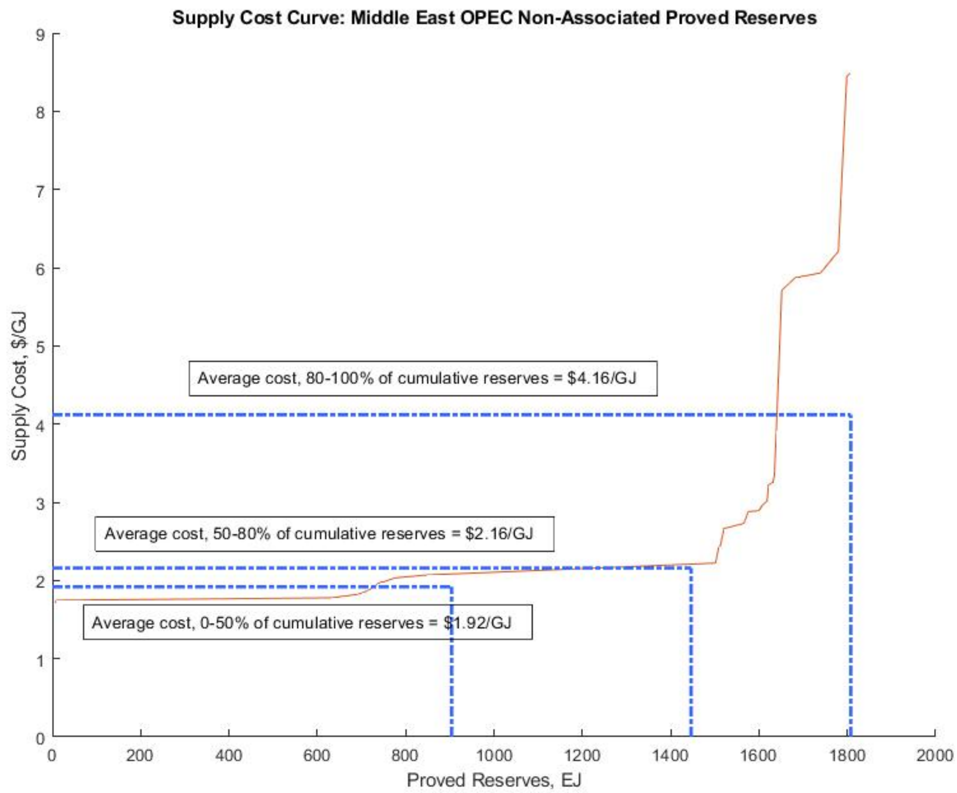

Figure A. 6. Example of three-step supply cost curve for the Middle East OPEC region in TIAM-UCL, for proved non-associated conventional gas reserves

Table A. 3 shows a cost range for some key natural gas mining technologies, constructed through a bottom-up analysis as part of the forthcoming PhD thesis by Welsby [24]. These costs were generated through a field-level database and a linear regression model applied to geological parameters to generate cost depletion curves.

Table A. 3. Cost range for natural gas mining technologies in TIAM-UCL

Resource category	Minimum cost, $/boe	Minimum cost region	Maximum cost, $/boe*	Maximum cost region
Proved non-associated onshore conventional reserves (includes sour)	5	AFR_OPEC	40	USA

[14] Despite the costs, which are far above the highly regulated pricing of many OPEC states in the Middle East, these fields have been developed in some countries to limit import dependency (e.g. UAE), and have therefore been included in the assessment of proved reserves.

Proved non-associated offshore shallow conventional reserves	10	MEA_OPEC	33	AUS
Proved non-associated offshore deep conventional reserves	20	CSA_N	44	USA
Conventional non-associated reserve additions	10	FSU	48	ODA
Undiscovered non-associated conventional	24	FSU	61	MEX
Sour natural gas undeveloped	30	USA	57	MEA_P
Arctic	31	-	64	-
Shale gas	16	USA	130	MEA_N
Tight natural gas	19	USA/CAN	66	CSA_N
CBM	18	USA	63	CHI

* Natural gas costs here have been expressed in $/boe so they can be directly compared to the oil extraction costs in Table 1.3.

A2.1.3 Oil

The representation of oil in TIAM-UCL is predominantly based on the work by McGlade [31], which focused on quantifying uncertainties in the outlook for oil and natural gas, and in particular in the availability and costs of these energy carriers. As with natural gas, oil is split into different geological categories, each with specific availabilities and supply cost dynamics:

- Conventional oil proved reserves
- Conventional oil reserve additions
- Conventional oil new discoveries
- Arctic oil
- Mined shale oil
- In-situ shale oil
- Light tight oil
- Mined oil sands
- In-situ oil sands (ultra-heavy oil)

The representation of uncertainty in TIAM-UCL for oil availability and costs differs between conventional and unconventional oil. For conventional oil, direct estimates of reserve and/or resource availability were taken from the literature and input into probability distributions, with corresponding assumptions on correlation between the estimates. For unconventional oil (e.g. mined bitumen), two parameters were assigned probability distributions: a range of estimates for original oil in-place (OOIP) and a range of estimates of a recovery factor (i.e. between 0 and 1, which determines the proportion of the in-place resource base which is technically recoverable). These two distributions were then combined using random repeated sampling (Monte Carlo simulations) to form regional estimates [31]. The combination is the product of the OOIP and the recovery factor, repeated a large number of times to generate an aggregated distribution. These estimates of the resource base for each category of oil were then combined with cost depletion curves, mostly formed from IEA data on cost ranges, and used to generate supply cost curves. Figure A. 7 from McGlade [31] shows a) a range of cost depletion curves and b) example supply cost curves for proved oil reserves, taking into account the inherent uncertainty in any volumetric estimates. In general, the depletion analysis for unconventional oil exhibits significantly more rapid cost escalation as the resource base is depleted, than for conventional oil.

a)

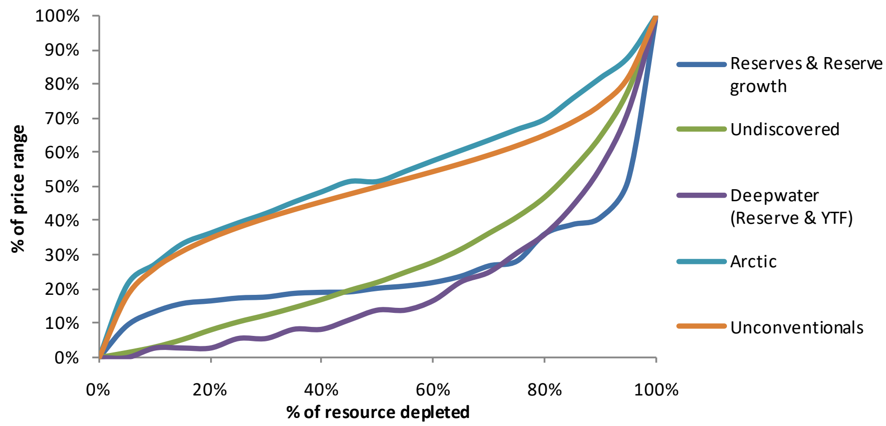

b)

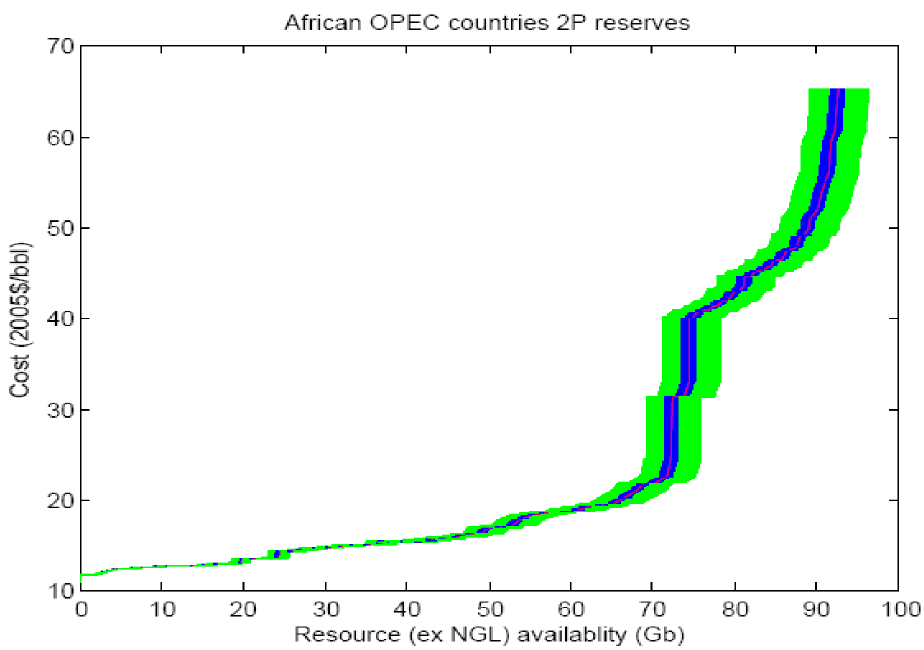

Figure A. 7. a) Cost depletion curves for a range of oil categories, and b) supply cost curves for African OPEC countries showing the range of uncertainty from the output distribution, and combined with representative cost depletion curves in a), to form a range of potential reserve-cost combinations.

Additionally, Table A. 4 shows the split of oil into each category. It should be noted that the resource availability is the central value taken from McGlade (2013).

Table A. 4. Global availability of oil by resource category in TIAM-UCL

Oil category	Resource availability, EJ	Share, %
Conventional	14842	52
Unconventional	13588	48
Global total	**28400**	

The mining processes for oil and natural gas match the geological categories listed previously. Unconventional oil has several more steps in the reference energy system to reflect that the output from these processes is initially several stages 'below' conventional oil. Table A. 5 below shows a range of costs in TIAM-UCL from McGlade [31] for the mining technologies in the upstream sector. Also included is the region in TIAM-UCL containing the minimum and maximum cost for each category. As with natural gas represented in Figure A2.6), the supply cost curve is split into three sections: the first 50% of the resource base considered the lowest cost, then the next 30%, and finally the most expensive oil representing the last 20% of the resource base.

Table A. 5. Cost ranges for oil resources in TIAM-UCL

Resource category	Minimum cost, $/boe	Minimum cost region	Maximum cost, $/boe	Maximum cost region
Proved reserves	11	MEA_OPEC	47	CSA_N
Reserve addition	21	MEA_OPEC	68	CSA_N
New discoveries	16	MEA_OPEC	94	IND
Arctic	48	-	102	-
Bitumen (mining)	35	-	44	-
Bitumen (in-situ)	29	-	37	-
Ultra-heavy oil	29	-	37	-
Oil shale	39	-	83	-

Due to limited development outside of certain countries (e.g. Canada for bitumen production), costs have largely been applied homogenously across the relevant TIAM regions. Figure A. 8 shows the global supply cost curve for oil in TIAM-UCL split by region (a) and resource category (b). It should also be noted that unconventional oil is split into three separate cost categories: variable O&M, fixed O&M, and an investment cost (i.e. capital cost). In order to incorporate these into a supply cost curve with conventional oil, a singular supply cost figure was required, therefore the O&M costs were summed, and then a per-unit investment cost was assigned to each category of unconventional oil (derived by dividing cumulative investment and cumulative production from each mining technology) which then yielded a supply cost figure.

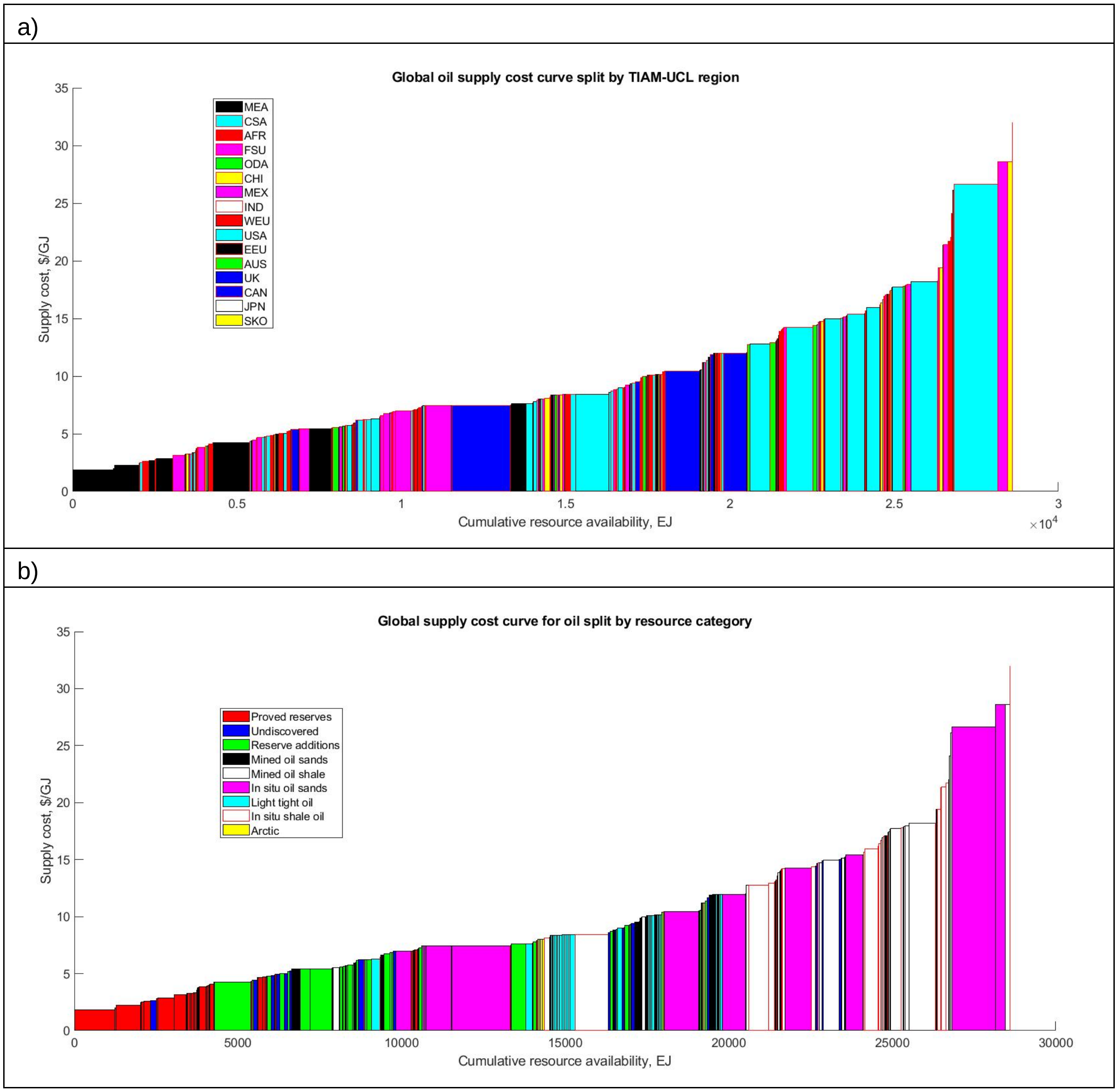

Figure A. 8. Global supply cost curve for oil split by a) TIAM-UCL region and b) oil resource category.

A2.2 Primary transformation (separation, upgrading and processing)

In addition to separating primary energy carriers in the upstream sector, TIAM-UCL also accounts for the use of fuels in the upstream itself (e.g. heat inputs required for the production of crude oil from the oil sands mining process).

A2.2.1 Coal

Coal requires far less upstream upgrading/processing than oil and gas. In general any impurities will result in lower energy content in its end-use, rather than being removed in the upstream as with oil and gas. One main exception is the production of coking coal from hard coal, which requires energy inputs and therefore incurs costs, losses, and emissions across the upstream sector. Coking coal, used predominantly in the production of iron and steel is represented in TIAM-UCL as a product of heating at huge temperatures (≥ 1000°C) hard coal (it is assumed lignite is not used), leaving very high concentrations of carbon.[15]

A2.2.2 Natural gas

Natural gas requires processing to ensure it is of pipeline / liquefaction quality. This involves removing any impurities which could undermine the integrity of transportation / further transformation infrastructure, such as:

- Hydrogen sulphide (H_2S)[16] and carbon dioxide (CO_2) corroding gas pipelines
- CO_2 in a liquefaction terminal which would freeze at a much higher temperature than methane liquefies, and therefore lead to blockages/system shutdown at the facility

After the mining process, a natural gas commodity carrier then passes to an upstream process which acts as a proxy for the collection and processing of natural gas from the well-heads to gas processing plants. Regionalised operation and maintenance costs are associated with this gathering/processing technology, as well as historical capacities. Additionally, a distinction is made between the gathering and processing of non-associated conventional natural gas, and unconventional natural gas. This process (taking into account emissions intensities, efficiencies, and any required energy inputs) turns the output gas from the mining process into an energy commodity which can either be traded internationally, via pipeline or LNG, or can be used as 'useful' input downstream, such as secondary transformation in the power generation sector, or directly used in the residential sector via transportation through smaller distribution networks (e.g. to satisfy residential heating service demand).

Due to its large regional-scale and intensive data requirements, TIAM-UCL is not able to accurately reflect the techno-economic characteristics of smaller downstream distribution networks for natural gas (e.g. distribution networks in urban areas which transport gas to individual households for cooking and heating service demand) due to the granularity required to effectively model such networks. However, additional user constraints have been added in the model to prevent excessively large and unrealistic uptake of downstream natural gas, particularly for the residential sector, in regions/sub-regions where this is highly unlikely, at least in the near-term. Some of these constraints have been discussed in more detail in the Buildings Sector (Section 6.2) part of this documentation.

Additionally, underlying capacities and new capacity costs have been added into TIAM-UCL for associated natural gas (Welsby, forthcoming), in order to reflect the fact that whilst it is produced as a relatively low cost by-product of oil, it still requires infrastructure to be in place, and is therefore a key reason behind large-scale flaring and venting in some regions. Table A. 6 shows a range of investment and O&M costs for associated natural gas projects, which have been incorporated in TIAM-UCL.

[15] World Coal Association website. https://www.worldcoal.org/coal/uses-coal/how-steel-produced (Accessed 22.02.20)

[16] Hydrogen sulphide is not explicitly modelled in TIAM-UCL, due to the fact it is not a greenhouse gas. However, as part of the cost database work described in 1.2.3, a binary variable was included in the linear regression to isolate the impact on field supply costs of the presence of hydrogen sulphide. This variable was found to be statistically significant. Therefore whilst the physical presence of H_2S is not modelled, TIAM does capture that natural gas with high concentrations of H_2S is generally more expensive to produce than 'sweeter' counterparts.

Table A. 6. **Range of associated natural gas[17] investment and operational costs**

Associated gas production field/region	CAPEX, $/MMBtu	OPEX, $/MMBtu	Region (Country)	Source
Bakken		0.31-0.67	United States (USA)	EIA [56],
Grand Rapids Bitumen	11.25	0.62	Canada (Canada)	AER [57]
Tengiz	2.40		Former Soviet Union (Kazakhstan)	Carbon Limits [58]
Middle East OPEC		0.8-1.3	Middle East OPEC countries	IPAA [59]
Utorogu	1.95		Africa (Nigeria)	OGJ (2016)[18]
Nigeria offshore		0.09-0.38	Africa (Nigeria)	World Bank [60]
El Merk		0.27	Africa (Algeria)	Aissaoui [61]
Gassi Touil		0.60	Africa (Algeria)	Aissaoui [61]
Cantarell		0.18	Mexico (Mexico)	IMCO [62]
Ku-Maloob-Zaap		0.11	Mexico (Mexico)	IMCO [62]

Source: Welsby (forthcoming)

These improvements led to a more accurate recalibration of actual production volumes of associated natural gas in the near-term. Additional capacity can be built in the model, with constraints placed on the build-out rates.

A2.2.3 Oil

Oil generally requires the most refining / upgrading / processing in the upstream sector before it can be sent further downstream (e.g. crude oil as a traded commodity, or derived naphtha as a feedstock into petrochemical production of plastics etc.). In particular for some forms of unconventional oil, a huge operation is required to upgrade the oil to 'useful' forms of energy (e.g. crude oil), which requires large scale investment in upgrading infrastructure and intensive energy inputs into the processes. For example, extra-heavy oil and bitumen oil require significant upgrading to reduce the viscosity of the oil from a tar-like liquid (hence the name tar-sands) to a less viscous compound which can be transported by pipeline. A significant part of the improvements made to the upstream sector of TIAM-UCL by McGlade [31] was to provide insights into the costs and availability of unconventional oil production.

---

[17] Associated natural gas is modelled differently, in the sense that the supply cost is the cost of separating and processing the natural gas to yield 'dry stripped gas'. This is because associated gas is based on oil extraction economics, and therefore a field level analysis was not possible. The TIAM-UCL energy systems model has been amended to include region-specific operational costs associated with separating and processing, as well as investment costs (CAPEX) for building new associated gas processing capacities if necessary.

[18] Oil and Gas Journal article. *Nigerian operator lets contract for gas processing plant*. https://www.ogj.com/refining-processing/article/17250582/nigerian-operator-lets-contract-for-gas-processing-plant (Accessed 20.02.20)

These costs and material[19] flows through the reference energy system could then be assessed until, for example, mined bitumen is upgraded to synthetic crude oil which can then be transported and/or used as a useful energy carrier. These upstream processes which upgrade and/or process the initial outputs of the mining process require energy inputs, which have a range of efficiencies and costs. Therefore the output commodity 'price' of these processes (useful energy carriers), will have a premium above the cost of the mining process. This was of particular importance for bitumen and extra-heavy oil, where the upgrading process can account for upwards of 50%[20] of the production cost (i.e. generating synthetic crude).

As mentioned in Section 1.4, TIAM-UCL has a detailed representation of the use of upstream energy fuels, whereby an energy commodity output from the upstream sector requires energy commodity inputs in order to produce a unit of output. An example of this would be the use of natural gas in in-situ and mined oil sands production, whereby the gas is used to generate steam/heated water which increases the temperature of the oil in the reservoir or separates the oil from the sand, increasing the viscosity which allows it to flow at sufficient rates[21]. Therefore, natural gas, electricity, etc. are all potential inputs into the upstream sector in TIAM-UCL which allows the upgrading of mined commodities into energy carriers which can be used further downstream. Each of these potential inputs incurs costs and efficiencies, examples of which are shown in Table A. 7, which shows a (simplified) section of the upstream for the production of crude oil from synthetic mined bitumen, as well as the upstream energy requirements (input commodities with subscript UPS_).

Table A. 7. Example of upstream transformation for mined oil sands into synthetic crude oil

Mining process	Output commodity	Primary transformation	Input commodity	Output commodity (efficiency)
Oil sands, mined bitumen	Oil sands	Production of synthetic oil from mined bitumen	Oil sands UPS_Natural gas UPS_Electricity UPS_Heat (Steam) UPS_Hydrogen UPS_Biofuels	Crude oil (72%) Heat Flared and vented natural gas CO_2 CH_4

[19] Including externalities associated with production of oil and gas, such as fugitive emissions, flaring, emissions from the upgrading process, etc.

[20] For example, McGlade (2013, p. 124) identifies the difference in costs (driven by energy requirements to upgrade, and the initial complexity/efficiency of the original mining process) between in-situ and mined bitumen, with mined the upgrading costs of mined bitumen reaching over 50% ($22/bbl) of the total production cost ($40/bbl). It should be noted these figures do not include fiscal regime costs.

[21] Canadian Energy Regulator website. *Market Snapshot: Natural gas plays an important role in Alberta's oil sands.* https://www.cer-rec.gc.ca/nrg/ntgrtd/mrkt/snpsht/2017/04-03ntrlgslbrtlsnd-eng.html?=undefined&wbdisable=true (Accessed 23.02.20)

A2.3 Secondary transformation in upstream sector

TIAM-UCL has a range of secondary transformation processes which produce refined petroleum products. As with the primary transformation processes, refinery activity in TIAM-UCL requires energy inputs, which have costs associated, as well as the efficiency of the technology. Table A. 8 gives a brief example of a secondary transformation process for a generic refining technology in TIAM-UCL, which produces (amongst other commodities) aviation fuel. Additionally, externalities of the process (i.e. emissions) are accounted for.

Table A. 8. Example of refinery process for secondary transformation in TIAM-UCL

Process	Region	Input commodity choice	Output	Efficiency	Investment cost, $M/PJ	Residual capacity (2005), PJ	Emissions intensity
Existing flexible refining	MEA_OPEC	Biofuels Natural gas Crude oil Natural gas liquids Refined petroleum products	Refinery gas Ethane Aviation fuels Naphtha Paraffin wax Oil lubricants Asphalt CO_2 CH_4 N_2O	0.88	6.84	11207	1600 t CO_2/PJ

A2.4 Fossil Trade

All traded commodities in TIAM-UCL must first be processed/transformed into 'transportable' energy carriers, as described in earlier sections. An underlying matrix is then defined by the user, which determines inter-regional trade flows. For flexible forms of transportation (i.e. by maritime transport), the number of trade links will thus be higher than more constrictive forms of trading energy commodities (e.g. by pipeline, which are not just restricted by cost but also by geopolitical and geographical constraints). Table A. 9a shows a representative trade matrix[22] for crude oil, with the number of trade links (represented by the number 1) significantly higher due to the flexibility of ocean tankers over pipelines[23], with the significantly lower number of trade links for natural gas via pipeline shown in Table A. 9b. The comments in Table A. 9b reflect some of the main uncertainty in pipeline

[22] Applied for all traded energy commodities

[23] Crude oil is also traded via pipeline, notably in Russia/Central Asia into Europe and China, and in North America (Canada-USA, USA-Mexico, etc.). Therefore, the activity costs of these trade processes in TIAM-UCL are reflected by the operation and maintenance costs of pipelines rather than crude oil tankers.

routes, with the several projects stalling over several years and with no final investment decision taken. Therefore, the decision whether to switch these trade links on/off rests with the user.

Table A. 9. Trade links between TIAM-UCL regions for a) crude oil and b) natural gas via pipeline

a)

~TradeLinks

OILCRD	AFR	AUS	CAN	CHI	CSA	EEU	FSU	GBL	IND	JPN	MEA	MEX	ODA	SKO	USA	WEU	UK	MINRNW	IMPEXP
AFR		1		1		1			1	1			1	1	1	1	1		
AUS				1						1									
CAN	1			1		1			1	1	1	1	1	1	1	1	1		
CHI																			
CSA	1			1		1			1	1		1	1	1	1	1	1		
EEU																			
FSU	1	1	1	1	1	1			1	1		1	1	1	1	1	1		
GBL																			
IND																			
JPN																			
MEA	1	1	1	1	1	1	1		1	1		1	1	1	1	1	1		
MEX															1				
ODA		1		1					1	1				1					
SKO																			
USA	1	1	1	1	1	1	1		1	1	1	1	1	1		1	1		
WEU															1		1		
UK			1												1	1			
MINRNW																			
IMPEXP																			

b)

~TradeLinks

GASNGA	AFR	AUS	CAN	CHI	CSA	EEU	FSU	GBL	IND	JPN	MEA	MEX	ODA	SKO	UK	USA	WEU	MINRNW	IMPEXP
AFR																	1		
AUS																			
CAN																1			
CHI														1					
CSA																			
EEU																	1		
FSU				1		1					1		1	1			1		
GBL																			
IND																			
JPN																			
MEA						1	1		1				1						
MEX																1			
ODA				1															
SKO																			
UK																	1		
USA			1									1							
WEU						1									1				
MINRNW																			
IMPEXP																			

Daniel Welsby: Take out for non-TAPI runs

Daniel Welsby: Constrain MEA_IND trade and no capacity start until 2025

Daniel Welsby: Dependent on the Iran Pakistan (India) pipeline being built

A2.4.1 Coal

It is assumed in TIAM-UCL that only higher grade coal is traded; i.e. sub-bituminous, bituminous and anthracite. All trade flows for coal have been recalibrated in the model to ensure that 2015-2020 flows of coal around the world are consistent with historical data [33–37,63–65]. As with natural gas (and oil) discussed subsequently, the trade of coal incurs costs, namely for its transportation via international shipping or across land-borders (i.e. by rail). The transportation costs, as with natural gas and oil, are determined based on average shipping/train capacities and rental rates, and the distance between the regions. However, unlike natural gas which requires processing, transformation and transportation infrastructure (e.g. liquefaction plants and pipelines), coal can be more easily transported and therefore no investment costs are required.

A2.4.2 Natural gas

Natural gas trade in TIAM-UCL is split between pipeline gas and liquefied natural gas (LNG). Both are constrained firstly by the underlying trade matrix shown above. Additionally, trade volumes and infrastructure have been calibrated to 2015/2020-2025, with **under construction** infrastructure (both pipeline and LNG) fixed to come online in the model by 2020/2025, depending on an estimated start-date [39–47]. For example, Figure A. 9 shows **under construction** regasification capacity for China between 2016 and 2022, which is used to bound the build rates of trade infrastructure capacity.

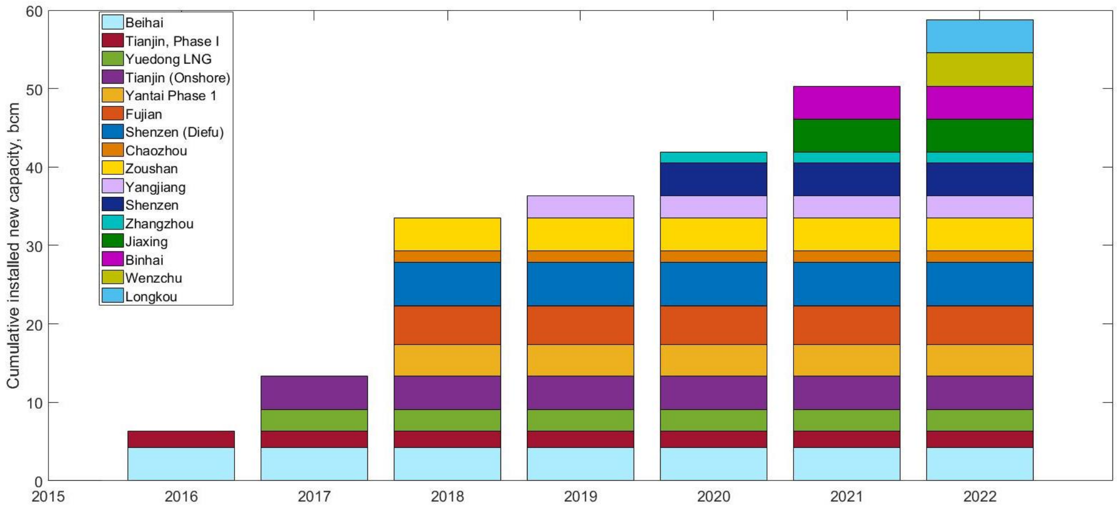

Figure A. 9. Under construction regasification capacity in China, 2016-2022 (Source: IGU, 2018; IGU, 2019; figure taken from Welsby [24]**).**

LNG

Liquefied natural gas trade in TIAM-UCL includes infrastructural parameters (liquefaction and regasification capacities and build constraints) and cost parameters (CAPEX on new infrastructure, OPEX on the liquefaction/regasification process, and a shipping cost).

Regionalised liquefaction costs have been included based on:

- Representative projects in each region, including the location of the liquefaction terminal and investment costs;
- Competition for E&P in recent years which led to real price inflation on projects built between 2010 and 2020 [66];
- Whether the project was a brownfield extension or conversion (e.g. conversion of regasification (import) terminals in the United States into liquefaction (export) facilities), or green-field integrated project (e.g. Yamal LNG field and export facility development in Russia, and several projects in Australia including Gorgon, Ichthys (floating), and Wheatstone).

Table A. 10 shows a range of investment costs for liquefaction terminals in TIAM-UCL, showing the cost inflation attributed to a large range of projects coming online at the same time, and the corresponding stabilisation of these costs. (For reference, these costs are an example and can be changed in the model to conduct sensitivity analysis). Table A. 10 clearly shows which regions have the potential to take advantage of cost de-escalation for brownfield conversions/expansions[67], i.e. the USA and the Middle East, before (at least in this example) costs converge across regions for green-field investments. Additionally, the amount of capacity which can be converted/expanded under these lower costs has been limited to existing regasification capacity and/or a maximum upper limit based on proposed brownfield extensions.

Table A. 10. Liquefaction investment costs by region and year in TIAM-UCL, $M/PJ

Year	AFR	AUS	CAN	CHI	CSA	EEU	FSU	IND	JPN	MEA	MEX	ODA	SKO	UK	USA	WEU
2006	6	6.1	6	6.1	6	5.9	6	6.1	6	5.8	6	6.1	6.1	5.9	5.8	5.9
2010	16	16	16	13.7	16	18.3	16	13.7	16	9.1	16	13.7	13.7	18.3	8.6	18.3
2015	9.9	20.4	16	13.7	16	18.3	16	13.7	16	9.1	16	13.7	13.7	18.3	8.6	18.3
2020	9.9	21.10	21.9	20.40	20.40	20.40	20.40	20.40	20.40	9.50	20.40	20.40	20.40	20.40	12.30	20.40
2025	25.30	21.10	21.9	20.40	20.40	20.40	20.40	20.40	20.40	9.50	20.40	20.40	20.40	20.40	12.30	20.40
2050	20.40	21.10	20.40	20.40	20.40	20.40	20.40	20.40	20.40	18.40	20.40	20.40	20.40	20.40	19.10	20.40

LNG VAROM (i.e. shipping) costs in TIAM-UCL are calculated based on a range of parameters (McGlade et al. [68]; Welsby [24]):

- Assumed distance between ports
- Average speed of tanker
- Average capacity of tanker; calculated based on average capacity of tankers which are assigned to fixed routes and/or average size of delivery
- Daily rental rate of tanker (the rental rate is highly volatile depending on available capacities in each basin and seasonal spikes in LNG demand (Platts, 2018), however for a long-term energy systems model a fixed figure is assumed based on McGlade et al. [68].
- Boil-off rate (i.e. efficiency of transportation process translated into losses of natural gas), which in turn is a function of journey time
- Loading/unloading time at each port

As part of the Welsby's thesis [24] a significant database of LNG transportation costs was constructed, with representative average shipping costs between the TIAM-UCL regions used if more than one trade route is used. An example of these shipping costs between individual liquefaction and regasification terminals is shown in Table A. 11 below. For reference, the exporters are in red, and the zeros reflect that a) there is no intra-regional trade in TIAM-UCL and b) some regions are exogenously determined (through the trade link matrix shown earlier) not to be able to trade with each other.

Table A. 11. Representative shipping costs for LNG between TIAM-UCL regions, $M/PJ

	AFR	AUS	CAN	CHI	CSA	EEU	FSU	IND	JPN	MEA	MEX	ODA	SKO	UK	USA	WEU
AFR	0	0	0	1.09	0.26	0	0	0.84	1.28	0.63	1.06	1.02	1.19	0.83	0	0.81
AUS	0	0	0	0.75	0	0	0	0.96	0.8	0	0	0.73	0.8	0	0	0
CAN	0	0	0	0.85	0	0	0	1.2	0.81	0	0.62	0.85	0.82	0	0	0
CHI	0	0	0	0	0	0	0	0	0	0	0	0	0	0	0	0
CSA	0	0	0	1.07	0	0	0	0.97	1.14	0.91	0.78	1.15	1.12	0.81	0	0.8
EEU	0	0	0	0	0	0	0	0	0	0	0	0	0	0	0	0
FSU	0	0	0	0.72	0	0	0	1.39	0.59	0	0	1.38	0.66	0.81	0	0.8
IND	0	0	0	0	0	0	0	0	0	0	0	0	0	0	0	0
JPN	0	0	0	0	0	0	0	0	0	0	0	0	0	0	0	0
MEA	0	0	0	0.83	0.81	1.02	0	0.6	0.94	0	1.28	0.74	0.92	0.97	0	0.85
MEX	0	0	0	0	0	0	0	0	0	0	0	0	0	0	0	0
ODA	0	0	0	0.66	0	0	0	0.71	0.73	0	0	0	0.69	0	0	0
SKO	0	0	0	0	0	0	0	0	0	0	0	0	0	0	0	0
UK	0	0	0	0	0	0	0	0	0	0	0	0	0	0	0	0
USA	0	0	0	1.09	0.84	0.91	0	1.21	1.11	0	0.72	1.1	1.09	0.85	0	0.9
WEU	0	0	0	0	0	0.63	0.64	0	0	0	0	0	0	0	0	0

Source: Welsby [24]; McGlade et al. [68]

User constraints for natural gas trade through LNG are employed for both the technology which covers overall export capacity (i.e. the liquefaction process technology) and the bilateral trade process itself. In short, this constrains the model from building new capacity over the space of a time-slice and sending all of the potential output in a single trade link. Equation 1.1 shows the formula for the user constraints on growth of LNG liquefaction capacity (the same functional form is utilised for individual trade routes).

$$LiquefactionCap_{r,t} = LiquefactionCap_{r,t-1} * LiquefactionGro^{ts} + Seed_{r,t} \tag{1.1}$$

For individual LNG trade routes, it is assumed that trade between two regions can double across each time-slice, with seed values (for initial growth or to allow some additional slackness on the constraint) based either on historical contract data or historical trade volumes [24].

Pipeline

For pipeline investment costs and capacity additions in the near-term, individual project costs and capacity have been added where appropriate (e.g. pipeline cost and maximum volume from Russia to China between 2015 and 2020 are based on the under-construction Power of Siberia pipeline, which is due to come online in 2020). Some examples of pipeline investment costs are shown in Table A. 12, with each pipeline at different development stage [24]. However, other factors need to be taken into account including whether the pipeline has to cross challenging physical barriers (e.g. a sea or mountainous territory).

Table A. 12. Pipeline investment costs for a range of representative projects used in TIAM-UCL

Pipeline Name	Status	Investment Cost, $M/PJ	Investment Cost, $MM/km
Power of Siberia	Under-construction	10.38-23.02	5.27-11.67
Central Asia-China	Operational	3.51	3.99
TAPI	Proposed	6.66-8.33	7.11-8.89

Additionally, a user constraint has been added as an upper bound on potential gas pipeline trade, with a similar functional form as the upstream constraints discussed in Section A2.5. In short, it is assumed that the model can, at a maximum double capacity across a ten year period for any trade route (e.g. add a new pipeline parallel to an existing one with the same capacity). Therefore, an exponential growth constraint is set in the following form shown in Equation 1.2:

$$PipeCap_{a \to b,t} \leq PipeCap_{a \to b,t-1} * PipeGro^{ts} + Seed_{r,t} \tag{1.2}$$

Where,

$PipeCap_{a \to b,t}$ = pipeline capacity between exporter *a* and importer *b*, in time period *t*

$PipeCap_{a \to b,t-1}$ = pipeline capacity between exporter *a* and importer *b*, in time period *t-1*, i.e. the preceding time period

$PipeGro^{ts}$ = pipeline growth coefficient, set at ~1.07 (i.e. allows a doubling of capacity over 10 years using the above formulation)

$Seed_{r,t}$ = seed value for region *r* and time-period *t*, which allows growth value to take hold if there is no historical trade link, or adds on to the growth constraint for absolute upper bound (i.e. slackness on the constraint). The seed value is added across the time-slice, rather than in each individual year. As with LNG, this is based on a maximum capacity addition across a time-slice.

For regions where volumes of trade are already well established and there is significant pipeline capacity in place, the seed value has been set to zero from 2020 (e.g. between the UK and Western Europe, and the USA and Canada). A seed value is included in these cases between 2006 and 2015 in case large increases in gas pipeline trade were in evidence, such as between the United States and Mexico after the expansion of shale gas in the Barnett shale play. In short, the seed value allows the model to expand trade up to the upper bounds which have been added for 2015 to calibrate natural gas trade to historical data. However, some trade links have a seed value from 2020 to allow the model to expand pipeline capacity over the growth coefficient alone. For example, the seed value for gas pipeline trade between the Former Soviet Union and China is bounded (upper) by the growth coefficient (1.07/a) and a seed value equivalent to the under-construction Power of Siberia pipeline operating between a minimum (70%) and maximum (90%) contracted quantity.

A2.4.3 Oil

The trade of oil commodities is split into various different products, which are outputs of processing/transformation processes in the upstream: crude oil, heavy fuel oil, naphtha, natural gas liquids[24], diesel. As with natural gas trade via LNG tankers, the variable cost of transporting oil via tankers is assumed to be a function of the distance between ports, the speed of the tanker, and the average capacity of a ship travelling from the exporter to the importer.

A2.5 Key upstream constraints

A2.5.1 Coal

Upstream constraints for coal extraction are not as widely applied for two main reasons:

1. The extraction of coal does not follow the same geological production profile of oil and gas extraction; i.e. the growth and decline of production profiles through time and different geological structures. As coal resources become depleted, the energy inputs required for extraction become more intensive, and increasingly risk intensive, and inefficient, production methods are employed (e.g. mountain top removal).
2. For decarbonisation scenarios meeting 2°C and below (a significant focus of recent work using TIAM-UCL), coal is rapidly phased out of the energy mix. Additional scenarios have been run by Welsby [24] which pushes the model to slow down the rate at which coal can be phased out,

[24] Longer chain hydrocarbons which are separated from the gas stream in processing plants, most of which form liquids at surface temperature and pressure, and includes ethane, propane, butane (Schlumberger, 2019)

before negative emissions (other than biomass with carbon capture and storage (BECCS)) are required.

A2.5.2 Oil and natural gas

As with natural gas (discussed subsequently), there are upstream user constraints which control the rate at which production of different categories of oil can grow/decline. In short, these user constraints model the natural growth and decline of oil and natural gas. The predominant form of constraint for these mining technologies is an exponential (constant) rate of growth/decline across a time-slice, using seed values if there is no residual (historical) productive capacity. Equation 1.3 shows the functional form of these growth (a) and decline (b) constraints, for mining technologies with historical production, and Equation 1.3 (c) and (d) shows the same equations for technologies which are new and require a seed value.

$$Production_{i,t} \leq (Production_{i,t-1} * Growth^{ts}) + Seed_{i,t} \tag{1.3 (a)}$$

$$Production_{i,t} \geq (Production_{i,t-1} * Decline^{ts}) + Seed_{i,t} \tag{1.3 (b)}$$

$$Production_{i,t} \leq Seed_{i,t} * Growth^{ts} \tag{1.3 (c)}$$

$$Production_{i,t} \geq Seed_{i,t} * Decline^{ts} \tag{1.3 (d)}$$

Where,

$Production_i$ = production of oil/gas for mining process i

$Seed_i$ = seed value from which growth/decline coefficients are assigned to if no historical (i.e. t-1) volumes, and which is added[25] to overall growth/decline constraint across each time-slice

t = time period in the model (therefore t-1 is the previous time-slice)

Growth = growth coefficient, where *Growth* ≥ 1

Decline = decline coefficient, where *Decline* ≤ 1

ts = time-slice length (i.e. $t - (t\text{-}1)$)

Therefore, for growth constraints, the production of an oil and/or gas mining technology in time slice *t* will be bounded (upper) by a maximum of production in time slice *t-1* multiplied by the growth coefficient to the power of the length of the time-slice. For decline constraints, the inverse applies: production in *t* will be bounded (lower) by a minimum of production in *t-1* multiplied by the decline coefficient to the power of the time-slice length.

Table A. 13 shows examples of the growth/decline coefficient parameters and seed values used in TIAM-UCL, for a range of oil (a) and gas (b) mining technologies.

Table A. 13 (a): User constraints for a range of oil mining technologies in TIAM-UCL

[25] N.B. for decline user constraints, the seed value is negative, therefore any addition is actually a subtraction to the production level relative to *t-1*

Mining technology	Growth coefficient	Decline coefficient
Conventional proved reserves	1.41 ($\sqrt{2}$)	0.93
Conventional reserve additions	1.41 ($\sqrt{2}$)	0.93
Conventional undiscovered	1.41 ($\sqrt{2}$)	0.93
Shale oil	1.07	0.8
Mined bitumen	1.07	0.8
In-situ bitumen	1.1	0.85

(b): User constraints for a range of gas mining technologies in TIAM-UCL

Mining technology	Growth coefficient	Decline coefficient
Conventional proved reserves	1.41 ($\sqrt{2}$)	0.95[26]
Conventional reserve additions	1.41 ($\sqrt{2}$)	0.92
Conventional undiscovered	1.41 ($\sqrt{2}$)	0.92
Shale gas	1.27	0.83
Tight gas	1.12	0.83
Coal bed methane	1.12	0.83

For example, shale gas decline rates were calculated using well-level data from the United States (Marcellus). Over 950 shale gas wells were assessed over a 10 month period; the rate of decline for these wells, when aggregated, best fit a hyperbolic profile. The rate of change between the first year and last year was then calculated to give a constant annual rate of decline. In order to generate a decline parameter which fits the formulation of user constraints in TIAM-UCL (Equations 1.3 (a-d)), this annual decline rate was then re-calculated to an equivalent rate of decline but as a constant exponential rate of decline. For the shale gas wells examined, this translated as a decline coefficient of ~ 0.83, which when raised to the power of 5 (assuming a five year time-slice), gives a maximum rate of decline of ~ 60% between *t-1* and *t*.

Additional constraints have been input as a proxy for controlling the expansion of associated natural gas. Whilst the production itself is a function of oil extraction (and oil economics), the infrastructural issues surrounding associated gas utilisation require some degree of user constraint. Therefore an

[26] Regional variations are taken into account; therefore the numbers above may differ between regions. Additionally, the decline rate for conventional oil and gas fields will vary depending on the size of the field, the stage of decline, and the geological structure of the reservoirs (IEA, 2009). For example, larger fields generally exhibit slower rates of production decline, as shown with the value for conventional proved gas reserves which is taken from a representative decline parameter calculated from super-giant gas fields in the Former Soviet Union (e.g. Urengoy) (Welsby, forthcoming).

upstream constraint is placed on the speed at which associated gas processing and separation capacity can be added.

Appendix 3. Climate module

The climate module used in the model enables the translation of greenhouse gas emissions from the energy system into atmospheric concentrations, radiative forcing and temperature change, which can in turn be constrained in scenarios. The module is mainly based on that developed by ETSAP [69], but has been subsequently recalibrated to the MAGICC model results [2]. The recalibration has been conducted by stages following the different variable calculations needed to obtain the temperature change from greenhouse gas emissions.

1) from emissions to atmospheric concentrations

2) from concentrations to radiative forcing

3) from radiative forcing to realised temperature

The full climate module, and the improvements introduced during the three steps is checked against the results from MAGICC. Different trajectories of future emissions were used in this calibration work, using scenarios based on the Representative Concentration Pathways (RCPs), specifically scenarios RCP3-PD, RCP4.5 and RCP8.6 [70]. RCP8.5 is a rising radiative forcing pathway leading to 8.5W/m2 in 2100; RCP4.5 is a stabilisation pathway without overshoot, resulting in 4.5W/m2 after 2100 (4.1W/m2 in 2100); RCP3-PD (or RCP2.6) sees a peak in radiative forcing before 2100 at 3W/m2 and decline after (2.6W/m2 in 2100). The purpose of using these different trajectories (two with increasing emissions/forcing and one with deceasing emissions/forcing after a peak) is to check how the simple module responds to different emission trajectories.

The climate module uses emissions both from the energy system (endogenous) other non-CO2 GHG emissions from other sectors not explicitly represented (exogenous). Successively, it calculates changes in the concentration of CO_2, CH_4 and N_2O, the change in radiative forcing over pre-industrial times from all three gases plus an exogenously defined additional forcing (for the other GHGs and radiatively active parameters such as aerosols and clouds) and finally the temperature change over pre-industrial times for the atmosphere and the deep ocean. Figure A. 10 provides a graphical overview of the module's structure.

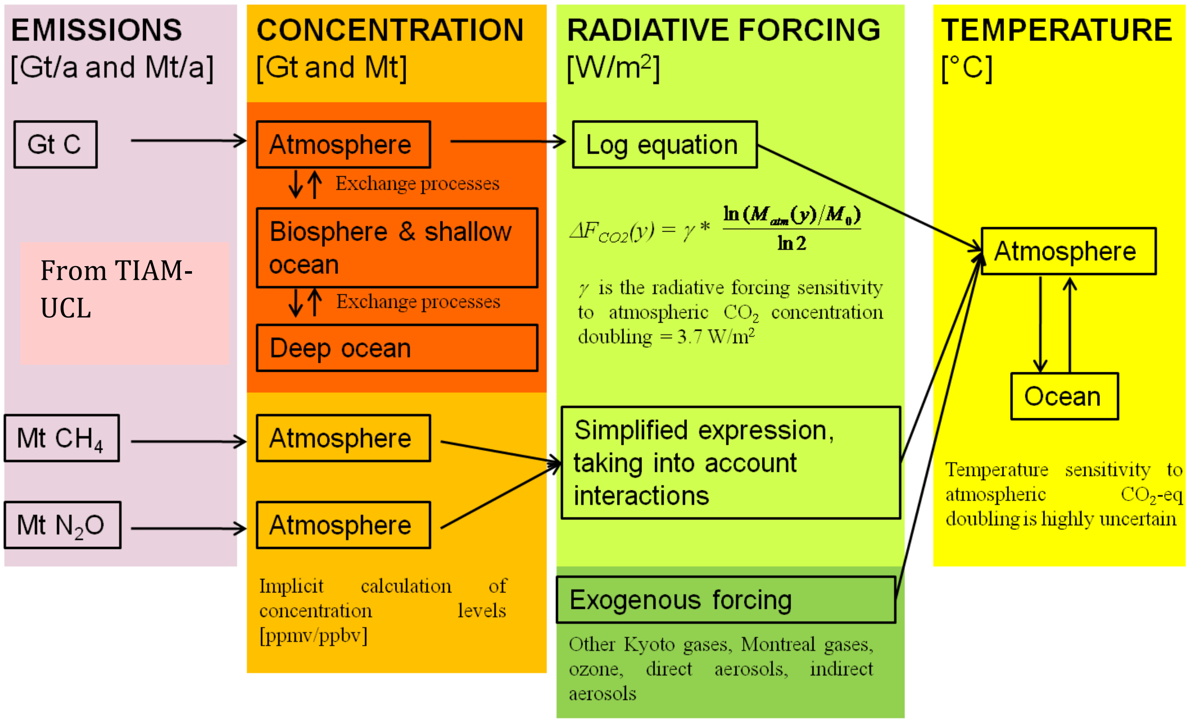

Figure A. 10. Illustration of the TIAM climate module

The underlying mathematical structure of the module is based on a linear recursive approach from Nordhaus and Boyer [71]. This is a well-documented, albeit simple approach, which gives a good approximation of more complex climate models [69]. Instead of converting non-CO_2 greenhouse gases into CO_2-equivalents and calculating concentrations and radiative forcing on this basis, the module models the life cycle of each endogenous emission separately.

Concentration

Carbon dioxide

The mass concentration of CO_2 is calculated with a three-reservoir model for the carbon cycle, including the atmosphere (ATM) , the biosphere and upper ocean (UP) , and the deep ocean (LO). CO_2 flows are modelled in both directions between adjacent reservoirs. The reservoirs are represented by the following equations, where the step of recursion is one year, *y*, and not a model period:

$$M_{atm}(y) = E(y) + (1 - \varphi_{atm-up})M_{atm}(y-1) + \varphi_{up-atm}M_{up}(y-1) \quad \textbf{(1)}$$

$$M_{up}(y) = (1 - \varphi_{up-atm} - \varphi_{up-lo})M_{up}(y-1) + \varphi_{atm-up}M_{atm}(y-1) + \varphi_{lo-up}M_{lo}(y-1) \quad \textbf{(2)}$$

$$M_{lo}(y) = (1 - \varphi_{lo-up})M_{lo}(y-1) + \varphi_{up-lo}M_{up}(y-1) \quad \textbf{(3)}$$

where $M_{atm}(y)$, $M_{up}(y)$, $M_{lo}(y)$ are the masses of carbon (not carbon dioxide) in the atmosphere, the quickly mixing reservoir of the biosphere and upper ocean, and in the deep ocean in year *y*. All masses are given in Gigatons (Gt) of carbon (C). This can be converted into a relative concentration in parts per million (ppm) by using the conversion factor of 2.13 ppmv/Gt C. $E(y-1)$ are the CO_2 emissions in the previous year in GtC. Finally $\varphi_{i,j}$ is the transport rate from reservoir *i* to reservoir *j* from year *y-1* to *y*.

Methane

The mass concentration of methane is represented in a simplified single-box model, where the atmospheric concentration is calculated in the following way assuming a constant annual decay rate:

$$CH4_{atm}(y) = EA_{CH4}(y) + (1 - \Phi_{CH4})CH4_{atm}(y-1) \quad \textbf{(4)}$$

where $CH4_{atm}(y)$ is the atmospheric concentration in Mt CH_4, and $EA_{CH4}(y)$ represents anthropogenic emissions of CH_4 in year y in Mt/year. Φ_{CH4} is the one-year retention rate of CH_4 in the atmosphere. Atmospheric mass concentration can be expressed in ppb by using the conversion factor of 2.84 ppbv/Mt CH_4.

Nitrous oxide

The mass concentration of nitrous oxide is calculated in the same way as for methane. Equally, a single-box is used where atmospheric N_2O mass concentration is calculated in the following way:

$$N2O_{atm}(y) = EA_{N2O}(y) + (1 - \Phi_{N2O})N2O_{atm}(y-1) \quad \textbf{(5)}$$

where $N2O_{atm}(y)$ is the atmospheric concentration in Mt N_2O, and $EA_{N2O}(y)$ represents anthropogenic emissions of N_2O in year y in Mt/year. Φ_{N2O} is the one-year retention rate of N_2O in the atmosphere. Atmospheric mass concentration can be expressed in ppb by using the conversion factor of 7.81 ppbv/Mt N_2O.

Radiative forcing

Radiative forcing in the TIAM climate module is assumed to be additive for the various gases, as is usually assumed in science [72]:

$$\Delta F(y) = \Delta F_{CO2}(y) + \Delta F_{CH4}(y) + \Delta F_{N2O}(y) + EXOFOR(y) \quad \textbf{(6)}$$

The calculation of the different elements of the sum in the above equations is explained in more detail below.

Carbon Dioxide

Radiative forcing caused by the accumulation of carbon dioxide in the atmosphere is derived from a widely used relationship [73]:

$$\Delta F_{CO2}(y) = \gamma * \frac{\ln{(M_{atm}(y)/M_0}}{ln2} \quad \textbf{(7)}$$

Where M_0 is the pre-industrial (circa 1750) reference atmospheric concentration of CO_2 of 596.4 GtC. γ is the radiative forcing sensitivity to atmospheric CO_2 concentration doubling, which is usually assumed to be 3.7 W/m^2 [73]. However the linear character of TIAM-UCL has once again constrained the modeller to the use of a linear approximation of the logarithmic curve that will be introduced later.

Methane and Nitrous Oxide

The radiative forcing due to accumulation of CH_4 in the atmosphere is based on an equation given in Ramaswamy et al. [73]. This considers interactions between CH_4 and N_2O:

$$\Delta F_{CH4}(y) = 0.036 * \left(\sqrt{CH4_y} - \sqrt{CH4_0}\right) - \left[f\left(CH4_y, N2O_0\right) - f\left(CH4_0, N2O_0\right)\right] \quad \textbf{(8)}$$

$$\Delta F_{N2O}(y) = 0.12 * \left(\sqrt{N2O_y} - \sqrt{N2O_0}\right) - \left[f\left(CH4_0, N2O_y\right) - f\left(CH4_0, N2O_0\right)\right] \quad \textbf{(9)}$$

where:

$$f(x, y) = 0.47 * ln[1 + 2.01 * 10^{-5} * (xy)^{0.75} + 5.31 * 10^{-15} * x(xy)^{1.52}] \quad \textbf{(10)}$$

N2O and *CH4* represent the mass concentration of nitrous oxide and methane respectively in Mt, while the subscript *0* indicates pre-industrial times (1750). $CH4_0$ is 1988 Mt CH_4 and $N2O_0$ is 2101 Mt N_2O.

The representation of the radiative forcing from these two species in TIAM-UCL is a simplification to a linear function with constant coefficients. The absorbance interaction between the two gases is just taken into account via the calibration to the MAGICC values. The linear functions used in TIAM for the two non-CO2 greenhouse gases are:

1) $\Delta F CH_4(y) = \alpha CH_4 + \beta CH_4$ [CH4]

2) $\Delta F N_2O$ (y) = $\alpha N_2O + \beta N_2O$ [N2O].

Table A. 14. TIAM climate module coefficients for the greenhouse gases radiative forcing calculations: CH_4 and N_2O in the CMLINFOR equation

CMLINFOR		Default values
CH4-PPB (N)	αCH_4	0.0003
CH4-PPB (FX)	βCH_4	-0.085
N2O-PPB (N)	αN_2O	0.003
N2O-PPB (FX)	βN_2O	-0.8

Exogenous forcing

EXOFOR(y) stands for the increase in total radiative forcing in year y in comparison to pre-industrial levels due to gases that are not taken into account in the model. TIAM accounts for CO_2, N_2O and CH_4, but does not cover other Kyoto gases, Montreal gases, ozone, water vapour, and aerosols. Such perturbations can be direct emissions such as CFCs (from cooling, refrigeration or firefighting systems) or black carbon aerosols (from carbon base fuel burning) that have a direct effect on the radiative forcing. Other perturbation may change some characteristic of the atmosphere such as its chemistry (ozone production from NOx and VOCs emissions) or its microphysics (cloud seeding from aerosols or aviation contrails) will also indirectly impact on the radiative characteristics of the atmosphere (greenhouse gases composition or albedo). Therefore, it is the analyst's responsibility to adjust *EXOFOR(y)* to the extent that it represents additional radiative forcing that is not captured within TIAM. After comparison of the RCPs radiative forcing data for these parameters, a rapid simplification allows us to regroup the three first scenarios (RCP3PD, RCP4.5 and RCP6) in one unique behaviour and keep RCP8.5 (high intensive energy use from fossil fuels) separate. The values are summarised in the table below.

Table A. 15. Simplified values of radiative forcing values for extra anthropogenic forcing to CO_2, CH_4 and N_2O contributions to be used in TIAM scenarios

EXOFORC	Non-RCP8.5	RCP8.5
2005	-2.66e-01	-2.66e-01
2025	-1.00e-01	
2040		1.00e-01
2095	-1.00e-01	2.25e-01

Linear approximation for CO2 radiative forcing.

As TIAM does only use linear equations, each of the three forcing expressions is replaced by a linear approximation. Two linear functions are used to approximate the concave functions, one is the chord from below and the other one is the tangent from above. Finally, the arithmetic average of both linear functions is used to approximate the original non-linear radiative forcing function. In order to keep the approximation accurate, an interval of concentration has to be specified by the analyst.

The TIAM-UCL linear function for the CO_2 radiative forcing is:

$\Delta F_{CO_2}(y) = \alpha + \beta\,[CO_2](y)$

(α and β calculated for concentrations in a given interval for the year y and have to be chosen interactively by the modeller prior the start of the calculation).

Temperature increase

An increase of the global mean surface temperature is a widely used figure to quantify climate change. The climate module in TIAM uses a two-reservoir model to represent global warming. Radiative forcing heats up the atmosphere and is then transmitted to the quickly mixing upper ocean. Both, the upper ocean and the atmosphere form one reservoir. The upper ocean then slowly warms the deeper layers of the ocean, which forms the second reservoir. An increase in the global mean temperature is described by the influence of radiative forcing and the exchange processes as follows:

$$\begin{aligned}\Delta T_{up}(y) = {} & \Delta T_{up}(y-1) \\ & + \sigma_1\{F(y) - \lambda\Delta T_{up}(y-1) - \sigma_2[\Delta T_{up}(y-1) - \Delta T_{low}(y-1)]\}\end{aligned} \tag{11}$$

$$\Delta T_{low}(y) = \Delta T_{low}(y-1) + \sigma_3[\Delta T_{up}(y-1) - \Delta T_{low}(y-1)] \tag{12}$$

where ΔT_{up} is the global mean surface temperature increase above pre-industrial levels and ΔT_{low} is the deep-ocean mean temperature increase above pre-industrial levels. σ_1 is the one-year speed of adjustment parameter for atmospheric temperature (lag parameter), σ_2 is the coefficient of heat loss from atmosphere to deep oceans, and σ_3 represents the one-year coefficient of heat gain by deep oceans. λ is the feedback parameter; it is defined as the ratio $\lambda=\gamma/C_S$, where C_S is the climate sensitivity parameter, defined as the change in equilibrium atmospheric temperature provoked by a doubling of the atmospheric CO_2 concentration. In contrast to most other parameters, C_S is highly uncertain with a possible range from 1°C to 10°C with a consensus estimate of approximately 3 °C ± 1.5 °C (high confidence in AR5).

Climate module parameters

Table A. 16. Default values of all parameters of the climate module

Parameter	Year	Default value	Unit
CO2-ATM	2005	807.27	Gt Carbon
CO2-UP	2005	1600	Gt Carbon
CO2-LO	2005	10010	Gt Carbon
Δ_{UP}	2005	0.86	°C
Δ_{LO}	2005	0.07	°C
$CH4_{up}$	2005	1850	Mt CH_4
$CH4_{atm}$	2005	3150	Mt CH_4
$N2O_{up}$	2005	2103	Mt N_2O
$N2O_{atm}$	2005	390	Mt N_2O
γ		3.7	W/m^2
φ_{up-atm}		0.0048	-
φ_{atm-up}		0.0127	-
φ_{lo-up}		0.000075	-
φ_{up-lo}		0.0005	-
λ		1.34	(W/m^2)/°C
C_S		2.9	°C
σ_1		0.043	
σ_2		0.31	
σ_3		0.005	
ϕ_{CH4}		0.087	-
ϕ_{N2O}		0.0081	-

Appendix 4. Power generation sector techno-economic data.

Key cost and efficiency assumptions are provided in Table A. 17 below.

Table A. 17: Power generation technology assumptions: costs and efficiencies

Technology	CAPEX, $2005 /kW					Efficiency, %			
	2010	2020	2030	2040	2050	2010	2020	2030	2050
MSW combustion	5236	4862	4488		4114	23	27	30	33
Bioenergy combustion	2618	2431	2244		2057	28	31	34	37
Bioenergy combustion (dcn)	2880	2674	2468		2263	28	31	34	37
Bioenergy gasification	3080	2860	2640		2420	31	34	37	40
Bioenergy gasification (dcn)	3388	3146	2904		2662	31	34	37	40
Coal IGCC	2376					44	48	51	54
Coal super critical	1870					41	42	42	42
Coal ultra super critical	2277					46	48	49	50
Gas CCGT	990					56	59	61	63
Oil generation (dcn)	659					31	31	31	31
Oil generation	495					38	39	40	42
Coal IGCC w/CCS		3802	3564		3326		38	43	48
Coal USC w/CCS		3643	3416		3188		39	42	46
Gas CCGT w/CCS		1584	1485		1386		49	53	57
Geothermal shallow	2376	2310	2255	2200	2129				
Geothermal deep	3911	3644	3383	3108	2846				
Geothermal very deep		4978	4510	4015	3564				
Hydro dam	1650-6050	1623-5913	1595-5775	1568-5638	1540-5500				
Solar CSP	5850	3330	2700	2385	2070				
Solar PV	2587	923	633		376				
Tidal	6600	5500	4400		3432				
Offshore wind		2921	1749	1047	627				
Onshore wind		1314	969	715	527				
Nuclear Advanced LWR	3726	3524	3443		3240				
Storage	3300	1336	1034	688	472	80	80	80	80

Source: Fossil and CCS technologies (Ekins et al. (2017) [17]; Rubin et al. (2015) [74]); CCS is available from 2030, and can see capacity growth of 5% per annum. Power generation technologies have capture rates of 90%, which do not improve over time. Future solar PV and wind reductions based on BNEF estimates (unpublished), recent cost estimates based on IRENA [75]. The maximum build rate of new solar PV and wind capacity each year is set at 30% of existing capacity in line with recent solar PV build rates [76]. Range for hydro denotes different resource tranches and cost of exploitation. In the above table, 'dcn' denotes 'decentralised'.

Appendix 5. Hydrogen techno-economic data.

Table A. 18. Hydrogen production technologies

Technology	Size	Fixed O&M costs (% capital costs)	Capital investment costs ($2005/GJ/y)			Fixed O&M costs ($2005/GJ/y)			Efficiency		
			2000	2025	2050	2000	2025	2050	2000	2025	2050
Coal gasification	Large	0.05	30.909	27.475	24.040	1.545	1.374	1.202	65%	65%	65%
SMR	Large	0.04	8.586	6.869	5.151	0.343	0.275	0.206	80%	85%	85%
SMR	Medium	0.04	20.606	17.172	13.737	0.824	0.687	0.549	75%	80%	80%
SMR	Small	0.04	77.272	17.172	13.737	3.091	0.687	0.549	65%	80%	80%
Biomass gasification	Large	0.07	25.757	25.757	25.757	1.803	1.803	1.803	50%	50%	50%
Biomass gasification	Medium	0.07	51.515	34.343	34.343	3.606	2.404	2.404	50%	50%	50%
Biomass gasification	Small	0.07	77.272	42.929	42.929	5.409	3.005	3.005	50%	50%	50%
Biomass oil pyrolysis	Medium	0.07	51.515	34.343	34.343	3.606	2.404	2.404	50%	50%	50%
Waste gasification	Medium	0.07	51.515	34.343	34.343	3.606	2.404	2.404	50%	50%	50%
Nuclear	Large	0.06		68.686	68.686		4.121	4.121		75%	75%
Electrolysis	Medium	0.05	30.909	17.172	17.172	1.545	0.859	0.859	75%	85%	90%
Electrolysis	Small	0.05	111.615	27.475	17.172	5.581	1.374	0.859	75%	85%	90%

Table A. 19. Hydrogen delivery technologies and data

Refuelling station							
Technology	start year	AF	Input H2	Input electricity	$/GJ/yr (2005)	FIXOM $/GJ/yr (2005)	Life
LH2-GH2 medium	2005	0.98	1	0.0202	46	2.3	20
LH2-GH2 medium	2025	0.98	1	0.0202	35	1.75	20
LH2-GH2 medium	2025	0.98	1	0.0202	27	1.35	20
GH2-GH2 medium	2005	0.98	1	0.068	51	1.7	20
GH2-GH2 medium	2025	0.98	1	0.068	35.5	1.275	20
GH2-GH2 medium	2025	0.98	1	0.068	26	0.95	20
GH2-GH2 medium-Distributed production	2005	0.98	1	0.068	65	3.25	20
GH2-GH2 medium-Distributed production	2025	0.98	1	0.068	51.5	2.575	20
GH2-GH2 medium-Distributed production	2025	0.98	1	0.068	35	1.75	20
Liquefaction medium	2005	0.96	1	0.301	25.757	1.80	20
Liquefaction medium	2050	0.96	1	0.301	17.171	1.202	20
Liquefaction large	2005	0.96	1	0.189	25.757	1.80	20
Liquefaction large	2050	0.96	1	0.189	10.3	0.721	20
Road tankers							
Road tanker (distance 100 km, delivery 240 days/year)	2005	0.98	1.0038		4.707	0.471	20
Road tanker (distance 100 km, delivery 240 days/year)	2025	0.98	1.0038		4.297	0.471	20
Road tanker (distance 800 km, delivery 72 days/year)	2005	0.98	1.1022		15.692	1.571	20
Road tanker (distance 800 km, delivery 72 days/year)	2025	0.98	1.1022		14.323	1.571	20
Road tanker (distance 800 km, delivery 72 days/year)	2050	0.98	1.1022		11.617	1.571	20
Pipelines							

Local pipeline (100 km)	2005	0.69	1.0638		16.524	0.414	80
Local pipeline (100 km)	2025	0.69	1.0638		15.767	0.395	80
Distribution pipeline (800 km)	2005	0.69	1.125		7.986	0.246	80
Distribution pipeline (800 km)	2050	0.69	1.125		7.089	0.218	80

Appendix 6: Techno-economic assumptions on BECCS technologies

Table A. 20. Techno-economics of BECCS, assumptions in TIAM-UCL v4.1.1

Technology Group	Technology Group	Start time	Life yr	Efficiency %		Investment cost $/kW		Fix cost $/kW		Variable cost $/GJ		Availability/ capacity factor	CO_2 Capture rate %	Build rate %
	Year			2030	2050	2030	2050	2030	2050	2030	2050			
Electricity	Energy Crop Combustion w CCS	2030	25	26	31	3060	2618	175	131	6.9	6.6	0.85	90	5
	Energy Crop Gasification w CCS			29	34	3600	3080	206	173	1.7	1.7			
	Solid Biomass Combustion w CCS			26	31	3060	2618	175	131	6.9	6.6			
	Solid Biomass Gasification w CCS			29	34	3600	3080	206	154	1.7	1.7			
Heat	Heat from biomass with CCS	2030	30	63	65	1671	1419	189				0.6	90	3
Hydrogen	Hydrogen from biomass gasification + CCS	2030	30	42	44	4594	3516	322	246			0.9	90	5
Advanced transport fuels	FT process w CCS using solid biomass	2030	30	34	42	3630	2509	218	150	5.9	3.9	0.9	50	5
	FT process w CCS using biomass co-fired with coal (50-50)			41	46	2636	1859	170	118	4.3	2.8			
	FT process w CCS using biomass co-fired with coal (20-80)			41	46	2636	1859	141	99	3.3	2.2			
	FT process w CCS using energy crops			34	42	3630	2509	218	150	5.9	3.9			

Note that the same processes are also available in the technology database without CCS. The efficiency of bioenergy w/o CCS is 10% higher than of those with CCS, and the investment costs are roughly 50% smaller. Also note that biotechnologies w/o CCS in TIAM-UCL can take any type of biomass feedstock, including waste fractions.

Appendix 7: Assumptions on biomass availability and cost

Biomass costs in 2050 vary between 4 and 16 $/GJ for solid biomass, and between 6 and 15 $/GJ for energy crops depending on the region. These costs do not include a potential increase of land costs due to increased bioenergy demand [77]. Note that all costs are considered in 2005 USD. The waste fraction costs are included in TIAM using an import cost, ranging between 6 and 8 $/GJ, for bringing the commodity into the energy system. The costs of processing these waste streams into energy feedstock are included as operational costs of the different processing technologies that deal with that waste on the upstream side of the subsequent energy chains.

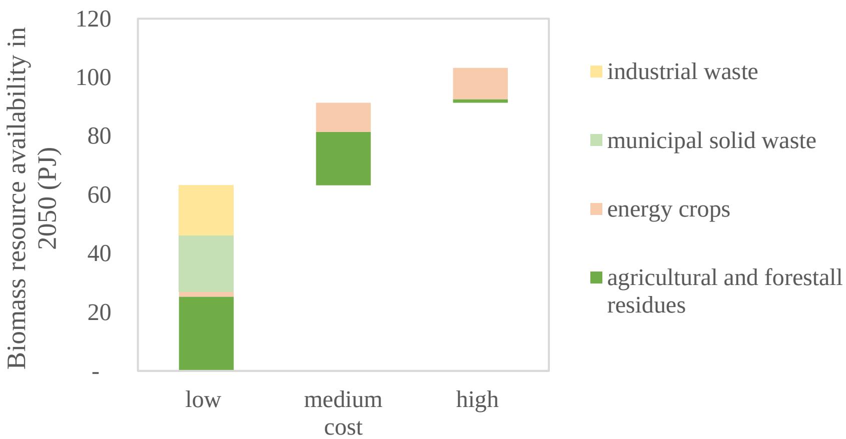

Figure A. 11. TIAM-UCL assumptions on global biomass resource potential. Agricultural and forestall residues (solid biomass) and energy crops are available at increasing costs, reflecting incremental difficulty of securing higher amounts of biomass.

The potential landfill gas resource is projected to be constant over time at about 7% of the total bioenergy feedstock potentially available in 2050. Similarly, the availability of first generation liquid biofuels is assumed to remain at 1% of the total biomass feedstock and is assumed not to expand in the future to account for concerns related to indirect impacts caused by the expansion of these crops [78,79]. Assumptions for the future availability of solid biomass are based on spatial modelling of the theoretical available potential, with the biomass fractions required for maintenance of soil quality and other uses subtracted, for the IMAGE model SSP2 baseline scenario [80]. Cost projections are also taken from the IMAGE model SSP2 baseline scenario, derived from a review of several literature sources; and include elements such as harvest, operations, storage and drying, forwarding, chipping and transport [80].

Availability assumptions for dedicated energy crops are based on regional modelling of 'abandoned agricultural land' [81] and so assume no competition for land with food crops or pasture. The most degraded and water scarce land is excluded. They are derived from the Ricardo-EE model for the UK Department for Business, Energy and Industrial Strategy [81]. This uses regional projections of abandoned agricultural land from the IMAGE model SSP2 RCP2.6 mitigation scenario. The most degraded and water scarce land is excluded by applying constraints derived from [82]. The land considered available for bioenergy crops globally thereby totals 199 Mha in 2020, 207 Mha by 2050 and is assumed constant up to 2100. Typical yields for perennial energy crops are applied for each region and a 1.3% yearly yield increase is assumed. This figure was estimated based on historic yield increases between 2010-2017 and a business-as-usual scenario regarding globalisation and investment [81]. The regional resources are split into 3 cost bands drawn from [83].

The distribution of bioenergy feedstocks between regions is derived from [80] for solid biomass, [83]and [81] for energy crops, and TIAM-WORLD for waste fractions, with some adjustments made to match the regions in TIAM-UCL. Assumptions on the regional distribution of biomass fractions are represented in Figure [77].

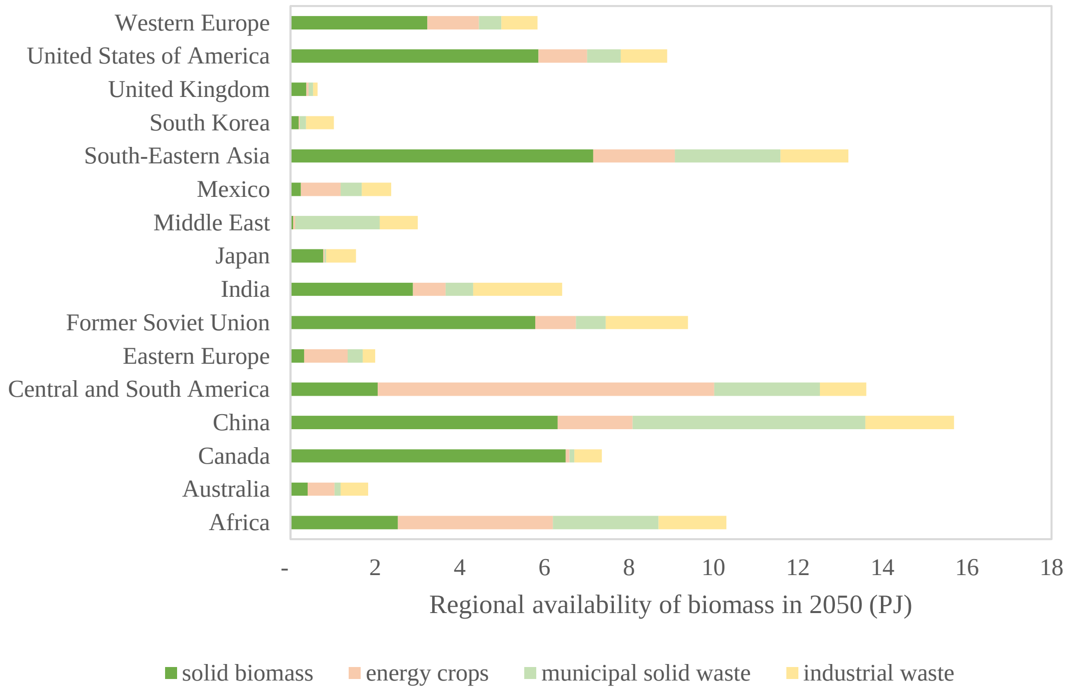

Figure A7.2. Assumptions on regional availability of biomass fractions in year 2050.

The global potential of bioenergy feedstock is assumed to increase from 65EJ/y in 2005 to 112 EJ/y in 2050. The main contributors to the global potential are solid biomass and energy crops, which cumulatively are assumed to reach 76 EJ/y in 2050. This is in line with current agreement on how much biomass feedstock could be produced sustainably by 2050 [84].

A7.1. Bio-commodity trade links

Tables Table A. 21 and Table A. 22 shows representative trade matrices for biomass feedstock and respectively bio-commodities. The trade links between each two regions are represented by the number 1.

Biomass feedstock	AFR	AUS	CAN	CHI	CSA	EEU	FSU	IND	JPN	MEA	MEX	ODA	SKO	USA	WEU	UK
AFR		1		1	1				1						1	1
AUS	1		1	1	1	1	1	1	1		1	1	1	1	1	1
CAN		1			1							1	1	1		
CHI	1	1			1		1						1	1	1	1
CSA	1	1	1	1		1	1	1	1		1	1	1	1	1	1
EEU		1			1		1	1						1		
FSU		1		1	1	1		1						1		
GBL																
IND		1			1	1	1					1		1		
JPN	1	1			1							1	1	1	1	1

MEA																
MEX		1			1									1		
ODA		1	1		1			1	1					1	1	1
SKO		1	1	1	1				1					1	1	1
USA		1	1	1	1	1	1	1	1		1	1	1		1	1
WEU	1	1		1	1				1			1	1	1		1
UK	1	1		1	1				1			1	1	1	1	

Table A. 21. Representative trade matrix showing trade links available for biomass feedstock. Note that from all biomass fractions, only energy crops and solid biomass can be traded in TIAM-UCL.

Biofuels	AFR	AUS	CAN	CHI	CSA	EEU	FSU	IND	JPN	MEA	MEX	ODA	SKO	USA	WEU	UK
AFR		1		1		1		1	1			1	1	1	1	1
AUS				1												
CAN	1			1		1		1	1	1	1	1	1	1	1	1
CHI																
CSA	1			1		1		1	1		1	1	1	1	1	1
EEU																
FSU	1	1	1	1	1	1		1	1		1	1	1	1	1	1
GBL																
IND																
JPN																
MEA	1	1	1	1	1	1	1	1	1		1	1	1	1	1	1
MEX														1		
ODA		1		1				1	1				1			
SKO																
USA	1	1	1	1	1	1	1	1	1	1	1	1	1		1	1
WEU														1		1
UK															1	

Table A. 22. Representative trade matrix showing trade links available for biofuel commodities, which include biodiesel, bio-naphtha and biojet kerosene.

.

Appendix 8. Techno-economic assumptions on DACS technologies

Table A. 23. Techno-economics of DACS, assumption in TIAM-UCL v4.1.1

DACS	Value	Unit	Source
Start time	2040	-	Chen and Tavoni [55] and Marcucci et al. [85] assume start time in 2060 vs. Fuss et al., [86] suggesting a CO_2 removal by DACS of 0.5-5 GtCO2/yr by 2050. Here we chose a start time by 2040.
Size	1	Mt CO2	IPCC report on CCS [87] defines Industrial – scale DAC on the order of 1 $MtCO_2$/yr.
Construction time	0	Years	No mention in literature, therefore is assumed zero here.
Lifetime	20	Years	As in Socolow et al. [54]
Learning effects	Expressed as less heat input	8.1 in 2060 to 5 GJ/tCO_2 in 2080	No learning effects in Socolow et al. [54] and Chen and Tavoni [55] vs. Marcucci et al [85] who consider an initial thermal energy requirement of 8.1 GJ/tCO_2 decreasing to 5 GJ/tCO_2 plus electricity consumption of 1.8 GJ/ tCO2 (0.5 MWh/tCO_2 captured). Here we use assumptions in Marcucci et al. [85].
Capital costs	2,900	$M\$/MtCO_2$	Based on Socolow et al. [54] and Chen and Tavoni [55], per total installed capacity (1 $MtCO_2$).
Fixed O&M	120	$\$/tCO_2/y$	Based on Socolow et al. [54] and Chen and Tavoni [55]; include maintenance, labour and chemicals.
Variable O&M	N/A	$\$/tCO_2/y$	Electricity and heat costs calculated by TIAM-UCL.
Technology hurdle rate	10	%	In line with new technologies hurdle rates in TIAM-UCL [88].
Build rate	7.5	%	Assume 7.5% increase of global DACS capacity per year (to get from 0.4 $MtCO_2$/yr currently to 40 $GtCO_2$/yr by 2100 as suggested possible by Fuss et al., [86].